

**ANNUAL REPORT**  
**2013**



# PREFACE

In 2013 the economic environment encountered some difficulties. Due to the expiration of current EU programs, fewer new EU projects were realized and the market situation for large R&D projects remained subdued.

Despite these difficult conditions the Fraunhofer IMS succeeded in asserting itself on the market and in achieving a consolidated budget. We were able to invest over €1 million in new facilities, in the extension of existing machinery as well as in the infrastructure of the Fraunhofer IMS. With regard to the number of employees, a slight increase was recorded and the operating budget amounted to €23.2 million at the end of the year. In 2013, the Fraunhofer IMS continued to achieve licensing revenues from its existing patent portfolio.

The cooperation with the company ELMOS in the field of "CMOS Processes" has been successfully continued and further expanded. Likewise, the cooperation with the company INFINEON in the field of "High-Voltage Devices in Silicon On Insulator (SOI) Technology" has been continued successfully and new products were co-developed.

The management of the Fraunhofer-inHaus-Center was taken over by Volkmar Keuter in the beginning of the year. Mr. Keuter, however, has been a part of the inHaus idea for a long time, coordinating the inHaus activities for the Fraunhofer UMSICHT in Oberhausen.

In July 2013, the "Hospital Engineering Labor" was inaugurated in the presence of important guests from politics, industry, and research. With its "Hospital Engineering Laboratory" the Fraunhofer inHaus-Center in Duisburg offers opportunities to test and demonstrate the performance of new developments in a realistic environment – for providers as well as users from the inpatient and outpatient fields. The research and test platform consists of a complete model hospital including lobby, hospital room, operating room, and rehabilitation area.

The development of circuits – with special regard to the requirements of functional safety according to ISO 26262 – is becoming increasingly important at the institute. In 2013, the business field "ASIC" was able to acquire a leading sensor provider as a new industrial partner for a development project. In the course of this project, a novel sensor front-end ASIC will be developed for application in the sensitive area of motor control.

In April 2013 Professor Kraft, who is in charge of the field of "Biohybrid Systems", opened the new biosensor laboratory, or "BioSensor Lab". In the future researchers and developers will be working together interdisciplinary in this laboratory, combining biotechnology with microelectronics to develop cost-effective analysis systems in miniature. The combination of biosensor, circuit and micro-electro-mechanical chip forms a so-called biohybrid system. These systems will be used in e.g. medical engineering, veterinary medicine and food analysis at home or in medical practice.

In collaboration with the Dutch start-up NovioSense BV the Fraunhofer IMS is developing a biosensor for diabetics and in 2013 the engineers made a significant step towards market maturity. The tiny sensor, which can be worn like a contact lens in the eye, is able to measure indirectly – via tear fluid – the blood sugar value, giving hope to millions of diabetics and therefore attracting wide public interest. During 2013, the high-temperature process (H035) of the Fraunhofer IMS in 0.35 µm Silicon On Insulator (SOI) CMOS technology has been further developed and first test circuits were successfully realized. A first version of the design kit was delivered to various customers in late 2013.

In comparison to already established high-temperature processes the Fraunhofer IMS achieved a unique selling point in terms of possible integration density. With a minimum feature size of 0.35 µm the SOI CMOS process provides the basis for integrated system solutions.



Another of 2013's milestones was the successful completion of the prototype development of QVGA-infrared detectors. These detectors are based on bolometers with integrated digital evaluation electronics. The Fraunhofer IMS succeeded for the first time in producing uncooled infrared sensors on the basis of bolometers in a chip-scale-package. To test the performance of these detectors an evaluation system especially for our industrial customers was developed.

The continuous technological development of bolometer processes is leading to a significant improvement of the core parameters. We will expand our activities in the field of uncooled infrared sensor technology and offer customer-specific sensors as well as infrared evaluation systems.

With the development of an intelligent solar cell for an international client, the Fraunhofer IMS was able to report another successful industrial project for the year 2013. This solar cell is applied onto a CMOS circuits via "post processing" and can be used for energy self-sufficient miniaturized sensor nodes. The technology used is based on customized amorphous silicon material, which can be isolated at a comparatively low temperature. The developed solar cell technology is matched to the existing L035 CMOS technology.

#### **Where do we go from here?**

The uncertainties of the global economy have not yet been overcome and the global growth remains subdued. The Fraunhofer IMS will accept the upcoming challenges with optimism. In addition to the planned acquisition of new industrial customers for various fields like high-temperature and microsystems technology, the Fraunhofer IMS will take part in the new founding opportunities of the "2020 Horizon" research and innovation program, which was launched in December 2013.

I would like to thank our employees for their tireless efforts which made the economic and scientific success of 2013 possible. We believe that we are well positioned for the future and the year 2014, despite the number of new challenges. I would particularly like to express my gratitude to you, our business partners, for our good cooperation during the past year, for your confidence in our institution, in our work and in our technologies.

We will do our very best to continue to achieve excellent results for you and we look forward to new and exciting tasks in 2014.

  
Anton Grabmaier



# CONTENTS

<b>Profile of the Fraunhofer Institute IMS</b>	<b>7</b>
<b>Development of the IMS</b>	<b>22</b>
<b>Selected Projects of the year 2013</b>	
<b>I CMOS Devices and Technology</b>	
Next generation high temperature SOI CMOS technology H. Kappert, S. Dreiner	26
Development of a CMOS-Integration technology for back side illuminated imagers based on direct bonding A. Goehlich, C. Eimers, Y. Celik, H. Vogt	29
Development of a high temperature resistant capacitor for micro systems technology Y. Celik, D. Dietz, A. Goehlich, A. Jupe, H. Vogt	32
Enhancement of the analog performance of PD-SOI mosfets using reverse body biasing (RBB) at high temperatures up to 400 °C A. Schmidt, H. Kappert	36
<b>II Silicon Sensors and Microsystems</b>	
FIR camera for thermal imaging D. Weiler	42
Optical sensors for time-resolved measurements E. Poklonskaya, O. Schrey	46
Measurement systems for optical properties of semiconductor devices A. Driewer, A. Schmidt, C. Busch	49
Implantable sensor to measure liquor pressure of a ventricular drainage system M. Görtz , G. vom Bögel, P. Fürst	52

### III CMOS Circuits

---

Customized Development of a CMOS compatible solar cell for autonomous sensor nodes M. Stühlmeyer, A. Goehlich, H. Vogt	56
---	----

---

### IV Wireless Chips and Systems

---

Smart flight case R. C. Jacobi, G. vom Bögel	59
---	----

---

Development of a wireless and selfsustaining sensor system in industrial applications for a high number of sensors G. vom Bögel, F. Meyer, M. Kemmerling	62
---	----

---

### V Systems and Applications

---

Sensor Based Care M. Munstermann	70
-------------------------------------	----

---

Electrochemical monitoring T. Zimmermann, A. Hennig	73
--	----

---

### List of Publications and Scientific Theses 2013

---

#### Chronical 2013

---

Opening of Hospital Engineering Laboratory V. Keuter	84
---	----

---

Microsystems technology congress S. van Kempen	85
---	----

---

Visit of the dutch commissioner, Ms. Annemieke Slow, at Fraunhofer IMS S. van Kempen, H. Vogt	86
--	----

---

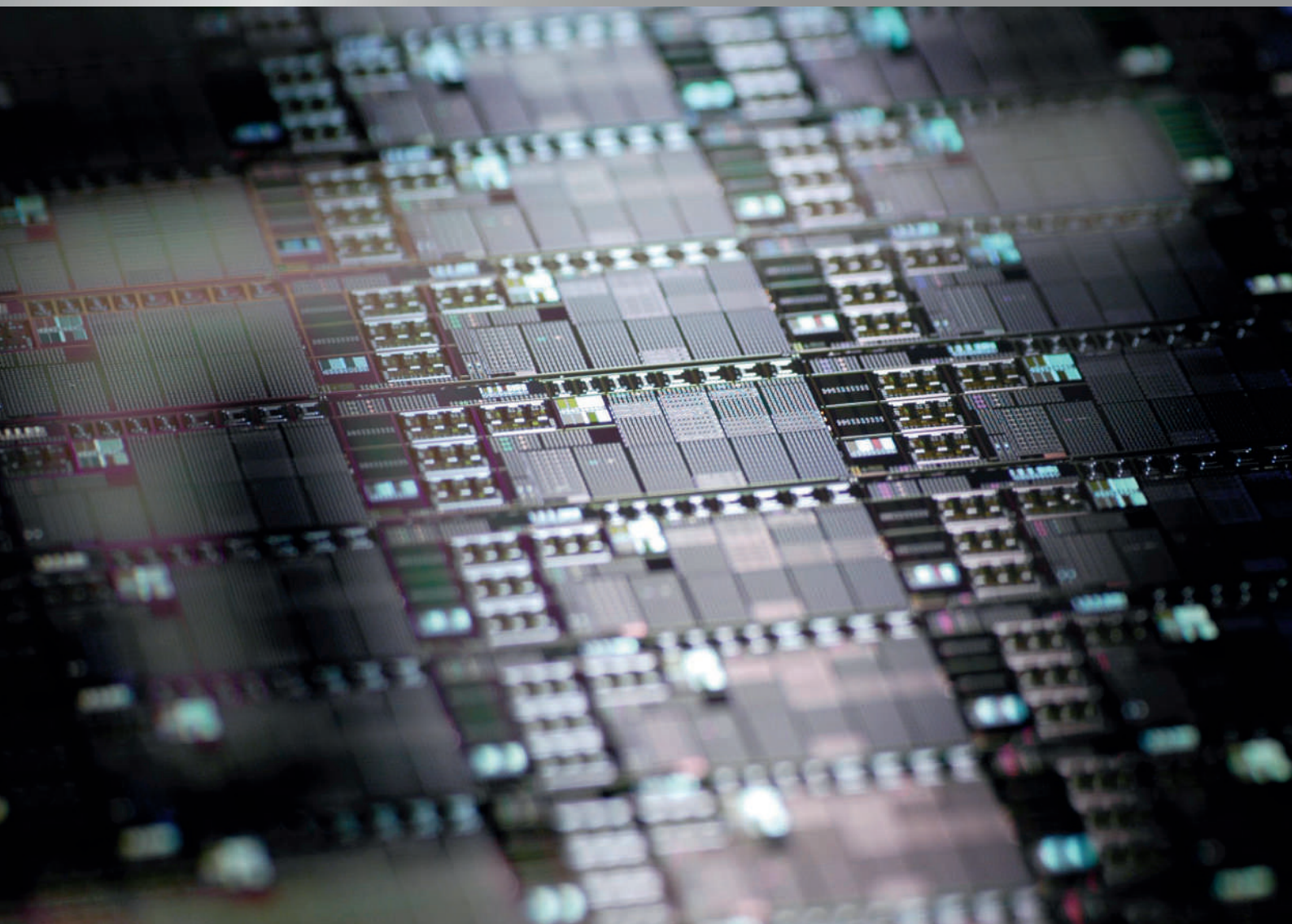
#### Press Review

---

PROFILE

FRAUNHOFER IMS

# PROFILE



# YOUR IDEA – WE WILL IMPLEMENT IT

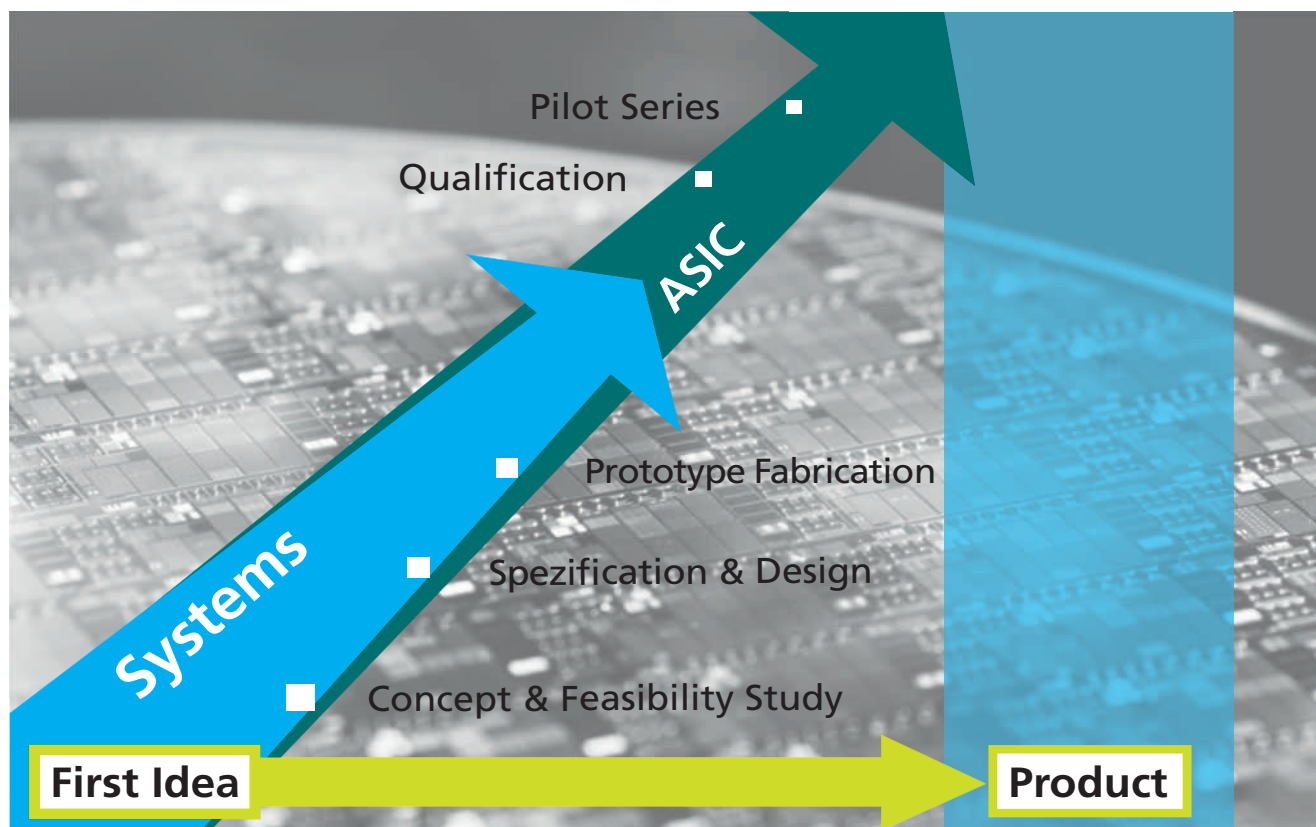
## Your Product Idea

In the beginning there's your idea or vision for a new product, but you don't know if it is feasible, which costs you will have to face, if there are potential risks and which is the technology that leads to the optimal product. As a research and development institute of the Fraunhofer-Gesellschaft we offer you our support.

We accompany your development with concept and feasibility studies from the first moment – via specification and design, draft and fabrication of prototypes through to the product qualification.

The pilot fabrication of your circuits and ICs is carried out by us as well. With us, you get microelectronics from a single source.

We provide our service and know-how across all industries. Our circuits and systems are especially used where it's all about the creation of unique selling points and competitive advantages for our customers. Then, our customer is able to serve his target market in an optimal way.





### Step by Step to Project Success

The way to a successful project is work-intensive and requires a good planning. Step by step, the following project phases are passed through:

- Concept & Feasibility Studies
- Specification & Design
- Demonstrator Development
- Prototype Development
- Qualification
- Pilot Fabrication (for ASICs)

### Quality Pays off

The Fraunhofer IMS is certified according to DIN EN ISO 9001 since 1995. The certificate is valid for all divisions of the institute: Research, development, production and distribution of microelectronic circuits, electronic systems, microsystems and sensors as well as consulting in these fields. The CMOS line is certified according to ISO/TS 16949.

Your project success is our mission.

---

### Our Business Units

---

- IC Design & ASICs
- Wireless Systems & Transponders
- Ambient Intelligence Systems
- Pressure Sensor Systems
- CMOS Image Sensors
- IR-Imagers
- Devices & Technology
- Biohybrid Systems



# FROM WAFER TO SYSTEM

Our technological home at Fraunhofer IMS is, since the foundation in 1984, the semiconductor technology and the development of microelectronic circuits and systems. The type and bandwidth of our infrastructure is extremely efficient; we have the experience and know-how in eight business units.

During our contract works we focus on strong, efficient and marketable developments. We offer comprehensive technologies and procedures which are applied in almost all industries. Application-specific adaptations to the requirements of our customers are the major focus of our work.

---

## Our Technological Core

---

- Semiconductor Processes
- CMOS & SOI-Technologies
- Microsystems Technology
- Component & System Developments
- Nano-(Bio)technologies

---

## Infrastructure

---

### CMOS Assembly Line

Wafer size	200 mm (8 inches, 0.35 $\mu$ m)
Cleanroom area	1,300 m <sup>2</sup>
Cleanroom class	10
Employees	150 in 4 shifts
Capacity	> 70.000 wafer/year

### Microsystems Technology Lab & Fab

Wafer size	200 mm (0.35 $\mu$ m)
Cleanroom area	600 m <sup>2</sup>
Cleanroom class	10
Capacity	5.000 wafer/year

### Cleanroom for Test & Assembly

Wafer size	200 mm
Cleanroom area	1.200 m <sup>2</sup>
Cleanroom class	1.000
Test	5 test systems
IC-Assembly	Sawing & thinning of wafer Chip-On-Board Die- and wire bonding

### Laboratories

Biohybrid sensors	45 m <sup>2</sup>
inHaus center	3.500 m <sup>2</sup>
Laboratory space	800 m <sup>2</sup>
High-frequency	
Measurement Chamber	24 m <sup>2</sup>



# AMBIENT INTELLIGENCE SYSTEMS



People spend a large part of their lives in rooms and buildings. Not only private living but also care processes – at home or in nursing homes – and the whole working life usually take place in buildings. Here, operating costs, a flexible adaption to user requirements and the feel-good factor are becoming increasingly important.

In our inHaus-center, supportive solutions for residential and building environment (AAL – Ambient Assisted Living) for our customers are developed and also tested. The installed products for facility management in commercial buildings are subject to criteria of high economic efficiency and sustainable energy efficiency.

The Fraunhofer IMS offers novel assistance systems for more efficiency in the nursing and hospital area. Innovative solutions in the area of energy & facility management up to solutions for the next generation office are the development priorities in the business unit Ambient Intelligence Systems.

We provide our service and know-how across all industries. Our circuits and systems are especially used where it's all about the creation of unique selling points and competitive advantages for our customers. Then, our customer is able to serve his target market in an optimal way.

---

## Supply and Services / Technology

---

- Hard- and software development
- Planning and consulting
- Building integration and practical tests
- Heterogeneous interconnection (also wireless)
- Field tests for long-term monitoring

# WIRELESS SYSTEMS & TRANSPONDERS



Industrial production and processing processes can only supply high quality products and work cost-effectively if the machines are optimally adjusted, if they haven't got much wear and possess a long durability. For the performance of these requirements it is indispensable to have measurement data which help to optimize the machine settings, to determine the maintenance requirements, to control the manufacturing steps and to make quality recordings.

Transponder systems – especially sensor transponder systems – and sensor networks feature an excellent technological basis for the registration of identification and sensor data.

The wireless communication and power supply open up new application areas – e.g. in medicine to get measurement data from implanted sensors for diagnostic and therapeutic purposes. Other interesting application areas are the building sector and logistics.

---

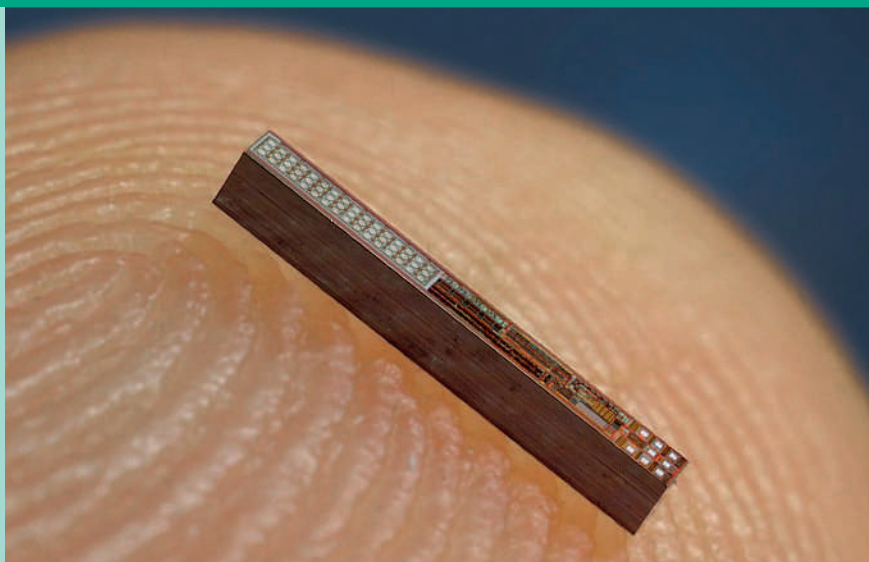
## Supply and Services / Technology

---

- Active and passive systems
- Sensor transponder integration
- Customized adaption
- Funk-frontends for LF-, HF- & UHF-frequencies
- Systems with high ranges
- Systems for "difficult" environments



# PRESSURE SENSOR SYSTEMS



In microelectronics the trend is toward smaller and smaller sensors even in pressure sensor technology. Our customized developments are not only particularly efficient and consume little power but they are also, due to their minimal size, implantable in the human body if required. For this reason, beyond classic applications of pressure sensor technology, new fields of application are opened up, particularly in medical engineering.

By the fabrication of these sensors as integrated capacitive pressure sensors in surface micromechanics a connection with any signal processing is possible.

Our miniaturized pressure transponders are also suitable for metrological applications in industry or for the measurement of tire pressures in automotive engineering. Due to the integration of the sensor system and signal processing in one ASIC the Fraunhofer IMS can cater to all realizable requirements and applications and can offer customized technologies for the future.

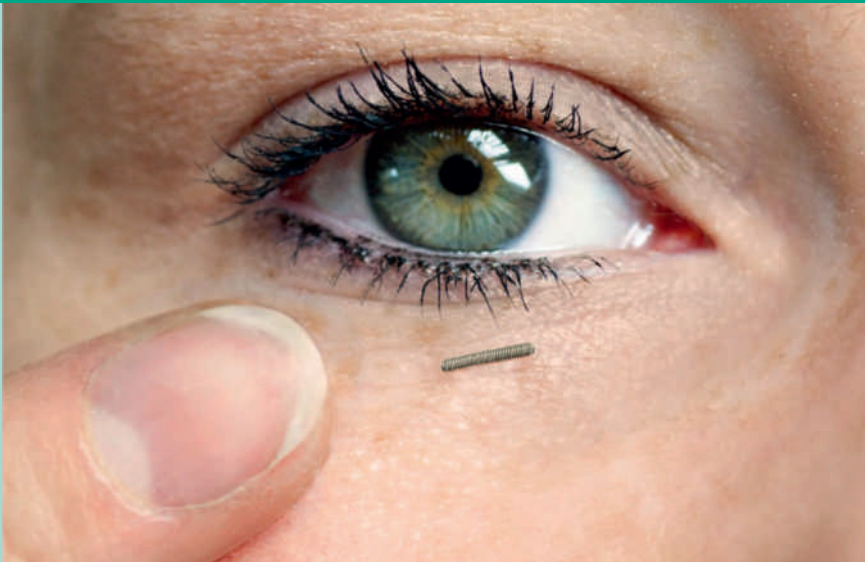
---

## Supply and Services / Technology

---

- Customized development of capacitive pressure sensors
- Measurement range of just a few mbar up to 350 bar
- Extremely high precisions
- Transponder ability due to low energy requirements
- Integrated temperature sensor
- Customized packages, tests & calibration

# BIOHYBRID SYSTEMS



The markerless identification of biological and chemical substances without extensive laboratory work is decisive for the progress in medical engineering. Sophisticated measuring technology is replaced by miniaturized systems which recognize substances via a biosensor (immuno or electrochemical sensor) by their electronic reaction.

We offer the development of these highly sensitive detection systems, which state a cost-effective and fast option to optical analyses in the laboratory. These nano systems can also be integrated into more complex biohybrid systems, such as Lab-on-chip, if required. This is particularly interesting for customers of medical engineering, who can offer simple ways

for real-time examinations via non-invasive, permanent diagnosis and monitoring systems in the future.

Because bioelectronic sensors can detect medical and physical parameters. These functions are also interesting for the food industry, which can profit by the simple and fast detection of biological-chemical variations of their products.

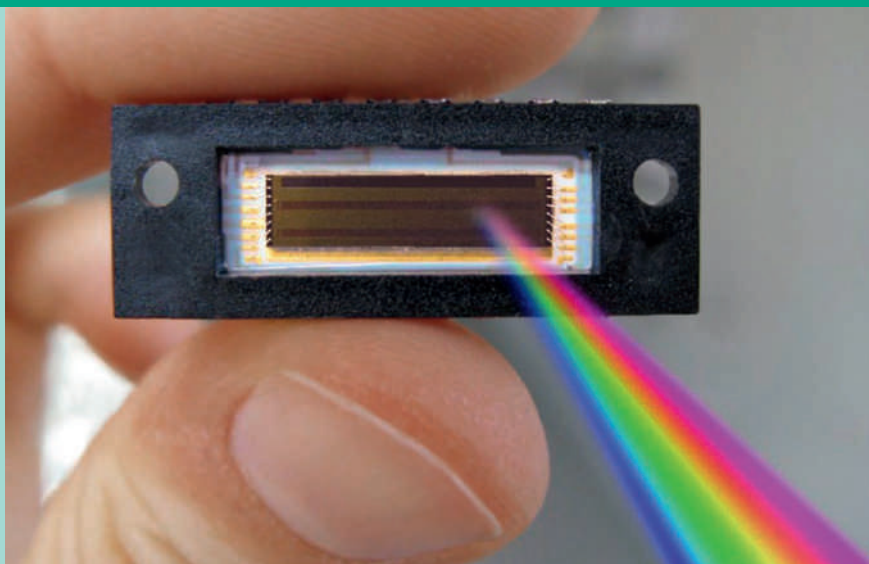
---

## Supply and Services / Technology

---

- Customized biosensor systems (e.g. glucose, lactose)
- Markerless and quantitative sensor technology
- Real-time monitoring in body fluid
- Customized electrochemical sensor technology
- Customized immuno sensor technology
- Customized packages and tests

# CMOS IMAGE SENSORS



Sensors for image capture based on CMOS technologies have reached a point where its quality and performance even surpasses the outmost mature CCD sensors. Development of special photo detector devices or the special treatments of the silicon surface boost the pixel attributes. Our long experience in designing CMOS photo detectors and imagers, as well as their processing and characterization enable custom solutions that meet customers' requirements.

Our customers profit from a 0.35  $\mu\text{m}$  "Opto" CMOS process optimized for photo sensing applications. »Pinned« photodiodes with low dark current and noise with color filters, micro lenses and also stitching can be integrated.

Our developments cover a wide spectrum from roentgen-rays to EUV, UV and the visible area up to the near infrared-range.

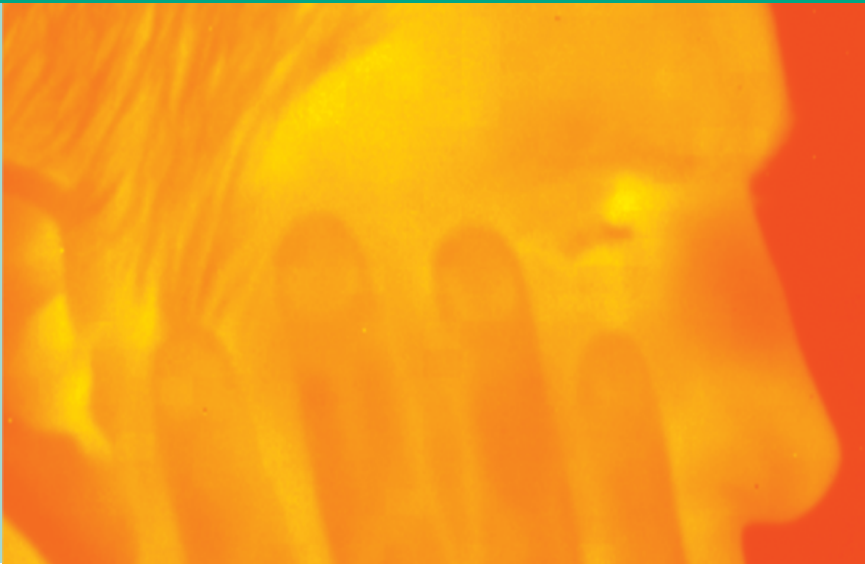
---

## Supply and Services / Technology

---

- Customized line and area sensors
- Special pixels for time-of-flight, spectroscopy et al.
- Stitching for large-area sensors
- UV- and XUV-sensitive sensors
- Color filters and micro lenses
- Customized packages and tests
- Pilot fabrication in the 0.35  $\mu\text{m}$  "Opto" CMOS proces

# IR SENSORS



Infrared imagers »see« in a wave length range from the near up to the long-wave infrared. These thermal image sensors are called focal plane arrays and are one- or two-dimensional lines of IR-sensitive pixels. They are based on radiation-sensitive structures on silicon technology, where CMOS read-out circuits are integrated on a chip. That's how complete image sensor chips are developed.

Our customer-specific applications are used in the automotive industry, where driver assistance, night vision and pedestrian detection are focal points of development.

In the industrial sector similar safety aspects, e.g. personal security, and also the measurement technology in the process monitoring matter. In the sensor system, the gas analysis is of increasing interest. Further applications are thermography in buildings or in medicine, but also for border and building security.

---

## Supply and Services / Technology

---

- Customized IR imagers
- Complete on-chip signal processing
- Budget chip-scale packages
- IR development and pilot fabrication
- Customized packages, tests & calibration

# IC DESIGN & ASICS



“From the concept up to the pilot fabrication” is the maxim of the Fraunhofer IMS. We provide our customers professional analogue or mixed signal ASIC design solutions – from the concept up to verified silicon for “ready to use” ASIC products for the application in several areas. In doing so, we support our customers with our large system know-how.

In addition to implementations in various standard CMOS technologies we especially allocate design and technology solutions for high temperature, high voltage and sensor systems applications.

Special circuit parts or sensor system components are individually and custom-designed developed and integrated with standard components like sensor readout, signal processing, interface components or embedded micro controllers on an IC.

---

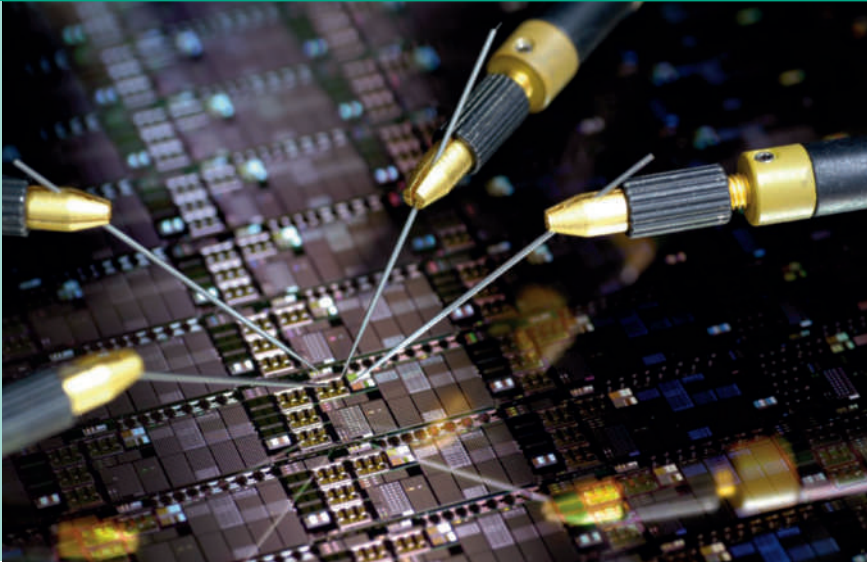
## Supply and Services / Technology

---

- Sensor interfaces
- Analogue ICs
- Signal conversion
- Digital signal processing
- Integrated sensors
- Customized packages and tests
- Energy-optimized solutions
- Pilot fabrication



# DEVICES & TECHNOLOGY



Our in-house CMOS line is the technological base of our institute. It supplies professionally operated and acknowledged automobile quality in robust 0.35  $\mu\text{m}$  technology on 200 mm wafer. The entire processes are developed in the Fraunhofer IMS and are extended by additional process modules, such as special optical devices, pressure sensors or high voltage components.

The integration of new materials or micromechanical structures is not possible by implication because a CMOS line has to be restricted to maintain the high level quality. Therefore, we have additionally assembled an own microsystems technology line (MST-Lab & Fab) for "post-processing".

CMOS wafers act as an "intelligent" substrate. They contain trigger and read-out circuits, signal processing and conversion as well as external interfaces up to the wireless power and data transmission. On these wafers, these "substrates", layers and structures are now deposited and by this new components are produced. The development's aim is to produce compact "intelligent" microsystems.

---

## Supply and Services / Technology

---

- MST process developments
- Integrated microsystems on CMOS
- Wafer size 200 mm (0.35  $\mu\text{m}$ )
- CMOS process development & devices
- SOI processes
- Development and consulting for the semiconductor industry

# DIRECTIONS & CONTACT



## Fraunhofer-Institut für Mikroelektronische Schaltungen und Systeme IMS

Finkenstraße 61, D-47057 Duisburg

Phone +49 203 37 83-0

E-mail [info@ims.fraunhofer.de](mailto:info@ims.fraunhofer.de)

Internet [www.ims.fraunhofer.de](http://www.ims.fraunhofer.de)

### Director

Prof. Dr. rer. nat. A. Grabmaier

### Contact

Martin van Ackeren

Phone +49 203 37 83-130

Fax +49 203 37 83-2 66

[martin.van.ackeren@ims.fraunhofer.de](mailto:martin.van.ackeren@ims.fraunhofer.de)

Michael Bollerott

Phone +49 203 37 83-2 27

Fax +49 203 37 83-2 66

---

## Access by car

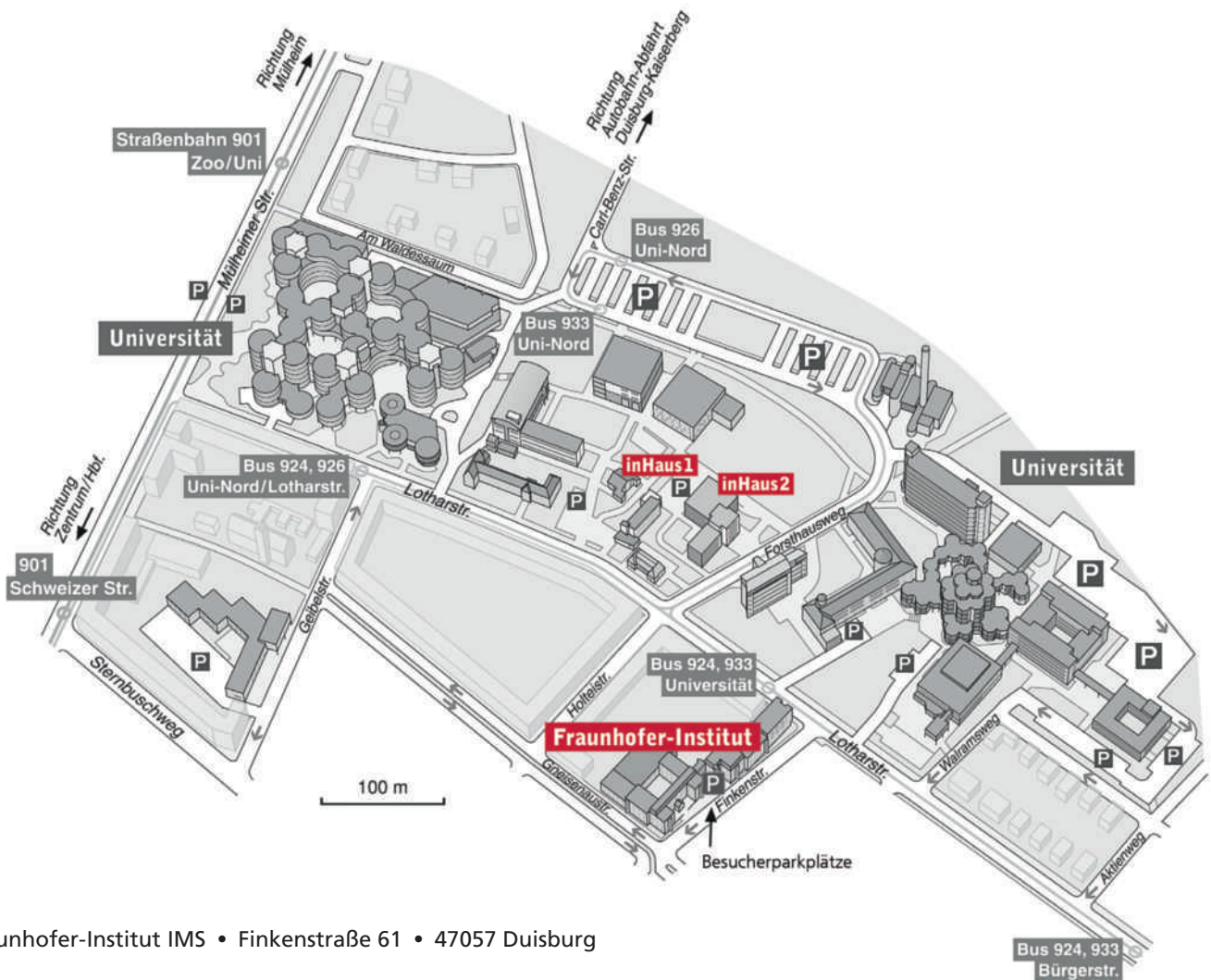
---

### via motorway A40

- exit "Duisburg-Kaiserberg"
- direction "Innenstadt", "Zoo"
- (Carl-Benz-Straße)
- after approx. 1 km (direction "Innenstadt") turn right into Mülheimer Str.
- pass the Zoo
- at first traffic light turn left into the Lotharstr.
- at third street turn right into Finkenstr.
- Institute is on the right side

### via motorway A3

- exit "Duisburg-Wedau"
- direction "Innenstadt" (Koloniestraße)
- at traffic light turn right into Mozartstraße, which turns into Lotharstr. in the following of the street
- after 800 m turn left into Finkenstr.
- Institute is on the right side



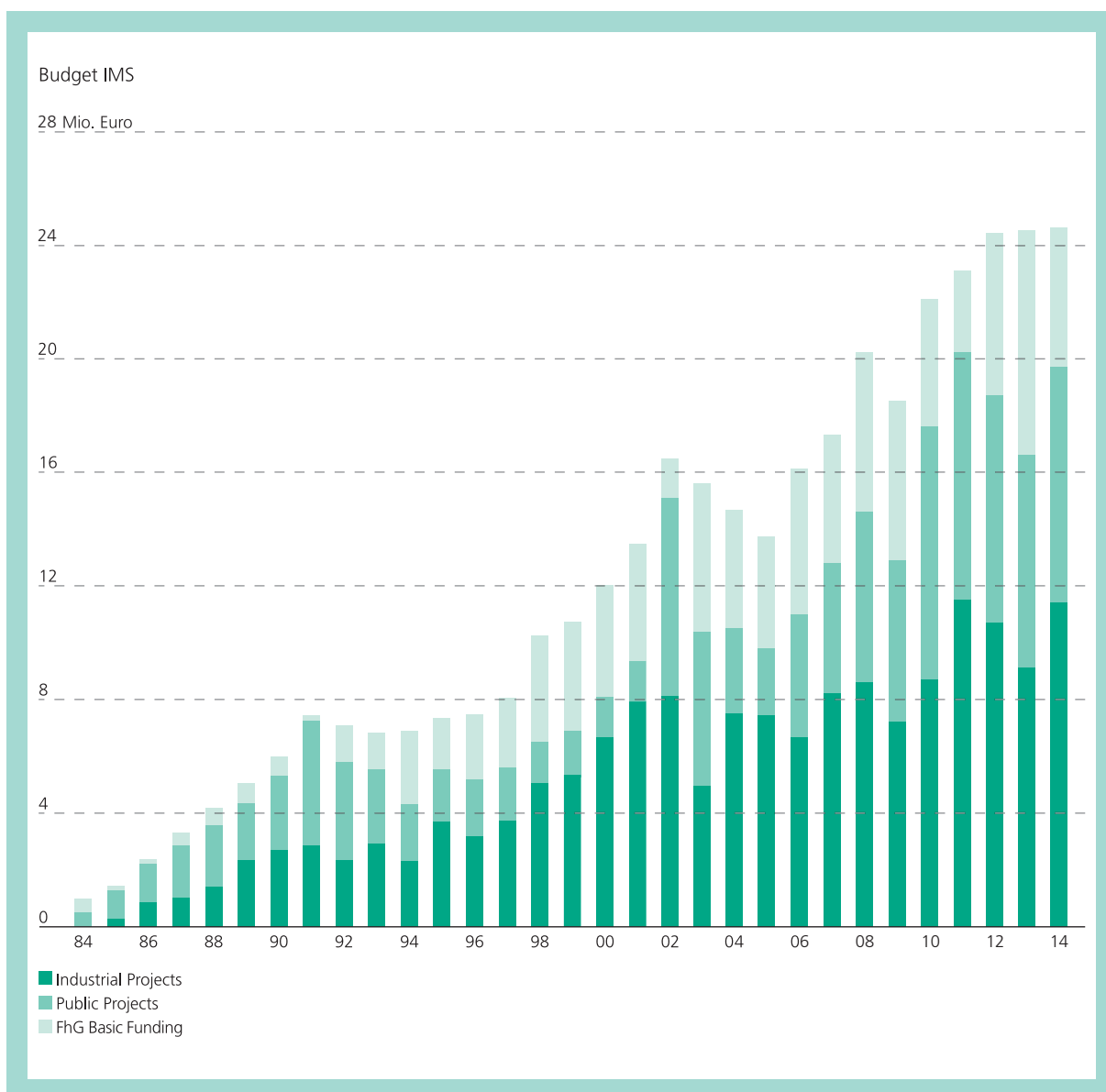
Fraunhofer-Institut IMS • Finkenstraße 61 • 47057 Duisburg

### Access by airplane

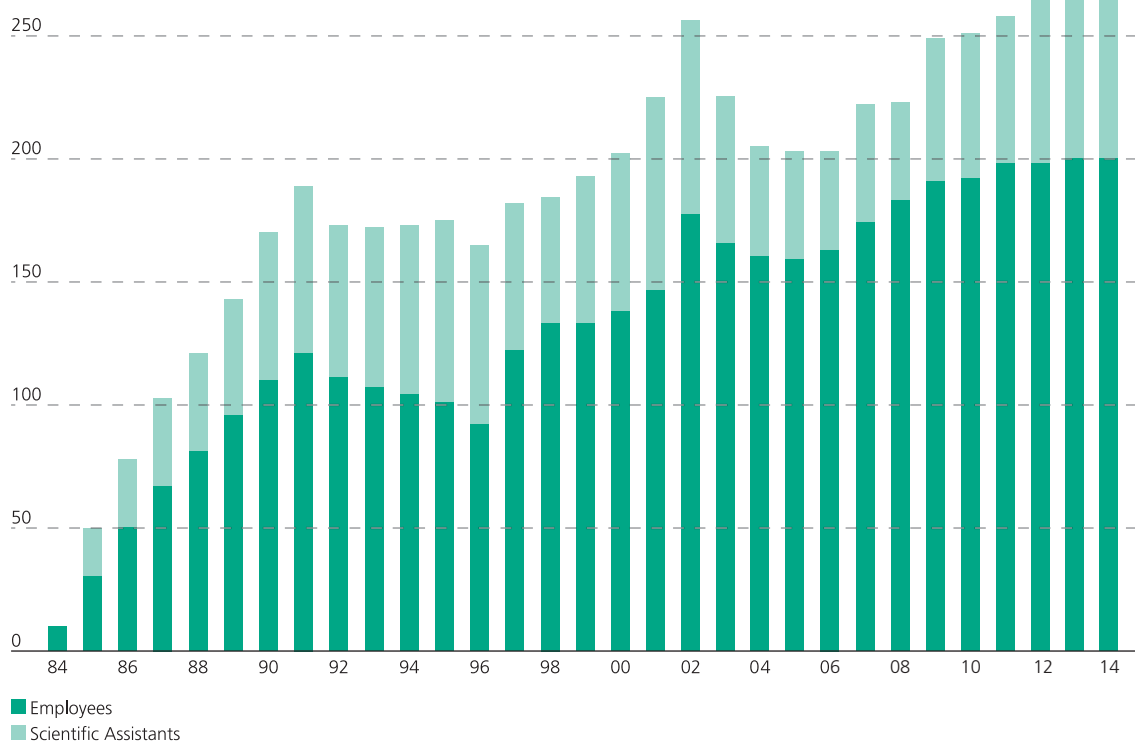
- Arrival at Airport Dusseldorf
- Taxi (duration 20 minutes)
  - to Duisburg Central Station by train  
from Duisburg Central Station take bus number 933 or 924 (direction Uni/Zoo), bus stop Universitat

### Access by train

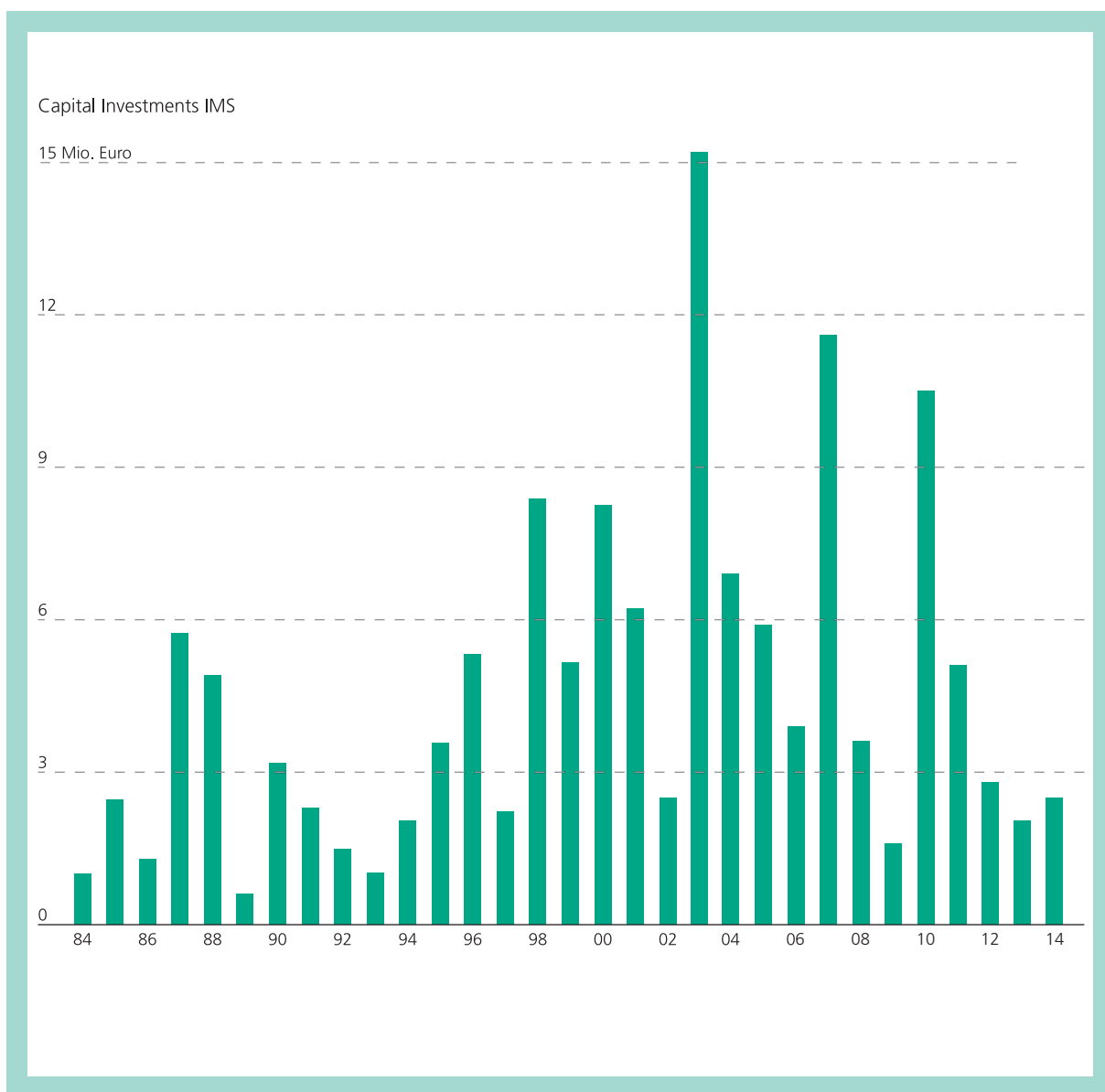
- Arrival Duisburg Central Station
- Taxi (duration 5 minutes)
  - Bus line 933 or 924 (direction Uni/Zoo), bus stop Universitat



Staff Members IMS







# SELECTED PROJECTS OF THE YEAR 2013

## Selected Projects of the Year 2013

---

I	CMOS Devices and Technology	26
II	Silicon Sensors and Microsystems	42
III	CMOS Circuits	56
IV	Wireless Chips and Systems	59
V	Systems and Applications	70

# NEXT GENERATION HIGH TEMPERATURE SOI CMOS TECHNOLOGY

H. Kappert, S. Dreiner

Fraunhofer IMS presents the next generation High Temperature Silicon-On-Insulator (SOI) CMOS technology H035. It's a 0.35  $\mu\text{m}$  SOI CMOS technology addressing the increasing complexity of mixed signal integrated circuitry even for high temperature operation up to 250  $^{\circ}\text{C}$  and more.

## Introduction

High temperature electronic is a specialized but continuously developing market. Several queries indicate that there is a demand for integrated circuits in harsh environments with operating temperatures of up to 250  $^{\circ}\text{C}$  and more. First developments for operating temperatures of up to 300  $^{\circ}\text{C}$  have been shown i.e. in the field of enhanced geothermal systems [1].

Today's high temperature semiconductor market is characterized by the use of less complex standard circuits e.g. references, operational amplifiers and large die sizes for memory or simple microcontroller circuitry. There is still a lack of an advanced high temperature CMOS technology, as known high temperature SOI CMOS technologies have a characteristic feature size of 0.8 to 1.0  $\mu\text{m}$ . Nevertheless the market demands for more complex systems even at high temperatures which often results in a multi-chip approach or in additional cooling effort.

First complex components like 32-bit microcontroller or flash memory are available, but with limited high temperature operation live of 1000 h at a maximum operation temperature of 210  $^{\circ}\text{C}$  [2]. Today no technology is known featuring a high gate density while supporting operating temperatures of up to 250  $^{\circ}\text{C}$  and more.

To fill this gap Fraunhofer IMS has developed a next generation high temperature SOI CMOS technology with a gate density which is about ten times higher than with comparable high temperature technologies. This new technology mainly addresses mixed signal applications e.g. sensor signal processing typically defined by analog signal conditioning and digital data processing. Furthermore, microcontrollers with application specific peripherals could be realized e.g. as controllers in motor driver or power converter applications. Due to the

increased gate density microcontrollers embedded in a mixed signal circuitry become feasible at a reasonable chip size.

## Technology

The new high temperature SOI CMOS technology H035 is based on the Fraunhofer IMS 1.0  $\mu\text{m}$  high temperature technology H10 and a proven 0.35  $\mu\text{m}$  automotive bulk CMOS technology.

Technology features:

- 0.35  $\mu\text{m}$  smallest structure size
- dual gate oxides
- gate density of about 8500 gates/ $\text{mm}^2$
- 3.3 V typical digital operating voltage
- up to 10 V analog operating voltage
- 30 V NSOI device
- various resistor types
- voltage independent capacitor
- pin and zener diodes
- EEPROM
- Silicided poly silicon and diffusion regions
- 4 layer reliable high temperature metallization
- operating temperatures up to 300  $^{\circ}\text{C}$

Figure 1 gives an impression of the shrink factor showing a single transistor drawn in H10 (1.0  $\mu\text{m}$ ) and in the new H035 (0.35  $\mu\text{m}$ ) technology, respectively.

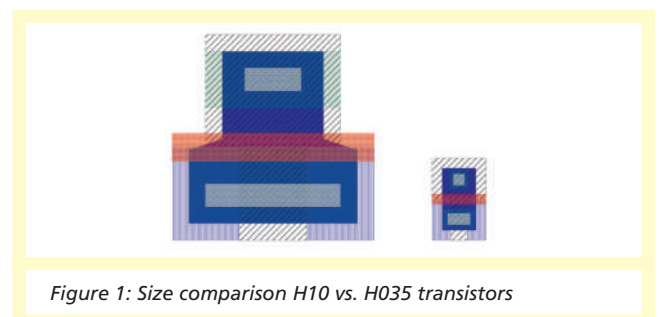


Figure 1: Size comparison H10 vs. H035 transistors

In Figure 2 a cross section of the H035 technology is depicted. H035 is a thin film SOI CMOS technology. All devices are built in a thin silicon film and are isolated against each other by silicon oxide. Due to the thin silicon film thickness and the insulation layer, leakage currents are reduced by about three decades at high temperature, which allows mixed signal operation up to 300°C. Measurements have been successfully performed even up to 400°C [3][4]. The technology is equipped with two gate oxides (9.4 nm and 40 nm).

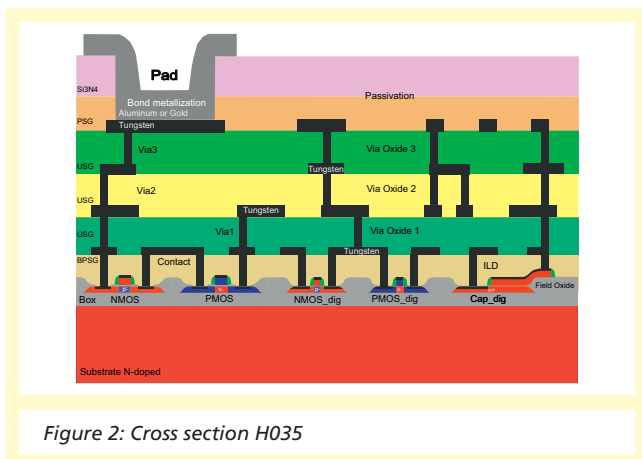


Figure 2: Cross section H035

Figure 3 three shows an SEM image of the silicon film, the poly silicon layer and the two different gate oxides. The thin gate oxide is typically used for digital 0.35  $\mu\text{m}$  devices, while the 40 nm gate oxide is utilized in the analog domain allowing operating voltages up to 10 V or even more for an NSOI device. These 40 nm devices are compatible to the H10 devices. To reduce source drain resistance as well as gate resistance, poly and diffusion regions of the digital devices are silicided. The technology is equipped with four layers of tungsten metallization allowing reliable operation up to 300 °C without any electromigration issue. Finally the H035 technology features nonvolatile memory based on EEPROM. One time programmable memory is in evaluation as a highly reliable permanent memory with extended data retention.

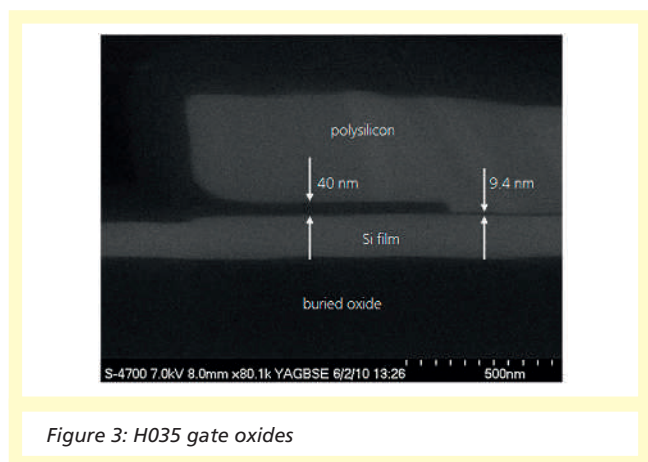


Figure 3: H035 gate oxides

### Process Design Kit

Fraunhofer IMS provides a process design kit (PDK) for the Cadence® design system. The PDK features:

- Technology library including all devices and simulation parameters
- Digital standard cell library
- IO cell library
- Memory generators are in development

Simulation parameters of the transistors are carried out for the BSIMSOI model. All parameters are extracted within a temperature range from -40°C to 300°C.

Cadence is a registered trademark of Cadence Design Systems, Inc.

### Test Circuitry

During the different development cycles various test circuits like ring oscillators, standard cells, a band-gap reference or an operational amplifier have been realized. Figure 4 shows an example test circuit including two band-gap references realized with the thin and thick gate oxide, respectively and an operational amplifier.

Measurement results have been successfully carried out over the whole temperature range. Additional test circuits and a complex mixed signal evaluation chip are planned for 2014.

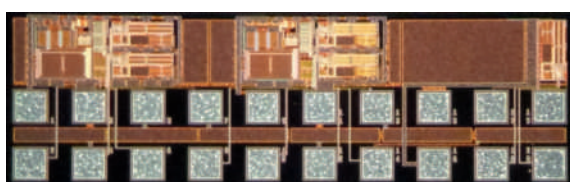


Figure 4: Analog test circuitry

#### Conclusion and future work

Fraunhofer IMS has developed a leading edge high temperature SOI CMOS technology. The great interest from fabless semiconductor companies as well as from application integrators shows that it is a long awaited technology.

Various test circuits were designed and performed successfully. Optimization and characterization of the technology, completion of the PDK and reliability tests are ongoing. A full feature evaluation chip and risk production is planned for 2014. Customers are invited to join the evaluation phase with first designs.

This work was supported by the Programme Inter Carnot Fraunhofer from BMBF (Grant 01SF0804) and ANR.

- [1] Bruce W. Ohme, Mark R. Larson:  
Analog Component Development for 300°C Sensor  
Interface Applications, Proceedings of IMAPS International  
Conference and Exhibition on High Temperature Electronics  
(HiTEC 2012), Albuquerque, New Mexico, USA
- [2] Texas Instruments:  
High-Temperature Guide 2013, [www.ti.com](http://www.ti.com), 3Q 2013
- [3] K. Grella, S. Dreiner, A. Schmidt, W. Heiermann,  
H. Kappert, H. Vogt, U. Paschen:  
High Temperature Characterization up to 450°C of MOS-  
FETs and basic circuits realized in a Silicon-on-Insulator (SOI)

CMOS-Technology, Proceedings of IMAPS International  
Conference and Exhibition on High Temperature Electronics  
(HiTEC 2012), Albuquerque, New Mexico, USA

- [4] Alexander Schmidt, Holger Kappert, Rainer Kokozinski:  
Enhanced High Temperature Performance of PD-SOI  
MOSFETs in Analog Circuits Using Reverse Body Biasing,  
Proceedings of IMAPS International Conference on High  
Temperature Electronics Network (HiTEN 2013), Oxford,  
United Kingdom



# DEVELOPMENT OF A CMOS-INTEGRATION TECHNOLOGY FOR BACK SIDE ILLUMINATED IMAGERS BASED ON DIRECT BONDING

A. Goehlich, C. Eimers, Y. Celik, H. Vogt

## Abstract:

Backside illuminated imager (BSI) technology with low pixel pitch is nowadays used more and more in the consumer market segment of imager chips, e.g. in smartphones. Within the Fraunhofer MEF project BackCis a highly sensitive BSI image sensor chip is developed that is intended for special applications such as optical emission spectroscopy (typically line type sensors), applications for 3D-distance measurements (e.g. for driver assistance) or for night vision. The applied technology is based on the T035 thick film SOI technology. This report focusses on the progress of the microsystem technology development.

## 1. Introduction

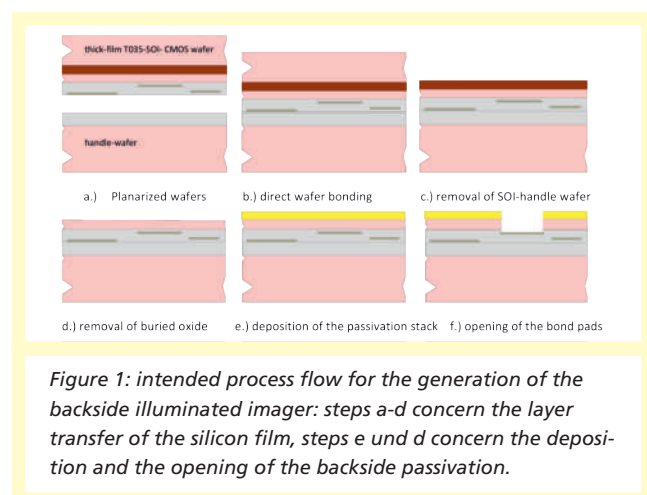
Backside illuminated imager (BSI) technology with low pixel pitch is nowadays used more and more in the consumer market segment of imager chips, e.g. in smartphones. A special advantage of such kind of image sensor consists in the fact that the illuminating light enters the image sensor from the backside, i.e. the side of the silicon substrate opposite to the metal wiring of photo diodes. This technology offers as compared to front side illuminated (FSI) sensors the inherent advantage of a high quantum efficiency and a high fill factor, since nearly the full available area can be utilized for the photo diodes without blocking and reflection effects by the metallization. However for special applications such as optical emission spectroscopy (typically line type sensors), sensor applications for 3D-distance measurements (e.g. for driver assistance) or for night vision high quality BSI- sensors with increased sensitivity in combination with low noise level are missing yet. Backside illuminated image sensors are realized with CCD- [1] and with CMOS-technology [2]. Two possible technological approaches are known so far: wafer bonding in combination with back thinning of a bulk wafer that comprises the image pixels [3] or the utilization of a silicon on insulator (SOI) technology in combination with a layer transfer technique [4].

The IMS has recently developed optical pixel structures with high gain comparable to single photon counting ability, which are ideally suited e.g. for spectroscopic applications such as optical emission spectroscopy. A thick film SOI-CMOS technology with trench isolation is available at IMS that enables the development of backside illuminated image (BSI) sensors with reasonable technological effort. In the frame of the internal

Fraunhofer program "BackCis" a BSI-demonstrator image sensor is developed. Within this project the image sensor chip is designed and the basic substrates are produced in the CMOS cleanroom with the aid of the T035 technology. A certain aspect of this project concerns the integration of the basic substrate towards the BSI camera chip. This report focusses on the progress of the microsystem technology development.

## 2. Process development for the back side illuminated image sensor

The technological approach for the realization of the BSI camera chip is based on the utilization of the existing thick film SOI technology in connection with the layer transfer of the silicon film on a separate handle wafer. A schematic drawing of the envisaged integration process flow is depicted in figure 1:



## CMOS DEVICES AND TECHNOLOGY DEVELOPMENT OF A CMOS- INTEGRATION TECHNOLOGY FOR BACK SIDE ILLUMINATED IMAGERS BASED ON DIRECT BONDING

The layer transfer is facilitated with the aid of the wafer-to-wafer bonding of the SOI wafer “top down” on a prepared handle substrate (see figure 1 a-c). The utilized bonding method is the direct oxide-to-oxide bonding, i.e. the CMOS-SOI substrate as well as the handle substrate is provided with an oxide bonding layer that is planarized by a chemical mechanical polishing process. This CMP process ensures a surface quality with a very low surface roughness (typically in the range of some angstroms). The mechanical interconnection of the CMOS SOI-wafer with the handle substrate is facilitated with the aid of a wafer bonding tool. The mechanical interconnection is enforced by a specially designed “low” temperature annealing step. The achieved bond strength enables the back grinding of the handle substrate of the SOI-wafer. The residual silicon of the SOI-handle wafer is removed subsequently by isotropic etching in a  $\text{SF}_6$  plasma. In this way the thick film containing the photo diodes is flipped down on a handle wafer enabling the backside illumination. This interconnection method ensures a robust mechanical interconnection in particular with respect to adapted coefficients of thermal expansion.

Photographs of a bonded wafer pair after grinding and etching are shown in figure 2. In this case a SOI-Wafer has been bonded on a planarized handle substrate. The SOI-wafer mimics the T035 substrate in this case. On both substrates a PECVD-oxide has been deposited and subsequently polished by CMP. The wafer bond has been performed in an AML-wafer bonding tool and has been annealed for a couple of 10 minutes at a temperature well below  $400^\circ\text{C}$ , in order not to influence the performance of a CMOS-circuit. The inspection of the bond interface in infrared light revealed only very view voids. The handle wafer of the SOI-wafer has been removed by a combination of mechanical grinding with a Disco DF 6841 grinder (see figure 2 left) and an isotropic plasma etch step using a Tegal 200 DRIE etcher in  $\text{SF}_6$  (see figure 2 right). This etch process stops very selectively with respect to the buried oxide. In the intended process flow the buried oxide is removed subsequently with the aid of a vapor phase HF-etch. The result of the direct bonding of a T035 trench wafer to a handle substrate after removal of the SOI handle-wafer is depicted in figure 3 as a SEM micrograph. As a result of the

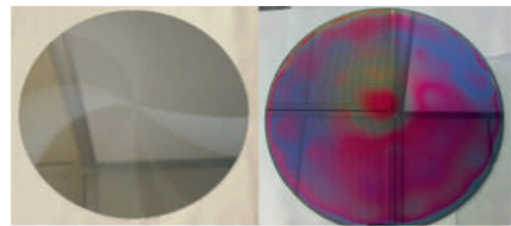


*Figure 2: left: bonded wafer stack after grinding, right side: bonded wafer stack after isotropic etch of residual silicon with stop on the buried oxide*

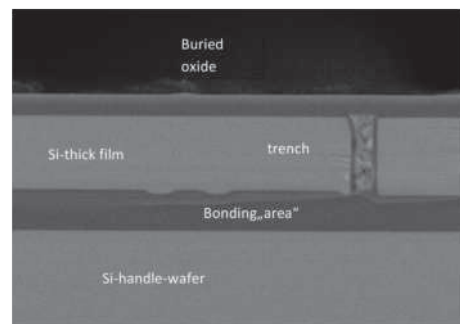


*Figure 3: SEM cross section of a thick film SOI-wafer with trench isolation bonded top down to the Si-handle substrate. The handle wafer of the SOI wafer has been removed by grinding and etching. No bonding interface is visible.*

bonding process the thick Si-film is flipped down on the handle substrate. No interface between the bonding oxides is visible. The subsequent process steps concern the removal of the buried oxide (see figures 1 d-e) and the deposition of a backside-passivation on the silicon film. The backside passivation has to fulfill several tasks. The passivation layer is intended on the one hand to confine the generated photoelectrons in the collection area, on the other hand the layer stack should exhibit a low optical absorption and in addition good anti-reflecting properties (ARC). Therefore the intended passivation layer stack is comprised of an insulating layer, a transparent conducting oxide (TCO) and a highly transparent passivation layer that acts as a protection layer against mechanical influences as well as a barrier against moisture.

Within this project aluminum doped zinc oxide (AZO) is used as the TCO layer and is deposited with the aid of the ALD- (atomic layer deposition) technique. A typical example of the transmission characteristics of the generated layer is shown in figure 4. A result of a transmission measurement of an AZO layer with a thickness of about 70 nm deposited on a glass substrate is represented. The measured transmission amounts to near 90% in the visible spectral range. The electrical conductivity of this layer is in the range of some milliohms and in good agreement with published data. The chemical precursors chosen for the base material is diethyl zinc (DEZ), the dopant is triethylaluminum (TMA). The electrical properties of the film are adjusted by a predefined ratio of DEZ to TMA cycles. For these layers dedicated low temperature processes have to be applied, in order not to disturb the electronic properties of the underlying CMOS-substrate.

The last process sequence (figure 1f) that has to be developed in this project concerns the opening of the bonding pads in order to obtain the access for the wire bonds. A reactive ion etch (RIE) step opens the passivation layer stack, the silicon film and the intermediate oxide layer underneath the first

metallization layer. This etching step “stops” selectively on the aluminum pad. In the course of the project this etch step has to be developed has to be figured out, if this layer stack etching could be performed in the same etching tool or if different tools have to be utilized.

### 3. Summary and Outlook

In the frame of the internal Fraunhofer Project “BackCis” a backside illuminated image sensor based on the thick film T035 SOI technology is developed. Applications such as optical emission spectroscopy or time-of-flight distance sensing are envisaged with this novel sensor. A special aspect of the development conducted in the MST Fab&Lab concerns the development of the layer transfer process by direct bonding and the development of a passivation layer stack. The results achieved so far are promising. In particular a layer transfer process based on oxide to oxide bonding has been demonstrated with a bonding strength sufficient to enable mechanical grinding. The observed void density is also very low. The developed passivation layer rely on atomic layer deposition technology and exhibits good transmission.

### 4. References

- [1] T. Arai et. Al. “A 252-V/lux-s, 16.7-Million-Frames-Per-Second 312-kpixel Back-Side-Illuminated Ultrahigh-Speed Charge-Coupled Device”, IEEE TRANSACTIONS ON ELECTRON DEVICES, VOL. 60, NO. 10, OCTOBER 2013
- [2] R. Fontaine: “The Evolution of Pixel Structures for Consumer-Grade Image Sensors” IEEE TRANSACTIONS ON SEMICONDUCTOR MANUFACTURING, VOL. 26, NO. 1, FEBRUARY 2013
- [3] S. G. Wu, “BSI Technology with Bulk Si Wafer,” 2009 International Image Sensors Workshop (IISW), June 2009
- [4] R.S. Edelstein et al.: „Process Integration aspects of back illuminated CMOS Imagers using Smart Stacking™ technology with best in class direct bonding”, 2011 INTERNATIONAL IMAGE SENSOR WORKSHOP, June 8–11, 2011 Hokkaido, Japan

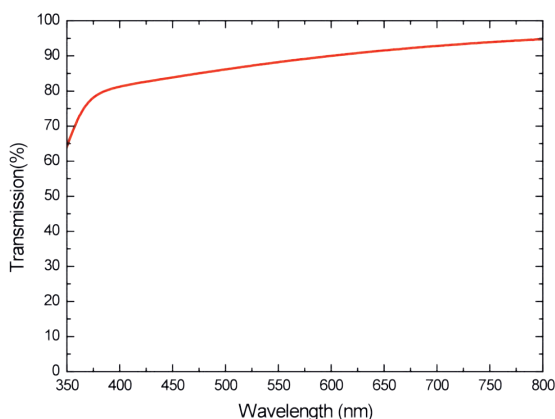


Figure 4: passivation layer development. The transmission curve of the TCO-layer deposited by ALD technology on glass substrate is shown.

# DEVELOPMENT OF A HIGH TEMPERATURE RESISTANT CAPACITOR FOR MICRO SYSTEMS TECHNOLOGY

Y. Celik, D. Dietz, A. Goehlich, A. Jupe, H. Vogt

Fraunhofer-Institut für Mikroelektronische Schaltungen und Systeme, 47057 Duisburg, Deutschland, Yusuf.Celik@ims.fraunhofer.de

## Abstract:

The development of a capacitor for the use at temperatures around 300 °C is presented. To avoid high leakage currents and low breakdown induced by critical steps such as dry and wet etching and layer deposition several concepts are presented. Preliminary etching results show sufficient low lateral scalloping. Further, it is shown that the dielectric layers generated by atomic layer deposition exhibit a good performance with a non-uniformity of 1 %. Preliminary electrical measurements with planar test structures give first insights into the performance of the dielectric layers. Capacitances of a few tens of nF are achieved. The breakdown voltage is about 7 V. A significant increase in of the breakdown voltage by tempering in air is observed.

## Introduction

There is a growing demand for high temperature resistant CMOS and MEMS components in automotive engineering, geothermal applications as well as in power electronics [1]. Sensors and electronics have to perform reliable operation even under extreme conditions at temperatures over 250°C which are easily found near the brakes or the motor of a vehicle. High temperature resistant CMOS- and MEMS components require new technologies using stable contact materials which allow the ICs to work at elevated temperatures. Therefore not only reliable high temperature devices but also a cost-efficient packaging of integrated circuits of high-temperature devices is needed [1].

Within the internal Fraunhofer MAVO project "High Temperature Microsystems: Reliable Packaging for Microelectronics and Microsystems at operation temperatures up to 300 °C" these aims are targeted with the participation of several Fraunhofer Institutes (ENAS, IKTS, IMS, IWM, IZM).

Inside the ICs, buffer capacitors ensure a constant current supply of the chips and short switching times for precisely working integrated circuits. Therefore, a work package within the MAVO is especially dedicated to the development of high temperature passive devices. In this contribution our approaches for the development of a high temperature resistant capacitor are presented.

## Method and process

The targeted process is a 4 mask process, where the substrate acts as one electrode and a metal layer on the etched structures as the other electrode. For this, a highly arsenic doped silicon substrate with a specific resistance lower than 4 milliohm-centimetres is used. To obtain a high capacitance density, geometries exhibiting a high surface-to-volume-ratio, i. e. a high aspect-ratio are preferred such as trenches and holes. Further, high- and medium k dielectric materials are preferred which are deposited either via sputtering, CVD or atomic layer deposition (ALD).

Within this project, aluminium oxide  $\text{Al}_2\text{O}_3$  with a dielectric constant  $\epsilon_r = 8$  or tantalum pentoxide with  $\epsilon_r = 26$  are deposited via ALD into the structured wafer. ALD has attained much interest as very thin layers are generated exhibiting very high conformity and uniformity. Moreover, very dense layers with a low concentration of defects (pinholes) are reported [2]. The counter electrode consists of a heat resistant metal such as ruthenium or titanium nitride deposited as well via ALD. The etched trenches will be filled with silicon dioxide. Subsequently, the contacts to the metal layer are etched. The packaging will be done via a heat resistant solid-liquid interdiffusion (SLID) process [3] which is successfully tested at IMS [4].

To ensure CMOS compatibility only processes with a low temperature budget < 400 °C are performed. Therefore, this process series can be used in the so called post-CMOS procedure.

Generally, the capacitor has to operate in a mode, where energy is stored within the capacitor to ensure a smooth and regular operation well below the break-down voltage  $V_B$  at which the capacitor starts to conduct charge carriers. Naturally, the breakdown voltage decreases with increasing thickness of the dielectric layer. However, the breakdown voltage is more sensitive to the choice of the dielectric medium. Jain et al. [5] estimated the theoretical limit of the electrical breakdown field as a function of the dielectric constant and derived the following empirical relationship:  $E_B^2 \epsilon_r = 400 \text{ (V/cm)}^2$ , where  $E_B$  is the breakdown field and  $\epsilon_r$  is the dielectric constant.

Another challenge is the limitation of the leakage current for  $V < V_B$  as it increases with the operation temperature. Here, it is important to avoid p-n-junctions. Furthermore, the leakage current increases with the band gap of the material, which in turn decreases with increasing dielectric constant [6].

On the other hand, the dielectric constant of the isolation layer should be large to obtain a high capacitance density.

Therefore, a trade-off between a high capacitance density, a low leakage current, and the breakdown voltage, must be found. For the designed layout of the trenches and holes a capacity density of a few hundreds of nF / mm<sup>2</sup> is calculated.

## Results

### Etching of geometrical structures and ALD

The geometrical structures such as trenches and pores are etched via the deep reactive ion etching method introduced by Bosch Company [7]. This so called "Bosch process" consists of a sequence of passivation ( $C_4F_8$ ) and etching ( $SF_6$ ) cycles, which generates vertical etched structures. For the capacitor development it is essential that the comb structure – typically caused in the Bosch process – exhibits a small waviness. Figure 1 shows a typical scanning electron microscope capture of a trench (AR 1:7) etched by the Bosch process at IMS site. The waviness is less than 20 nm. During etching special attention has to be paid to smooth edges as any sharp edge results in

an early voltage breakdown.

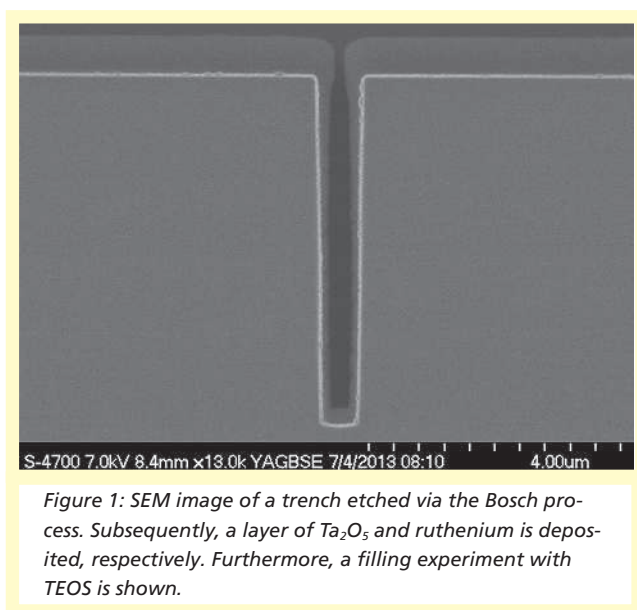


*Figure 1: SEM image of a trench etched via the Bosch process. Subsequently, a layer of Ta<sub>2</sub>O<sub>5</sub> and ruthenium is deposited, respectively. Furthermore, a filling experiment with TEOS is shown.*

The dielectric layer and the counter electrode of the capacitor are deposited via ALD. As shown in figure 1 both layers are deposited with high conformity and uniformity. Excellent uniformity for ALD aluminium oxide layers are attained with a standard deviation of less than 1 % throughout a 200 mm wafer (5 mm edge exclusion).

### Electrical measurements

To gain insight into the electrical performance of the micro structured trenches a single mask experiment with macroscopic plane structures is performed. The dielectric ALD layers (Al<sub>2</sub>O<sub>3</sub>) are deposited onto the n<sup>++</sup> substrate. The counter electrode is a 900 nm thick aluminium layer which subsequently is structured chemically with a high selectivity against the dielectric layer.

Preliminary electrical measurements were performed; the current voltage characteristic is shown in figure 2a.



CMOS DEVICES AND TECHNOLOGY  
DEVELOPMENT OF A HIGH TEMPERATURE RESISTANT CAPACITOR FOR MICRO SYSTEMS TECHNOLOGY

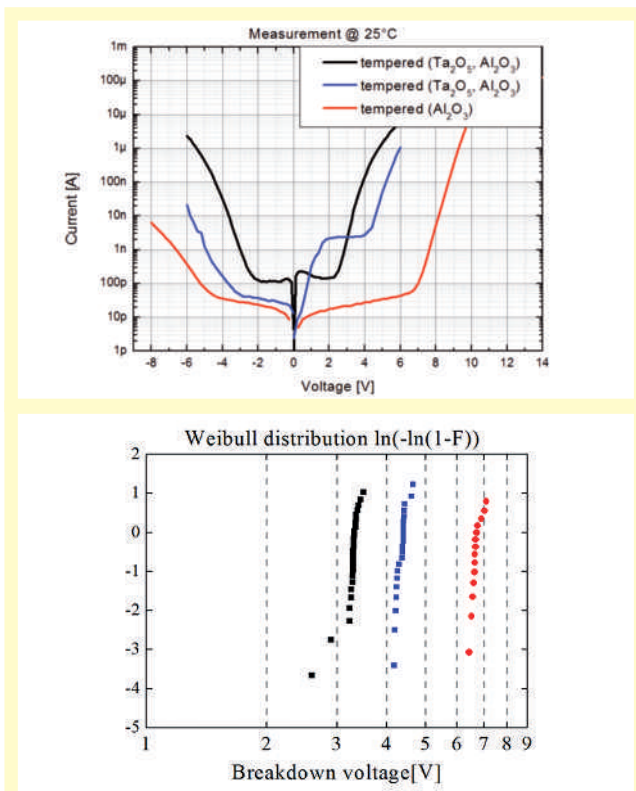


Figure 2: a) Current voltage characteristics on a semi-logarithmic scale of the plane structures measured at 25 °C. Here, every curve represents a measurement of a single capacitor. The voltage ramp always starts from 0 V. The black curve represents measurement with an untempered device whereas the blue curve shows the characteristics measured after an annealing step. b) Change of the breakdown voltage  $V_B$  visualised as a Weibull distribution for an un-tempered (black) and a tempered sample (blue). The red curves represent results obtained in a capacitor with a single aluminium oxide layer.

The black line in figure 2a represents measurements of the capacitors. A symmetric curve w.r.t. the positive and the negative branch is observed. The breakdown voltage  $V_B$  is low. In the literature, it was observed that an annealing step e.g. in ozone results in an increased breakdown voltage [6]. However, such an increase was not observed here. Instead it was found that an annealing step at 250 °C in ambient air improved the

electrical performance of the capacitors. The blue line in figure 2 shows the characteristics of the capacitors after the treatment at elevated temperature. Clearly, a significant shift of the breakdown voltage towards higher voltages is observed. This is also visualised in the Weibull plots – a common method to visualise the failure rate – shown in figure 2b. A possible explanation of the better performance after tempering is the saturation of traps, i.e. the oxygen vacancies in the dielectric layer lattice are filled [6].

Furthermore, the measurements show that for negative voltages the capacitors behave differently. Here, the leakage current decreases significantly after the tempering step. The asymmetry could have his origin in polarization effects originating from the different dielectric behaviour at the interfaces [8].

The leakage current was also measured at elevated temperatures (50 °C, 100 °C, and 250 °C). An exponential increase of the leakage current confirming an Arrhenius like relationship was observed. For negative voltages a leakage current of few tens of pA for is recorded.

The capacitances of the plane structures were measured using bridge circuits. A very reasonable agreement between the measured values and the calculated value for the dielectric layer stack is achieved.

### Summary and outlook

Several preliminary experiments and studies for the development of heat resistant capacitors are presented. The process flow and the targeted parameters were outlined. Crucial steps in the etching, the filling, and the deposition process are currently under investigation. The dielectric layers show promising performance, however optimization towards higher break through voltage is required yet. Moreover, the trench etch process and the filling of the trenches will be optimised. Electrical measurements of plane structures show encouraging trends to fulfil the targeted specifications.

## References

- [1] P. Hagler, P. Henson, R. W. Johnson: Packaging Technology for Electronic Applications in Harsh High-Temperature Environments; IEEE Trans. Industrial Electronics; Vol. 58; 2011 pp. 2673-2682
- [2] R. L. Puurunen: Surface chemistry of atomic layer deposition; J. Appl. Phys. Vol. 97, 2005, pp. 121301-1 – 121301-51
- [3] A. Munding, H. Hübner, A. Kaiser, S. Penka, P. Benkart, E. Kohn: Cu/Sn Solid-Liquid Interdiffusion Bonding in Wafer Level 3-D ICs Process Technology ed. C. S. Tan, R. J. Gutman, L. R. Reif, Integrated Circuits and Systems 2008, pp 131-170
- [4] M. Stühlmeyer, A. Goehlich, H. Vogt: Hybrid sensor integration by wafer to wafer bonding; Fraunhofer IMS, Annual Report 2012, pp- 38-40
- [5] P. Jain, E. J. Rymaszewski: Embedded Thin Film Capacitors-Theoretical Limits, IEEE Trans. Adv. Packaging, Vol. 25, 2002, pp. 454-458
- [6] M. K. Matters-Kammerer, K. B. Jinesh, T. G. S. M. Rijks, F. Roozeboom, J. H. Klootwijk: Characterization and Modeling of Atomic Layer Deposited High-Density Trench Capacitors; IEEE Trans. Semiconductor Manufacturing; Vol. 25; 2012; pp. 247-254
- [7] F. Laermer, A. Schilp, K. Funk, M. Offenberger: Bosch Deep Silicon Etching: Improving Uniformity and Etch Rate for Advanced MEMS Applications; Micro Electro Mechanical Systems, 1999. MEMS '99. Twelfth IEEE International Conference on, 1999, pp. 211-216
- [8] L. K. H. Van Beek: The Maxwell-Wagner-Sillars effect, describing apparent dielectric loss in inhomogeneous media, Physica, Vol. 26, 1960, pp. 66-28

# ENHANCEMENT OF THE ANALOG PERFORMANCE OF PD-SOI MOSFETS USING REVERSE BODY BIASING (RBB) AT HIGH TEMPERATURES UP TO 400 °C

A. Schmidt, H. Kappert

## Abstract

Analog circuits realized in a PD-SOI (Partially-Depleted Silicon-on-Insulator) CMOS technology for wide temperature range operation up to 400 °C are significantly affected by the transistor characteristics at high temperatures. As leakage currents increase with temperature, the analog device performance, e.g. intrinsic gain and bandwidth tend to decrease. Both effects influence the precision of analog circuits and lead to malfunction of the circuitry at high temperatures. Enhancement of the MOSFET device performance and improved design techniques are required to handle these issues. It is demonstrated that RBB (Reverse Body Biasing) is a useful method to improve the analog performance of PD-SOI transistors and also to push the limit of analog circuit design in SOI technology beyond 300 °C. It allows beneficial FD (fully depleted) device characteristics in a 1.0 μm PD-SOI CMOS technology by manipulating the depletion condition of the silicon film. Due to reduced leakage currents, operation in the moderate inversion region of the SOI transistor device up to 400 °C is feasible.

## Introduction

Analog circuit design in an SOI (Silicon-on-Insulator) technology for wide temperature range operation up to 400 °C is significantly affected by transistor device leakage currents. Within the temperature range of the target application, e.g. measurement technologies for use in harsh environments, analog circuits have to meet requirements like sufficient accuracy and operating speed. High leakage currents within these circuits lead to reduced accuracy and also cause malfunctions at high temperatures. In addition, the decrease of intrinsic gain and bandwidth of SOI-MOSFET (Metal-Oxide-Semiconductor-Field-Effect-Transistor) devices at high temperatures has to be considered. Solving these issues will allow analog circuit design for a wide temperature range up to 400 °C. The DC and RF behavior of SOI transistors at high temperatures has been studied intensively [3-7]. Body biasing has been found useful in influencing the threshold voltage and the breakdown characteristics of SOI-MOSFET devices and is also well known for reducing the off-state leakage current in digital circuits [9].

However, in the presented work we demonstrate that reverse body biasing (RBB) is also an elementary design technique facing analog circuit design issues at high temperatures. The influence of RBB on leakage currents of PD-SOI (Partially depleted Silicon-on-Insulator) MOSFET devices in a 1.0 μm PD-SOI CMOS (Complementary Metal-Oxide-Semiconductor)

technology, as well as the impact on the analog performance parameters, e.g. the  $g_m/I_d$  factor and the intrinsic gain are discussed. Body contacted SOI-MOSFET devices with an H-shaped gate (HGATE) are used for this investigation. The following consideration focuses on N-channel devices but has also been demonstrated for P-channel devices as well [11].

## SOI Technology & Devices

Figure 1 shows a photograph of an NHGATE device, fabricated in the Fraunhofer IMS 1.0 μm PD-SOI CMOS technology. The silicon film thickness  $t_{Si}$  is 150 nm with a gate oxide thickness  $t_{OX1}$  of 40 nm. The buried oxide thickness  $t_{OX2}$  is 400 nm. The minimum channel length for analog devices at a supply voltage of 5 V is 1.6 μm. The silicon film (body) of

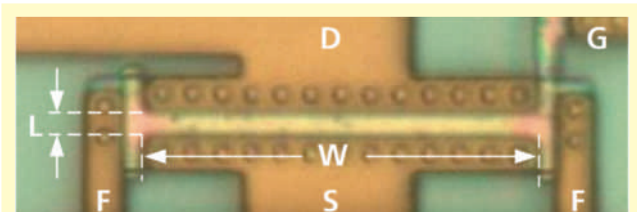


Figure 1: NHGATE SOI-MOSFET manufactured in the Fraunhofer IMS 1.0 μm PD-SOI CMOS technology with device width (W), device length (L), source (S), gate (G), drain (D) and film-contact (F).

the transistors is connected on both sides of the channel via a p+ body-contact for NHGATEs and an n+ body-contact for PHGATEs, respectively.

### Reverse Body-Biasing (RBB)

#### A. Influence on the Depletion State of the Silicon Film

In thin-film SOI technology, two basic depletion states of SOI-MOSFETs may be distinguished: partially depleted (PD) and fully depleted (FD). Figures 2 a) and b) show partially depleted and fully depleted SOI-MOSFET devices, respectively.

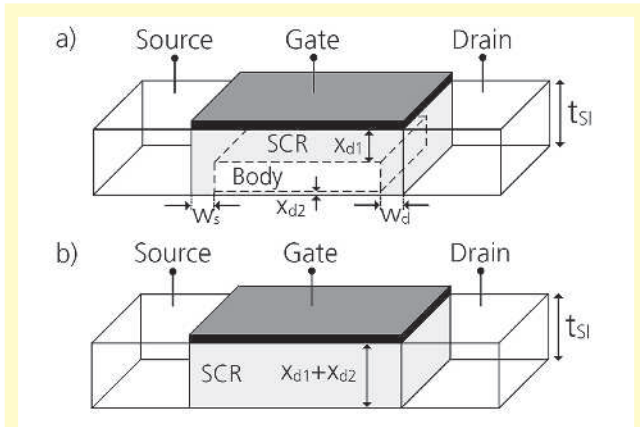


Figure 2: Partially depleted (PD) SOI-MOSFET (a), fully depleted (FD) SOI-MOSFET (b).

The SOI-MOSFET is partially depleted in case the sum of front gate depletion region  $x_{d1}$  and back gate depletion region  $x_{d2}$  is smaller than the silicon film thickness  $t_{Si}$  [2].

$$(x_{d1} + x_{d2}) < t_{Si} \quad (1)$$

In this case, an electrically neutral region, referred to as body, is present in the silicon film [2]. In a partially depleted SOI-MOSFET, depletion also occurs at the drain- and source regions, represented by the depletion region widths  $w_d$  and  $w_s$ .

The SOI-MOSFET is fully depleted in case the sum of front gate depletion region  $x_{d1}$  and back gate depletion region  $x_{d2}$  are

equal to, or greater than the silicon film thickness  $t_{Si}$  [2].

$$(x_{d1} + x_{d2}) \geq t_{Si} \quad (2)$$

In a partially depleted device, the calculation of both depletion depths can be done separately since there is no coupling between the front gate surface potential  $\phi_{s1}$  and the back gate surface potential  $\phi_{s2}$  [2]. Figure 3 shows a cross section of the SOI-MOSFET in the center of the device including front gate and back gate interface.

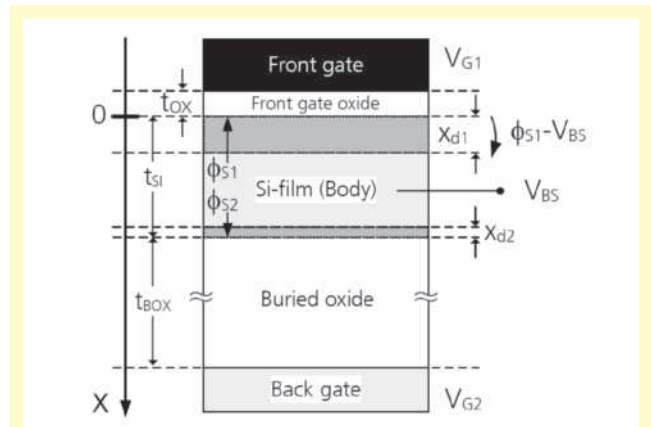


Figure 3: Metal-Oxide-Semiconductor-Oxide-Semiconductor structure of an SOI-MOSFET device including the depletion depths  $x_{d1}$  and  $x_{d2}$  and surface potentials  $\phi_{s1}$  and  $\phi_{s2}$ .

The silicon film (body) is connected to the body-source voltage  $V_{BS}$ . For the following investigation, an N-channel device with a film doping concentration  $N_A$  is considered. The voltage across the depletion region  $x_{d1}$  is then equal to  $\phi_{s1} - V_{BS}$ . The depletion depth  $x_{d1}$  can be written as [10]

$$x_{d1}(\phi_{s1}, V_{BS}) = \sqrt{\frac{2\epsilon_{si}(\phi_{s1} - V_{BS})}{qN_A}} \quad (3)$$

In Equation (3),  $\epsilon_{si}$  is the dielectric constant of silicon and  $q$  is the elementary charge. With increasing reverse bias ( $V_{BS} < 0$ ), the depletion depth  $x_{d1}$  extends to its maximum,

i.e. the film thickness  $t_{Si}$ . With the use of a sufficient reverse bias voltage, fully depleted SOI-MOSFET devices can be achieved in a partially depleted SOI technology.

### B. Influence on Threshold Voltage

The change in depletion region depth  $x_{d1}$  directly affects the threshold voltage of the partially depleted SOI-MOSFET, since the number of ionized charges inside the depletion region is changed. The threshold voltage of a partially depleted N-channel SOI-MOSFET with the influence of  $V_{BS}$  (including the body effect) can be written as [2]

$$V_{thPD} = \phi_{ms1} + 2\phi_F + \frac{\sqrt{2\varepsilon_{si}qN_A(2\phi_F - V_{BS})}}{C'_{ox1}} \quad (4)$$

In Equation (4),  $\phi_F$  is the Fermi potential,  $\phi_{ms1}$  the metal-semiconductor work function difference at the front interface and  $C'_{ox1}$  the front gate oxide capacitances per unit area. The temperature dependence of the threshold voltage of the partially depleted device is then given by [2]

$$\frac{d}{dT}V_{thPD} = \frac{d\phi_{ms1}}{dT} + \frac{d\phi_F}{dT} \left( 1 + \frac{q}{C'_{ox1}} \sqrt{\frac{\varepsilon_{si}N_A}{kT \ln(N_A/n_i)}} \right) \quad (5)$$

The front gate depletion depth  $x_{d1}$  increases with increased reverse bias ( $V_{BS} < 0$ ), which results in a fully depleted silicon film and an increased threshold voltage. In FD state, the depletion charge within the channel is constant and determined by  $t_{Si}$ . The temperature dependence of the threshold voltage is then determined by the metal-semiconductor work function difference  $\phi_{ms1}$  and the Fermi potential  $\phi_F$ . The temperature dependence of the threshold voltage of a fully depleted SOI-MOSFET is therefore given by [2]

$$\frac{d}{dT}V_{thFD} = \frac{d}{dT}(\phi_{ms1} + \phi_F) \quad (6)$$

The threshold voltage was experimentally investigated for NHGATE devices using RBB and is shown in Figure 4. The measurements were taken with a drain-source voltage of  $V_{DS} = 0.1$  V using the tangent method at the point of maximum slope in the linear  $I_d/V_{GS}$  input characteristic curve. The back

gate voltages for NHGATE devices is  $V_{BG5} = 0$  V. For a body bias voltage of  $V_{BS} = 0$  V, the NHGATE device turns PD at approximately 150 °C. At this point, the variation of  $x_{d1}$  with temperature dominates the temperature dependency of the threshold voltage. At 400 °C, the threshold voltage is approximately 150 mV, which results in significant device channel leakage currents in analog circuits. By applying a negative body bias of  $V_{BS} = -1$  V, this transition point is shifted to higher temperatures, whereby a lower temperature dependency in good agreement with Equation (6) was verified by our results. An adequate threshold voltage of 800 mV remains when RBB is applied at 400 °C.

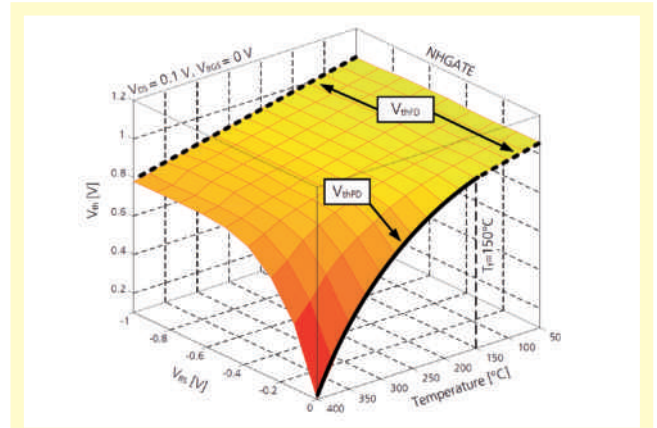


Figure 4: Measured threshold voltage  $V_{th}$  and its dependency on temperature and body bias voltage  $V_{BS}$  of NHGATE SOI-MOSFETs [11].

### C. Influence on SOI-MOSFET Leakage Currents

Three main leakage mechanisms contribute to the overall leakage current in the SOI-MOSFET, namely the PN-junction leakage current  $I_{PN}$ , the subthreshold leakage current  $I_{sub}$  and the sidewall leakage current  $I_{sw}$  [2]. The sidewall leakage current is effectively suppressed by the use of the H-shaped gate. Short channel effects (SCE) are neglected in this consideration, since long channel devices in the range of several microns in channel length are usually preferred for analog circuit design.



The PN-junction leakage current  $I_{PN}$  is related to the reverse bias of the drain- and source PN-junctions. Two components contribute to the PN-junction leakage current, i.e. the diffusion current  $I_{DIFF}$  and the generation current  $I_G$  [2].

In case of a fully depleted SOI-MOSFET, the depletion depth  $x_{d1}$  extends to the maximum silicon film thickness  $t_{Si}$ . The generation current  $I_G$  thereby slightly increases with applied RBB. Since diffusion occurs on the edge of the depletion region in SOI-MOSFET devices, the diffusion current  $I_{DIFF}$  can be neglected in FD state but should be considered in PD state [2]. The PN-junction leakage current was investigated with the use of RBB. The weak inversion input characteristics of an NHGATE SOI-MOSFET are shown in Figures 5 a) and 5 b) without RBB and with applied RBB, respectively [11]. The measurements were also carried out with a drain-source voltage of  $V_{DS} = 0.1$  V.

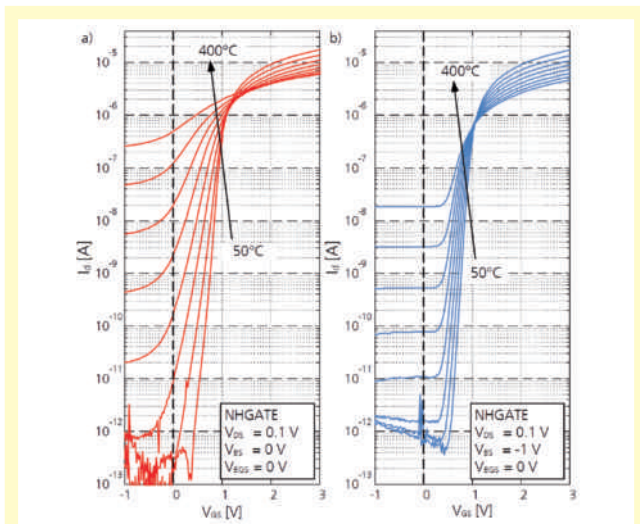


Figure 5: Weak inversion input characteristic curves of an NHGATE SOI-MOSFET without RBB (a) with applied RBB (b) [11].

Focusing on a gate-source voltage of  $V_{GS} = 0$  V at high temperatures in Figure 5 a), one can see that the channel current  $I_d$  is an exponential function of the gate-source voltage  $V_{GS}$ .

At this point, the subthreshold leakage current dominates the overall leakage current of the device. The high subthreshold leakage current is a consequence of the device's channel entering weak inversion ( $\phi_F < \phi_{S1} < 2\phi_F$ ) at high temperatures. Hence, weak inversion of the SOI-MOSFET in this case is primarily initiated by temperature rather than by gate-source voltage. If RBB is applied at  $V_{GS} = 0$  V, the partial derivative  $\partial I_d / \partial V_{GS}$  is significantly reduced, even at high temperatures. RBB effectively reduces the back gate surface potential of the SOI-MOSFET device [11]. The front gate surface potential decreases due to the coupling of the front gate surface potential and the back gate surface potential in a FD SOI-MOSFET device [11]. Thereby the device's channel does not enter weak inversion at high temperatures, eliminating the subthreshold leakage current as it can be recognized from Figure 5 b).

## Improved Analog Device Performance

### A. Transconductance efficiency $g_m/I_d$

The transconductance efficiency  $g_m/I_d$  as a figure of merit is most suitable to determine the analog performance of transistor devices [1]. It is separately defined in weak inversion (WI) and strong inversion (SI) and is given in Equation (8) [3] [1].

$$\left. \frac{g_m}{I_d} \right|_{WI} = \frac{1}{nV_t}, \quad \left. \frac{g_m}{I_d} \right|_{SI} = \sqrt{\frac{2\mu_0 C'_{ox1} W}{nI_d L}} \quad (8)$$

In Equation (8),  $I_d$  is the drain current,  $n$  the body factor,  $V_t$  the thermal voltage and  $\mu_0$  the zero-field charge carrier mobility. The center of the moderate inversion region can be obtained from the  $g_m/I_d$  over  $I_d$  measurements and lies in the range of 100 nA to 300 nA. Since  $n$  is significantly smaller when RBB is applied, the  $g_m/I_d$  factor can be directly influenced by reverse body biasing [11]. Two effects are responsible for an increase of  $g_m/I_d$  at high temperatures compared to the non-biased device. First of all, the maximum value of  $g_m/I_d$  in FD state, as noted in Equation (8), decreases only by the influence of  $V_t$  while  $n$  remains constant with increasing temperature. As a second effect, the leakage current in the device is decreased as mentioned before. A decreased overall leakage current results in a higher  $g_m/I_d$  value. The  $g_m/I_d$  factor was measured

**CMOS DEVICES AND TECHNOLOGY**  
**ENHANCEMENT OF THE ANALOG**  
**PERFORMANCE OF PD-SOI MOSFETS USING**  
**REVERSE BODY BIASING (RBB) AT HIGH**  
**TEMPERATURES UP TO 400 °C**

for NHGATE devices and is presented in Figure 6. In case of no RBB is applied, leakage currents tend to increase intensively with temperature, resulting in a very low  $g_m/I_d$  value especially in the weak inversion region (WI) and moderate inversion region (MI). By applying RBB to the NHGATE device, the normalized operating current can be reduced to 100 nA. Thereby the  $g_m/I_d$  value can be increased significantly at low and high temperatures. Choosing a normalized drain current of 100 nA for the NHGATE, a  $g_m/I_d$  value of  $6.7 \text{ V}^{-1}$  can be reached at  $400^\circ\text{C}$ , which represents an improvement of roughly a factor of 6 compared to the non-biased condition. Summarizing these results the  $g_m/I_d$  factor can be increased significantly, especially in the moderate inversion region when RBB is applied.

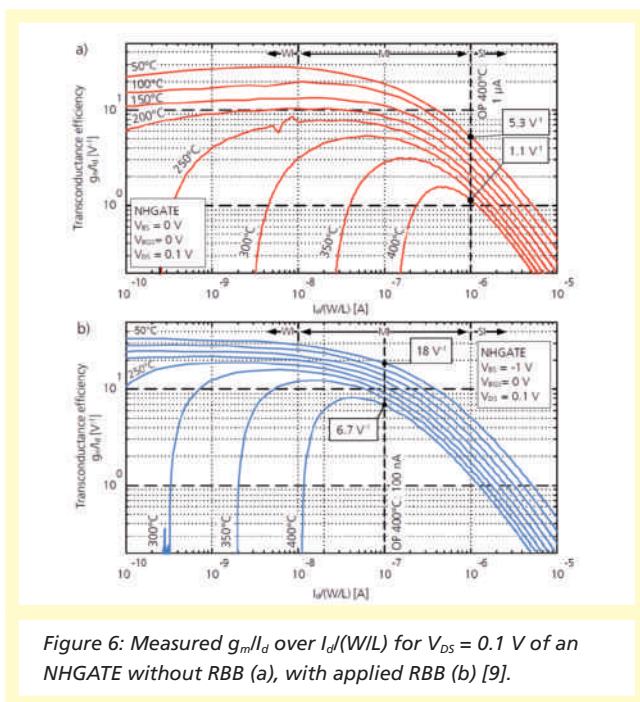


Figure 6: Measured  $g_m/I_d$  over  $I_d/(W/L)$  for  $V_{DS} = 0.1 \text{ V}$  of an NHGATE without RBB (a), with applied RBB (b) [9].

**B. Intrinsic Gain  $A_i$**

Intrinsic gain is one of the most important parameters in analog circuit design, especially for applications where high DC gain is required. The intrinsic gain of NHGATE devices is investigated for  $V_{DS} = 3 \text{ V}$  and is shown in Figures 7 a) and b) for the

NHGATE without RBB and with RBB, respectively. A high drain-source voltage was chosen for these measurements in order to make sure that the subthreshold leakage current is considered and that the device operates in saturation. In order to keep a safety margin to leakage currents, an operating current of  $5 \mu\text{A}$  is chosen. The intrinsic gain at  $400^\circ\text{C}$  is then  $40.2 \text{ dB}$ . By applying RBB, an operating current of  $100 \text{ nA}$  can be chosen. Thereby also the intrinsic gain at low temperatures increases about  $12 \text{ dB}$ . At  $400^\circ\text{C}$ , the intrinsic gain of the NHGATE is improved by  $14 \text{ dB}$ . Considering an application where two gain stages are cascaded, e.g. a two-stage op-amp, an improvement of the overall DC gain of more than  $20 \text{ dB}$  at  $400^\circ\text{C}$  seems feasible. Similar to the results of the  $g_m/I_d$  factor, the intrinsic gain is significantly improved in the moderate inversion region and below, since these regions are more affected by leakage current compared to the strong inversion region.

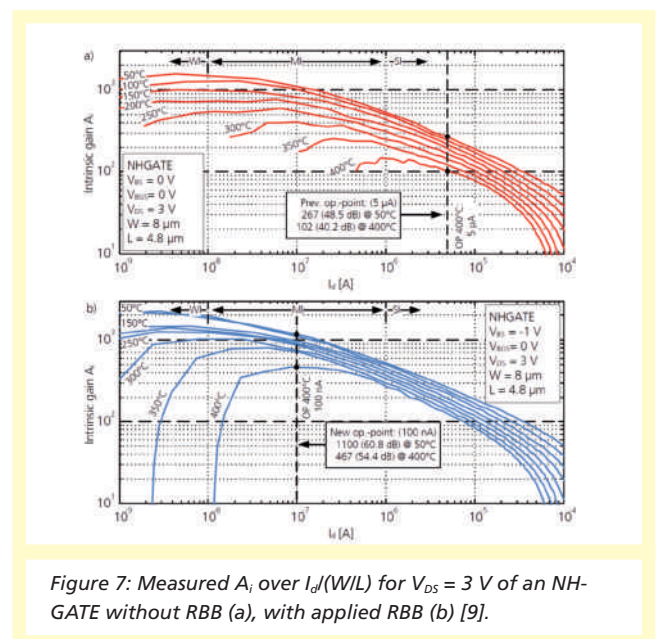


Figure 7: Measured  $A_i$  over  $I_d/(W/L)$  for  $V_{DS} = 3 \text{ V}$  of an NHGATE without RBB (a), with applied RBB (b) [9].

**Conclusions**

The experimental results presented in this work show that RBB is an appropriate circuit design technique, allowing analog

circuit design with significantly reduced leakage currents and improved device performance in a wide temperature range up to 400 °C. By applying RBB to the HGATE device, superior FD device characteristics are available in a PD-SOI technology. It was found that these devices remain fully depleted up to the considered temperature of 400 °C when RBB is applied. The non-linear decrease of the device's threshold voltage at high temperatures can be effectively reduced. The subthreshold leakage current is the dominating portion of the overall leakage current at high temperatures. A fully depleted silicon film results in improved subthreshold slope characteristics and thereby reduced subthreshold leakage currents at high temperatures. As a result, SOI-MOSFET device leakage currents are reduced by more than one order of magnitude. In addition, the  $g_m/I_d$  factor is improved significantly, especially in the moderate inversion region. By applying RBB, SOI-MOSFET devices are able to operate in the mid moderate inversion region, while achieving intrinsic gain values of 54.4 dB at 400 °C, compared to 40.2 dB without RBB. Due to the operation in moderate inversion, the intrinsic gain is increased by more than 14 dB per device. The enhancement of the high temperature device characteristics of PHGATE devices has also been investigated with the use of RBB and is presented in [11]. In addition, RBB was applied to essential analog building blocks, e.g. current mirrors, an analog switch, a two-stage operational amplifier and a bandgap voltage reference in [11]. These results not only prove the enhancement of analog SOI-MOSFET device characteristics using RBB at high temperatures, they also demonstrate the resulting impact on essential analog circuits for high temperature applications.

## References

- [1] D. Binkley. "Tradeoffs and Optimization in Analog CMOS Design". Wiley and John Wiley, Hoboken and N.J and Chichester, 2007.
- [2] J.-P. Colinge. "Silicon-on-insulator technology: Materials to VLSI". Kluwer Academic Publishers, Boston, 3. Edition, 2004.
- [3] J.-P. Eggermont, D. d. Ceuster, D. Flandre, et al. "Design of SOI CMOS operational amplifiers for applications up to 300°C". IEEE Journal of Solid-State Circuits, 31(2), 1996.
- [4] M. Emam, D. Vanhoenacker-Janvier, and J.-P. Raskin. "High Temperature DC and RF Behavior of Partially Depleted SOI versus Deep n-Well Protected Bulk MOSFETs". In IEEE Topical Meeting on: Silicon Monolithic Integrated Circuits in RF Systems (SiRF), 2009.
- [5] M. N. Ericson, M. Hasanuzzaman, et al. "1/f Noise and DC Characterization of Partially Depleted SOI N-and P-MOSFETs from 20°C - 250°C". IEEE Aerospace Conference, 2005.
- [6] K. Grella, S. Dreiner, A. Schmidt, et al. "High temperature characterization up to 450°C of MOSFETs and basic circuits realized in a Silicon-on-Insulator (SOI) CMOS technology". High Temperature Electronics Conference (HiTEC), 2012.
- [7] Guo-Wei Huang, Kun-Ming Chen, Han-Yu Chen, et al. "Impact of body bias on the high frequency performance of partially depleted SOI MOSFETs". Microwave Conference, APMC, 2008.
- [8] C. Neau and K. Roy. "Optimal body bias selection for leakage improvement and process compensation over different technology generations". International Symposium on: Low Power Electronics and Design, ISLPED, 2003.
- [9] A. Schmidt, H. Kappert, R. Kokozinski. "High Temperature Analog Circuit Design in PD-SOI CMOS Technology Using Reverse Body Biasing". 39th IEEE European Solid-State Circuits Conference (ESSCIRC), Bucharest, RO, 2013.
- [10] S. M. Sze and K. K. Ng. "Physics of semiconductor devices". Wiley-Interscience, Hoboken and N.J, 3. Edition, 2007.
- [11] A. Schmidt, H. Kappert, R. Kokozinski. "Enhanced High Temperature Performance of PD-SOI MOSFETs". European Conference on: High Temperature Electronics (HiTEN), 2013.

# FIR CAMERA FOR THERMAL IMAGING

D. Weiler

## Abstract

Fraunhofer IMS has developed an uncooled far infrared (FIR) camera as an evaluation kit for our digital IRFPAs (infrared focal plane arrays) based on a commercial available camera head. A thermal imaging camera is used for different applications like thermography, building inspection, pedestrian detection for automotive night vision systems, firefighting, predictive maintenance, quality control and vision enhancement for security and military applications. The FIR-camera detects the emitted FIR-radiation in a scene and displays it as a thermal image by using a PC. The FIR-camera is a platform for different digital IRFPAs (infrared focal plane array) using microbolometers developed by Fraunhofer IMS as the IR-detector. Apart from the IR-detektor the FIR-camera consist of an IR lens, a shutter, and the camera electronics. An USB2.0 interface transmits the video data to a PC and receives the configuration data for adjusting the FIR camera.

## Introduction

Commercial uncooled thermal imaging cameras typically based on microbolometer. These FIR-cameras display the temperature distribution by detecting the emitted infrared radiation of a scene similar to a visible camera. Warm bodies like humans or animals emit radiation in the far infrared band ( $8\ \mu\text{m} \dots 14\ \mu\text{m}$ ) according to Planck's law as a function of their temperature. Due to this emitted radiation an uncooled IRFPA can detect hot spots passively without any active illumination even at worse optical conditions. A FIR-camera estimates the surface temperature of an object due to its infrared radiation and emissivity. Uncooled FIR-cameras use infrared focal plane arrays (IRFPAs) as the image detector operating at ambient temperature. Typical applications for FIR-cameras besides pedestrian detection for automotive driving-assistance systems are thermal imaging, fire fighting, biological imagery, or military applications like target recognition.

## Digital IRFPA

An uncooled IRFPA based on microbolometers is the main component of a FIR-camera and determines the overall electro-optical performance in combination with an IR-lens. Fraunhofer IMS has fabricated in 2009 the first uncooled infrared focal plane array (IRFPA) throughout Germany. The digital IRFPAs are completely fabricated at Fraunhofer-IMS on 8" CMOS wafers with an additional surface micromachining process [2]. The IR-sensitive element is realized as a microbolometer based on amorphous silicon as the sensing material.

The microbolometer converts the infrared radiation absorbed by a membrane into heat energy and this induces a temperature rise resulting in a change of the electrical resistance. Two SEM images of a microbolometer are shown in Figure 1.



Figure 1: SEM image of a microbolometer (top view and cross section)

The microbolometers are fabricated by post-processing CMOS wafers. The vertical and lateral pixel geometry was kept very simple and straightforward to ensure a solid baseline process with high pixel operability [3].

Microbolometers have to operate in a vacuum-package to reduce thermal losses by gas convection. For reducing packaging costs Fraunhofer-IMS uses a chip-scaled package consisting of an IR-transparent window with an antireflection coating and a soldering frame for maintaining the vacuum [4]. For thermal imaging applications the chip scale package is mounted onto a detector-board as a chip-on-board solution, which is used in a FIR-camera system. The realization of the chip scale package

and the detector-board is depicted in Figure 2.

The IR-transparent lid consists of silicon with a double-sided antireflection coating and is placed using a solder frame on top of the CMOS-substrate which includes the readout electronics and the microbolometers. The use of silicon as a transparent lid results in lower production costs compared to germanium and causes lower mechanical stress due to equal expansion coefficients between the lid and the substrate.

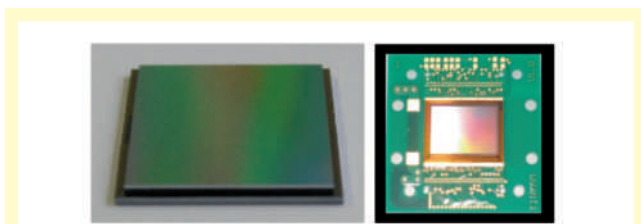


Figure 2: Realization of a chip scale package and a detector board

The microbolometer array is read out by using massively parallel Sigma-Delta-ADCs located under the array which results in a high performance digital readout. Blind microbolometers with a reduced responsivity are located in a ring around the active microbolometer array. The blind microbolometers are read out identically to the active microbolometer. The  $\Sigma\Delta$ -ADCs convert the scene dependent resistor change directly into 16 bit digital signals. These 16 bit image signals are fed into the digital video interface by a multiplexer. A sequencer controls the readout pattern by selecting each  $\Sigma\Delta$ -ADC using a line and row control block.

Fraunhofer IMS has developed several digital IRFPAs with different optical resolution like QVGA or VGA and 25 $\mu$ m and 17 $\mu$ m pixel pitch.

### Realization of the FIR-camera

The realized FIR-camera uses a digital IRFPA developed by Fraunhofer IMS as the IR-detector and consist of an IR lens, an

electro-mechanical shutter, and the camera electronics.

The block diagram of the developed FIR-camera is shown in Figure 3.

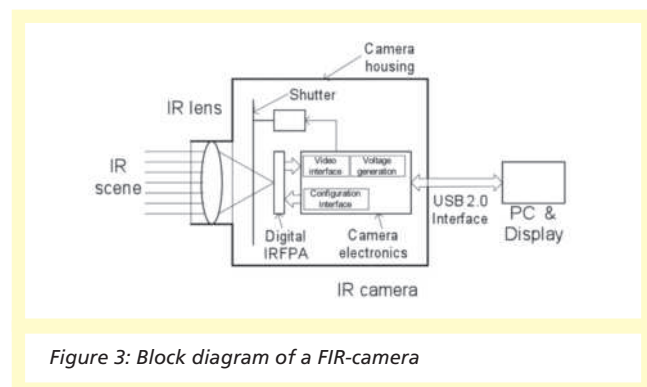


Figure 3: Block diagram of a FIR-camera

The IR-lens focuses the IR-radiation of the scene onto the surface of the digital IRFPA. Typically IR-lenses consisting of germanium with low f-numbers are used in uncooled FIR-cameras. An electro-mechanical shutter is needed for calibration purposes. The shutter is closed periodically approximately every 2–4 minutes to recalibrate the digital IRFPAs by placing a homogeneous tempered plate in front of the IRFPA.

The image data of the digital IRFPA are read out by using a camera electronic. The camera electronic consists of three main components: the video interface, the voltage generation, and the camera interface. An USB2.0 interface transmits the video data to a PC and receives the configuration data for adjusting the FIR camera.

The camera electronics without shutter and IR-lens is depicted in Figure 4.

The camera electronics consists of three PCBs: an adaptor board as the interface for the digital IRFPA, a reference board for generation of the reference and power supply voltages, and a FPGA board for the digital communication from and to the PC. The FIR-camera needs one supply voltage of 12 V and provides the



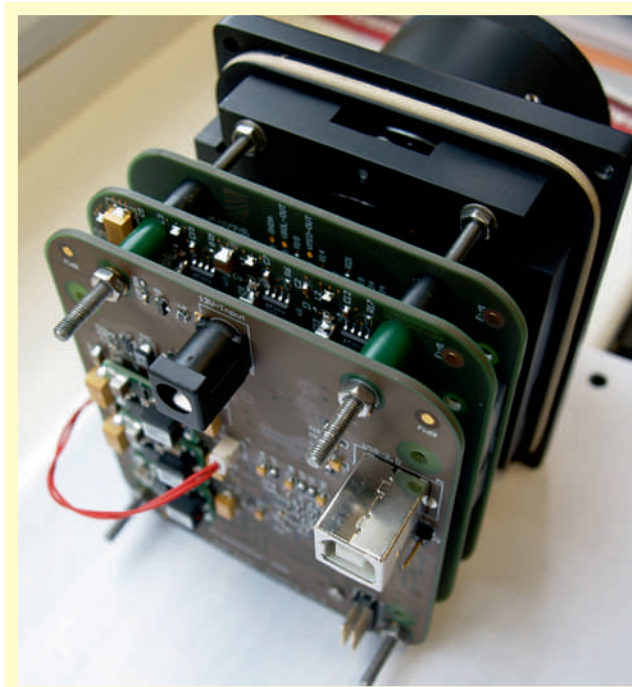


Figure 4: Camera electronics (without shutter and IR-lens)

raw digital video data via a USB2.0-interface to a PC, which displays the thermal image after a simple offset correction.

The complete FIR-camera shows Figure 5.



Figure 5: Realized FIR-camera

### Electro-optical results

An uncompensated IR image of road scene received by the FIR-camera is shown in Figure 6.



Figure 6: Uncompensated IR image of a road scene

Apart from a simple offset correction the shown image is uncompensated, i.e. no gain, defect pixel, or noise correction has been done. High temperatures in the scene are displayed as light gray, low temperatures as dark gray. Pedestrians can be detected easily by using FIR-camera even at worst environmental conditions.

### Conclusion

Fraunhofer IMS has developed an uncooled FIR-camera as an evaluation kit for our digital IRFPAs. A digital IRFPA based on microbolometer is used as the IR-detector. The video data is transmitted to a PC using a USB2.0-interface. The thermal image is displayed on a PC screen after a simple offset correction. A false color mapping to enhance the thermal image is implemented into the software.

## References

- [1] D. Weiler, et al., "A far infrared VGA detector based on uncooled microbolometers for automotive applications", International Forum on Advanced Microsystems for Automotive Applications (AMAA '11) <15, 2011, Berlin>; pp. 327 – 334, 2011
  
- [2] D. Weiler, et al., "Improvements of a digital 25µm pixel-pitch uncooled amorphous silicon TEC-less VGA IRFPA with massively parallel Sigma-Delta- ADC readout", SPIE Conf. on Infrared technology and Applications XXXVII, Orlando, Proc. of SPIE Vol. 8012, 80121F-1 - 80121F-7 , 2011
  
- [3] M. Ruß, J. Bauer, and H. Vogt, "The geometric design of microbolometer elements for uncooled focal plane arrays", Proc. SPIE Conference Infrared Technology and Applications XXXIII, Volume 6542, 2007
  
- [4] J. Bauer, et al., "Fabrication method for chip-scale-vacuum-packages based on a Chip-to-Wafer-Process"; Conference on Electro-Optical and Infrared Systems: Technology and Applications VII; Toulouse; Proc. of SPIE Vol. 7834, 78340S-1 – 78340S-8, 2010

# OPTICAL SENSOR FOR TIME-RESOLVED MEASUREMENTS

E. Poklonskaya, O. Schrey

## 1. Introduction

Many industrial applications require linear photosensors which exhibit high sensitivity and low noise. The optical emission spectroscopy (spark or laser induced spectrometry) is one of those. Such a spectroscopic method delivers the information about the qualitative and quantitative composition of an analyte.

From 1960 the photomultiplier tubes (PMT) were used as standard detectors in the field of spark spectrometry due to their extremely high sensitivity in the ultra-violet (UV) region and the possibility for time-resolved measurements (TRM). Since a PMT can detect only one signal at a distinct position in the spatially distributed spectrum, lots of PMT's are needed to equip a universal spectrometer. Therefore, these devices could not fully satisfy the market demands. On the other hand, widely used charge coupled device (CCD) line sensors are able to detect the emitted visible spectrum from 400nm-1000nm simultaneously, but usually require multiple integrations to pick up the information from the emission lines of interest. A CMOS approach can be a good alternative to PMT's and CCD's, as it potentially offers both time-resolved measurement capability (TRM) and spatial resolution. A lateral drift-field photodetector (LDPD) based CMOS line sensor offers the possibility of time gating accompanied by non-destructive readout and charge accumulation over several cycles, which enhances the signal-to-noise ratio (SNR) [1].

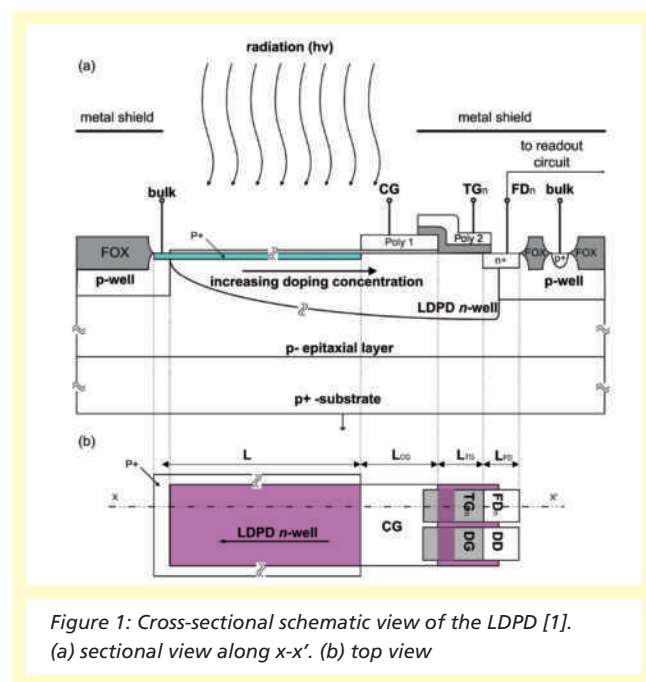
## 2. LDPD Line Sensor

### 2.1. Pixel structure

The light sensitive area of the developed pixel consists of an n-well incorporating a non-uniform lateral doping profile (Fig.1). It remains fully depleted during the operation, if sandwiched between the substrate and a grounded pinning layer, localized on the surface of this n-well. The built-in concentration gradient within the n-well in the direction of the readout node and the unpinned region of the detector generates an electrostatic potential gradient i.e., a lateral drift-field [2], which enables not

only a better charge collection within the considerably extended photoactive area (200  $\mu\text{m}$ ), but also a higher speed of the charge transfer from this photoactive area to the readout node.

A collection-gate (CG), two transfer-gates (TG and DG), a floating diffusion (FD) and an  $n^+$  diffusion directly connected to a higher potential and thus called draining diffusion (DD) (Fig.1) all form part of the unpinned area of the deployed LDPD.



Correctly biasing the TG, a potential barrier can be created within the well to prevent the charge carriers from being transferred to the FD during the charge readout cycle. On the other hand, during the charge collection cycle, the properly biased TG enhances the lateral drift-field mechanism and supports charge carrier transfer into the FD.

The DG serves to prevent the electrons being drained out to the high potential ( $V_{dd}$ ) during the collection cycle of the desired photogenerated charges, and serves to drain the non-desired charge out of the pixel when necessary, providing the system with the time-controlled charge collection ability [1].

## 2.2. UV Sensitivity

Due to the special UV-enhanced silicon-nitride based passivation layer, the LDPD structure provides good quantum efficiency in the blue and UV parts of the spectrum down to 220 nm. A comparison of the quantum efficiency curves of the LDPD pixels using a standard passivation present in the CMOS process, and the UV-enhanced passivation, can be observed in Fig. 2.

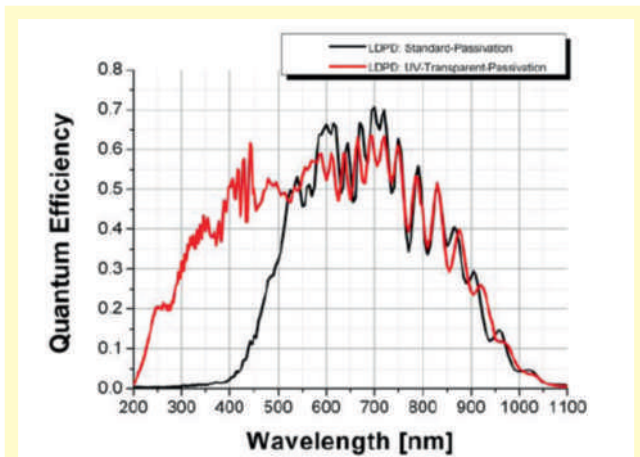


Figure 2: Wavelength dependent quantum efficiency curves obtained from LDPD line sensors using two different types of passivation layers [1]

## 3. Results

A test array with several different 5-pixel test clusters was fabricated using the 0.35  $\mu\text{m}$  LV/HV CMOS process with an LDPD and a specially designed UV-enhanced silicon-nitride passivation. Consistent with Fig.1, here  $L = 200 \mu\text{m}$  is the length of the pixel photoactive area. The distance between the n-wells of the neighboring pixels is  $5.5 \mu\text{m}$  for a  $10 \mu\text{m}$  pixel pitch [3]. The developed LDPDs were characterized by means of the photon-transfer method (PTM) and based on the EMVA 1288 standard. The LDPD yielded  $43 \text{ pA/cm}^2$  of dark current at room temperature (normalized to the entire pixel area),  $59.000 \text{ e}^-$  of saturation capacity, a spectral responsivity of  $530 \text{ V}/\mu\text{J/cm}^2$  for  $\lambda=525 \text{ nm}$  of impinging radiation, and a sensitivity of  $17.3 \mu\text{V/e}^-$ . All additional parameters specified and measured are presented in Table 1.

The transfer time is a major concern during the development of a CMOS line sensor due to the extra long photoactive area, which introduces difficulties in the collection and transport of the charge carriers. The increase of the electrostatic potential gradient generated from the correctly biased CG and TG make the transfer of the charge carriers fast and efficient. For the developed LDPD pixel, a transfer time of  $6 \mu\text{s}$  under an illumination of  $905 \text{ nm}$  wavelength and an irradiance level of  $714 \text{ W/m}^2$  was obtained.

Specification parameter	Units	Result
Responsivity (R)	$[\text{V}/\mu\text{J/cm}^2]$	530
Saturation Capacity (SC)	$[\text{ke}^-]$	59
Sensitivity (S)	$[\mu\text{V/e}^-]$	17
Signal-to-Noise Ratio (SNR)	$[\text{dB}]$	46
Dynamic Range (DR)	$[\text{dB}]$	52
Transfer Time	$[\mu\text{s}]$	6
Dark Current	$[\text{pA/cm}^2]$	43
$T = 25 - 26^\circ\text{C}$ $t_{\text{INT}} = 0 - 20 \text{ s}$	$[\text{e}^-/\text{s}]$	5380

Table 1: Electro-optical parameters of the developed LDPD pixel with a length of the photoactive area of  $200 \mu\text{m}$  verified by means of PTM. The integration time is  $t_{\text{INT}} = 60 \mu\text{s}$  while the sensor was illuminated with monochromatic radiation at  $\lambda = 525 \text{ nm}$  and varied from 0 to  $80000 \text{ nW/cm}^2$  illumination intensity.

## 4. Summary and Outlook

Within the framework of this project, an LDPD line sensor has been developed suitable for time-resolved measurements. The designed detector is sensitive in the UV part of the spectrum and exhibits a very high sensitivity as required for the application. High dynamic range (DR), achieved among other parameters, also through the accumulation of the signal charge over several measurement cycles without the need of resetting the sense node (and without introducing kTC noise after each cycle) and low dark current makes the proposed LDPD an ideal candidate for optical emission spectroscopy applications. A CMOS line sensor consisting of 368 pixels, each with a

length of 200  $\mu\text{m}$ , has been fabricated and characterized. The performance analysis of the developed LDPD-based CMOS line sensor will be presented for the first time at SPIE Photonics Europe 2014 and later published online in the conference proceedings

A CMOS line sensor consisting of 368 pixels, each with the length of 200  $\mu\text{m}$ , is currently fabricated. It is scheduled to be characterized by the end of 2013.

#### 5. References

- [1] D. Durini, W. Brockherde and B. Hosticka, Detector for detecting electromagnetic radiation with transfer gate and draining gate," U.S. Patent 0 134 299 A1, May. 30, 2013.
  
- [2] D. Durini, "Lateral drift-field photodiode for low noise, high-speed, large photoactive-area CMOS imaging applications," Nuclear Instruments and Methods in Physics Research A, vol. 624, pp.470-475, 2010.
  
- [3] E. Poklonskaya. (2013, May). Line sensor for fast, time-resolved spectroscopy measurements. Presented at AMA Conference 2013.[Online].Available:<http://www.ama-science.org/ama-conferences-2013/>

# MEASUREMENT SYSTEMS FOR OPTICAL PROPERTIES OF SEMICONDUCTOR DEVICES

A. Driewer, A. Schmidt, C. Busch

Since Moore's Law was formulated in the middle of the sixties, i.e. the hypothesis that the complexity of integrated circuits will double every 18 months, it was pretty much fulfilled by the development of the silicon technology. This could be realized by the steady shrinking of transistors during the last decades. This progress is now approaching both physical and economical limits and therefore another trend, known as „More than Moore“, is emerging and gets more and more attention within the silicon semiconductor industry. This trend no longer pursues the sole downscaling of devices, but to broaden the versatility of applications that can be addressed with silicon technology. Tailored processes allow the integration of custom devices – e.g. transistors for high temperature [1], high speed or high power applications, microelectromechanical systems (MEMS) or optoelectronic sensors.

Charge Coupled Devices (CCDs), first introduced in 1969, initiated the wide use of solid state sensors and they advanced well with the development of the silicon technology. These days CMOS image sensor (CIS) [2] [3] technology dominates this field. Applications in industry, aerospace, science, automotive and consumer are the driving forces for its advancement while mainly the latter ones are dominant considering the propagation of smart phones and portable computers. Applications span the whole range from the UV and visible to the infrared regime of the electromagnetic spectrum.

One crucial challenge during the development is the characterization of sensors while operating in these spectral regions. The following sections will give an overview of the possibilities of Fraunhofer IMS which are available for development purposes as well as for customer services. Two similar setups determine the spectral sensitivity of image sensors and single test structures by the use of monochromatically split white light sources. A third setup is equipped with an LED illuminator which allows a variation of the irradiance thus offering the option of measurements based on the photon transfer method.

## Spectral Sensitivity

Basically, the available characterization setups used to determine the spectral dependence of the quantum efficiency of a device under test (DUT) can be divided into three components.

The optical part consists of a light shield which screens the light sensitive components from disruptive stray light, a light source, a monochromator, an integrating sphere and an optical bench to guide the light beam on the DUT. The two setups for UV and VISNIR (visible & near-infrared) deviate in the used light source and hence the attainable wavelength range. Their combination gives the opportunity to characterize optoelectronic devices in the spectral range from 200 to 1100 nm. The optical path of the two setups is shown in Figure 1.

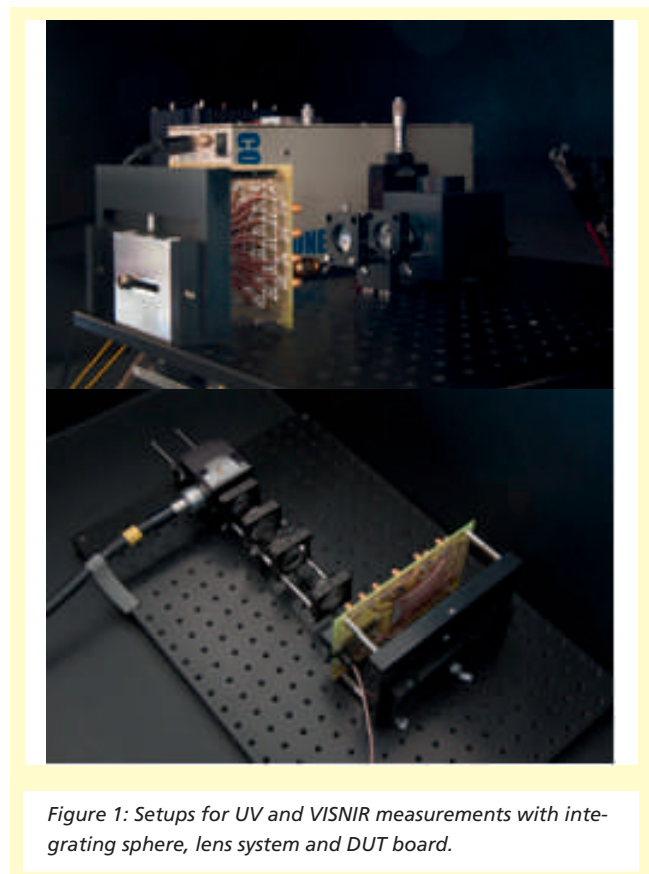


Figure 1: Setups for UV and VISNIR measurements with integrating sphere, lens system and DUT board.



The electrical part in each setup consists of a pre-amplifier and an instrument measuring the signal of the sensor as a response to the optical stimulation. A custom made PCB-board is used to mount the DUT and is capable of different package standards.

The third component is a custom-made software which controls the communication between the aforementioned elements via GPIB. Parameter settings, i.e. the amplification, resolution and spectral range, are software controlled as well and may be individually tailored to the demands of the DUT.

To ensure the system to be calibrated at every time a calibrated reference detector is used to detect any possible changes of the setup and consider them in a corrective manner.

Figure 2 shows the spectral quantum efficiency of two exemplary photodiodes characterized with the setups as described.

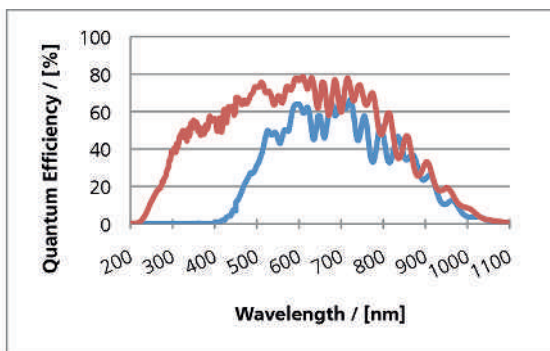


Figure 2: Spectral distribution of the quantum efficiency of UV and visible light sensitive photo diode, respectively.

### Photon Transfer Method

As mentioned in the introduction a third setup is used to perform irradiation dependent measurements. Instead of an arc lamp in combination with a monochromator the monochromatic radiation is generated by an LED illuminator which is shown in Figure 3. The illuminator covers the visible and

infrared spectrum by using four different LEDs: 470 nm (blue), 525 nm (green), 625 nm (red) and 850 nm (infrared). As a second light source a pulsed infrared laser with a wavelength of 905 nm is installed. Its 30 ns pulses are indispensable for measurements of charge transfer times within pixels and the characterization of Time-of-Flight sensors.

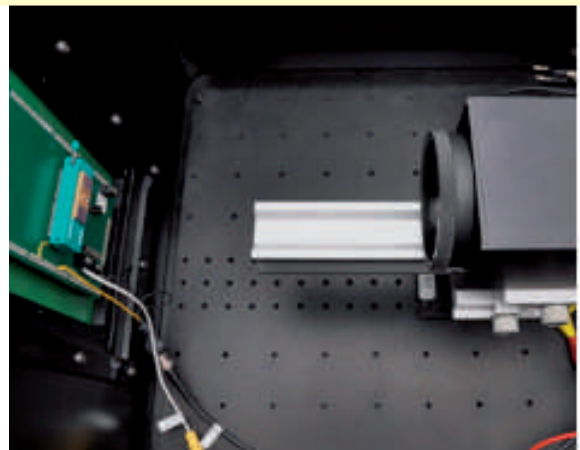


Figure 3: Illuminator on optical bench.

For the characterization of image sensors the system is equipped with 12 bit analogue-to-digital converters in combination with frame grabbers. The chips are controlled by a state machine which applies digital control signals and a wide range of available reference voltages and currents, respectively.

Within the software an automatic test sequence can be predefined. This includes in-situ data analysis with customizable software algorithms. The flexible interface including the control, the mounting and the read-out of the imager allow a diverse variety of measurements.

In order to provide standardized measuring methods and definitions for the most significant parameters of image sensors, Fraunhofer IMS performs the characterization according to the EMVA standard 1288 of the European Machine Vision Association [4].

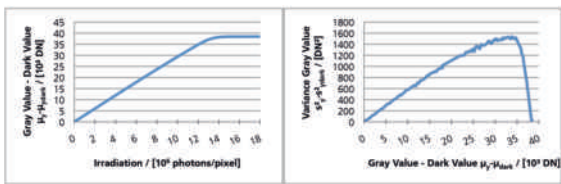


Figure 4: Example measurement according to the photon transfer method.

Figure 4 depicts two curves that were produced during measurements according to the photon transfer method. The left graph shows the mean photo-induced gray value versus the irradiation. On the right-hand side the mean photo-induced gray value and its variance is shown. From such type of measurements important parameters like the full well capacity, noise behavior, dynamic range and gain for optical sensors and imagers can be determined.

### Conclusion & Outlook

The available setups allow the characterization of the important parameters of optical sensors, i.e. the responsivity and quantum efficiency. In the near future this capability will be further extended. In addition to temperature dependent measurements, it will be possible to quantify the dynamic response to an optical stimulation, to vary the applied light intensity in the UV and to perform all the tasks in an early stage of development on wafer level.

By using the described measurement solutions the development of sensors for a wide range of applications can be driven by Fraunhofer IMS and its customers. This will support CMOS image sensor technology for further forward-looking applications.

- [1] K. Grella, S. Dreiner, A. Schmidt, W. Heiermann, H. Kappert, H. Vogt und U. Paschen, „High temperature characterization up to 450°C of MOSFETs and basic circuits realized in a Silicon-on-Insulator (SOI) CMOS-technology,“ *Journal of microelectronics and electronic packaging* 10 (2013), Nr.2, S.67-72,.
- [2] A. Spickermann, W. Brockherde und J. Noell, „Neuartige CMOS-Photodetektoren für die schnelle Flugzeit-Sensorik,“ *Photonik*, Bd. 44, Nr. 3, pp. 42-45, 2012.
- [3] E. Poklonskaya, D. Durini, M. Jung, O. Schrey und W. Brockherde, „Line Sensor for Fast, Time-Resolved Spectroscopy Measurements,“ in *AMA Conferences*, 2013.
- [4] „EMVA Standard 1288,“ *European Machine Vision Association*, [Online]. Available: [http://www.emva.org/cms/upload/Standards/Stadard\\_1288/EMVA1288-3.0.pdf](http://www.emva.org/cms/upload/Standards/Stadard_1288/EMVA1288-3.0.pdf).

# IMPLANTABLE SENSOR TO MEASURE LIQUOR PRESSURE OF A VENTRICULAR DRAINAGE SYSTEM

M. Görtz, G. vom Bögel, P. Füst

## Background

The human brain is filled with cerebrospinal fluid (CSF), which is produced in the ventricles. Normally the production and resorption of CSF are balanced. Patients suffering from normal pressure hydrocephalus (NPH) [Adams 1965] produce more CSF as they resorb. This leads to an increase of the intracranial pressure (ICP) in the skull, what may cause progressive enlargement of the head, convulsion, tunnel vision and mental disability due to shortage of oxygen and nutrients.

Recent population-based studies have estimated the prevalence of NPH to be about 0.5% in those over 65 years old, with an incidence of about 5.5 patients per 100,000 population per year [Brean 2008][Tanaka 2009].

To reduce the intracranial pressure the implantation of a drainage system (shunt) which removes excessive CSF e. g. into the abdominal cavity is necessary.

## Development

In corporation with the companies Aesculap AG and Christoph Miethke GmbH & Co KG a system was developed for wireless measurements of the cerebrospinal fluid pressure in the shunt. The system is approved for use as a long-term implant in humans.

This article describes a sensor transponder system to measure liquor pressure in a ventricular drainage system which is connected to the human brain. It focuses on the development of an application specific integrated circuit (ASIC) with a micro machined pressure sensor as well as the principle of a wireless readout system using a handheld reader device.

## Mobile Reader Device

If sensors do not require continuous activity it is a good choice to use a transponder based approach [Hennig 2010]. This ensures that batteries do not need to be changed for long term implants.



Figure 1: Illustration of the implantable shunt sensor in the drainage system.

Low frequency transponder systems are the method of choice for medical implants, especially if the transponder is encapsulated in metal. The system consists of a passive transponder equipped with sensors, and a reader device which powers the transponder by an electromagnetic field and transmits back information from the transponder. The metal of the shunt sensor housing has a significant influence on the wireless transmission. An analysis of the influence of metal on the reader circuit impedance and the energy transfer is given in [Jacobi 2012].

In passive transponder systems, load-modulation is used to transmit data from the transponder to a reader. Thereby, the impedance of the transponder is changed and modulates a carrier wave which is generated by the reader. The transponder is supplied with energy by this carrier. Using a metal encapsulation modifies the communication in both directions – in the downlink, for the energy transfer from reader to transponder and in the uplink, for data transmission from transponder to reader. To overcome the damping caused by the metal encapsulation, the handheld reader was designed with a high quality factor of the transmitter coil, to optimize

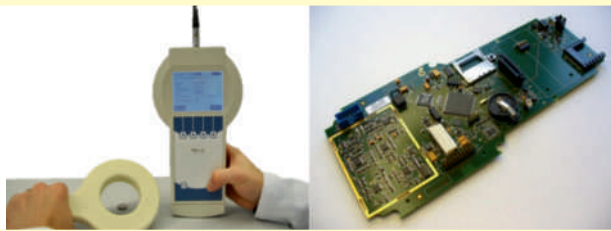


Figure 2: Mobile reader device with antenna handle (left); Main-PCB of the mobile reader (right)

the performance regarding reading distance and lifetime of the reader battery. For the power amplifier a free-running principle was chosen to compensate detuning effects of the metal.

To handle the detuning effects in the uplink, a customized receiver was implemented in analogue hardware together with digital programmable control. Core components of the receiver are a carrier suppression scheme as well as a special equalizer and a chain of low-noise amplifiers to recover the data signal.

The reader device is a medically approved component of the system including certification for medical device software and software life cycle processes.

### The Shunt Sensor ASIC

The ASIC receives energy from the electromagnetic field ( $f_c = 133 \text{ kHz}$ ) emitted by the mobile reader device. Due to the coupling between the antenna of the reader and the ASIC, a voltage is induced and the ASIC is activated. After a power-on criterion is fulfilled the sensor automatically measures and transmits the pressure, the temperature and voltage of the power supply of the Implant.

As shown in Figure 4 the shunt sensor ASIC consists of six main building blocks: HF-front-end, digital part, EEPROM, biasing & voltage regulation, pressure sensor and sensor readout with A/D-Converter.

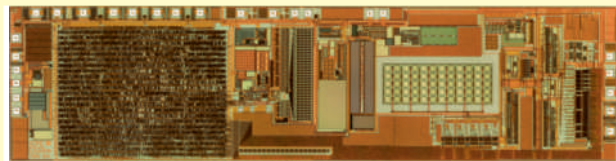


Figure 3: Shunt sensor ASIC (9.4 mm \* 2.5 mm)

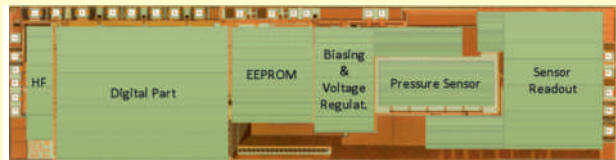


Figure 4: Shunt sensor ASIC with highlighted components

The following subsections give a more detailed overview and description of the building blocks.

### HF

The main functions of the HF-frontend are:

- Half-wave rectification of the RF signal at the antenna of the ASIC
- Extraction of a clock signal from the incoming RF signal and detection of clock failure
- Generation of a power-on signal for the digital part and the sensor readout
- High voltage protection of the shunt sensor using a limiter circuit
- Modulation of the RF carrier for data transmission

### Digital Part

The digital part of the shunt ASIC consists of several control modules, which are responsible for the interaction of the individual blocks of the ASIC.

- A state machine is the central control of the ASIC. Starting with the initial "power on" signal, it generates sequences of control signals for all other modules to implement the measurement and transmission protocols.
- The serial processor module stores the serial ADC output for transmission, computes the CRC during transmission and

## SILICON SENSORS AND MICROSYSTEMS

### IMPLANTABLE SENSOR TO MEASURE LIQUOR PRESSURE OF A VENTRICULAR DRAINAGE SYSTEM

stores and performs the error correction for the option bits.

- The clock digital module provides the clock signals for all modules. The main clocks are derived from  $f_c = 133 \text{ kHz}$ . All clocks are synchronous and constructed using two non-overlapping phase clocking feedback circuits.
- The test control module is a JTAG test access port that implements the IEEE 1149.1 protocol.
- The ADC control module provides the necessary clock and control signals for the ADC. It incorporates the clock generating circuit for the ADC clocks.
- The modulation control block converts the serial data input into a Manchester code or NRZ signal.

#### Pressure Sensor

The shunt ASIC consists of surface micro-machined capacitive sensor elements which are arranged in an array. The diameter of one element is approx.  $100\mu\text{m}$  and the capacitive change between minimal and maximal pressure is approximately 50fF.

#### EEPROM

The EEPROM control unit generates the necessary control signals for reading and writing EEPROM cells comprising

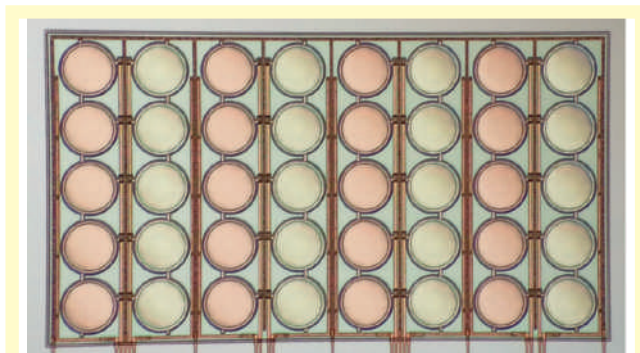


Figure 5: Array of capacitive pressure sensor elements

256 x 1 bit. The EEPROM control unit provides 32 data and error control bits for implant configuration, and 224 bits for calibration, manufacturer and ID data and their respective error control bits.

#### Biasing & Voltage Regulation

In this block all bias currents and regulated voltages for the sensor readout and are generated.

#### Sensor Readout

The main components of the sensor readout are:

- The differential  $C/V$  converter transforms the capacitance of the pressure sensor into a voltage signal. This conversation is adjustable in offset and gain to compensate fabrication related tolerances of the pressure sensor parameters. The  $C/V$  converter is realized in a switched capacitor technique.
- The RSD cyclic  $A/D$  converter transforms the analogue output of the  $C/V$  converter into a digital signal. Its output is a serial 13 x 2 bit data stream. The cyclic conversion algorithm is based on the conventional restoring numerical division principle. It comprises the multiplication by two of the signal to be converted followed by a comparison of the result with a reference voltage. At each bit decision, two comparison levels P and Q are used instead of one (with P positive and Q negative): If the signal is larger than P, the output code bit is set to 1 and the reference is subtracted; if the signal is smaller than Q, the bit is set to -1 and the reference is added; else, the bit is set to 0 and no arithmetical operation is carried out. The RSD cyclic conversion has several advantages: it does not require accurate comparators and is more insensitive against loop offset and gain errors.
- A multiplexer connects the  $A/D$  converter either to the output of the  $C/V$  converter, the temperature sensor or the supply voltage sensor.

#### Calibration of the Shunt Sensor

The calibration of the nonlinear and temperature dependent output of the shunt sensor is performed in a temperature controlled pressure chamber. Figure 6 shows a typical pressure characteristic of a complete in metal encapsulated sensor. The typical calibration error is better than 0.8 mm Hg as depicted in Figure 7.

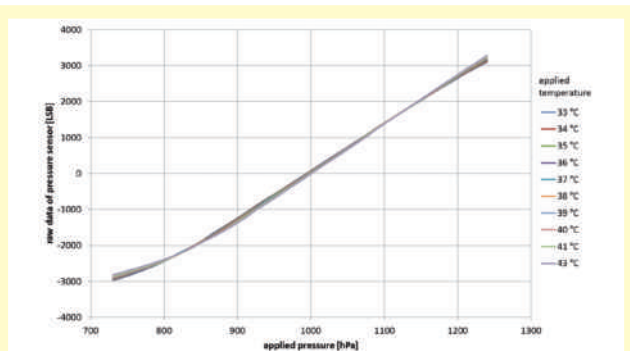


Figure 6: Pressure measurement example of a complete in metal encapsulated shunt sensor.

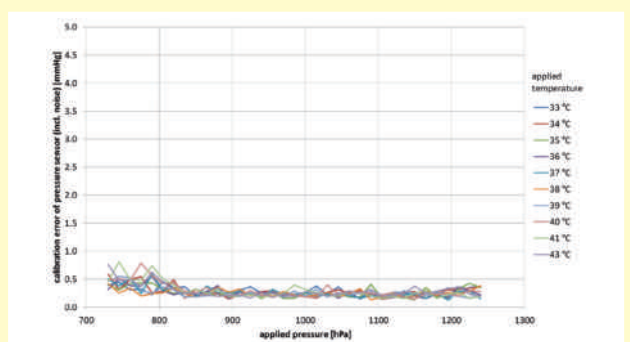


Figure 7: Typical calibration error including 1 sigma noise example of a complete in metal encapsulated shunt sensor.

[Adams 1965] Adams, R. D.; Fisher, C. M.; Hakim, S.; Ojemann, R. G.; Sweet, W. H. (15 July 1965). "Symptomatic Occult Hydrocephalus with Normal Cerebrospinal-Fluid Pressure". *New England Journal of Medicine* 273 (3): 117–126.

[Brean 2008] Brean, A.; Eide, P. K. (1 July 2008). "Prevalence of probable idiopathic normal pressure hydrocephalus in a Norwegian population". *Acta Neurologica Scandinavica* 118 (1): 48–53.

[Tanaka 2009] Tanaka, Naofumi; Yamaguchi, Satoshi; Ishikawa, Hiroyasu; Ishii, Hiroshi; Meguro, Kenichi (1 January 2009). "Prevalence of Possible Idiopathic Normal-Pressure Hydrocephalus in Japan: The Osaki-Tajiri Project". *Neuroepidemiology* 32 (3): 171–175.

## References

- [Hennig 2010] Andreas Hennig, Gerd vom Bögel: A Data Transmission Technique for Passive Sensor-Transponders in Medicine, Proceedings of IEEE RFID Conference 2010, Orlando, 2010
- [Jacobi 2012] Rebekka C. Jacobi, Gerd vom Bögel, Anton Grabmaier, Low Frequency Reader Design Approach for Metallic Environments, Conference Proceedings of SmartSystem 2012, München



# CUSTOMIZED DEVELOPMENT OF A CMOS COMPATIBLE SOLAR CELL FOR AUTONOMOUS SENSOR NODES

*M. Stühlmeier, A. Goehlich, H. Vogt*

The demand for autonomous low power applications such as sensors network and wireless devices has increased over last decades. Novel applications such as the “internet of things” [1] and “smart dust” [2] networks will drive these markets. All these applications require a continuous power source for operation. Nowadays typically a battery is used for this purpose. However, these batteries have a limited lifespan and produce a considerable amount of toxic waste. The main idea of energy harvesting is to replace these batteries with an ambient background energy source. Typical power sources are piezoelectric (vibration), thermoelectric (heat) or photovoltaic (solar) energy converter. The great advantage of solar cells is the fact that light is almost always available over long periods of time with a certain amount of power. In collaboration with SolChip Ltd. Fraunhofer IMS has developed a process to manufacture a thin film solar cell directly on top of an Applications Specific Integrated Circuit (ASIC) minimizing wiring and chip area.

## **Light as energy source**

Sensor networks made up of a multitude of individual intelligent sensor nodes, that are able to communicate wirelessly have the capability to measure local parameters (such as environmental data e.g. temperature, humidity and pressure) over large areas, and then are able to pass these data to a central data evaluation station. This makes sensor networks suitable for a wide range of applications, e.g. for fire prevention or environmental monitoring of large areas of farmland. The realization of the energy source for the individual sensor nodes remains a sticking point in these kinds of applications. Wiring the sensors together is hardly a viable option nowadays due to the cumbersome and costly installation. Moreover many applications require the sensor network to blend unobtrusively into the surroundings and not to have any impact on the aesthetics. Therefore also the miniaturization of the sensor nodes is desirable. Using batteries to power the sensor network does eliminate the need for inconvenient cables, but the amount of maintenance involved in replacing the batteries regularly as required should not be underestimated, in particular in large networks.

The technology developed in the MST Lab & Fab by the Fraunhofer Institute for Microelectronic Circuits and Systems IMS in collaboration with Solchip Ltd. utilizes special process steps to place a miniaturized solar cell directly on sensor modules (ASICs). Typically these sensor modules are manufactured on a

“piece of silicon” that has been treated with several processing steps, including ion implantation, oxidization or metal deposition. The ASIC structures are in general sensitive with respect to the additional processing steps, e.g. the thermal load, which makes the subsequent processing tricky. During the processing the silicon chip must not be interfered in anyway by later steps. For this reason a special “soft” processing technology of the solar cell has been developed.

## **CMOS integrated Solar Cell**

The CMOS integration of the solar cell follows closely the post-CMOS integration concept by depositing additional layers to a preprocessed CMOS-substrate. In this case the intelligent CMOS-substrate is realized in the CMOS-Fab “FEDU” and the additional processing of a solar cell is facilitated in the MST-Lab & Fab of IMS.

Subsequent to the basic processing of the CMOS circuitry with the established L035-technology of IMS, the surface of the CMOS-substrate is planarized with the aid of chemical mechanical polishing (CMP) in order to generate a smooth and nearly defect free surface. This is quite important, since any defect could result in a defective solar cell. Furthermore the plain surface of the CMOS-substrate facilitates the following process steps such as photolithography. The essential post-CMOS steps performed in the MST Lab & Fab of Fraunhofer IMS concern the deposition of an efficient photovoltaic (PV)

layer stack based on amorphous silicon together with the required collection electrodes. The active PV stack is generated with the aid of a cost effective CMOS compatible deposition technology that does not interfere with the performance of the CMOS substrate. With the aid of an optimized optical coating stack reflection losses are minimized. The light enters the active volume of the cell through the optical coating stack and generates electron-hole pairs that are collected by respective collection electrodes. This photo-generated current is utilized as a source to power the autonomous sensor node. An inherent advantage of this modular solar-CMOS technology consists in its flexibility, e.g. the area of the cell can be adapted to match the power requirements of the low power electronic circuitry and very miniaturized sensor nodes can be achieved in this way. Moreover, the established technology can be also transferred to external CMOS substrates. It has been demonstrated in the course of this project that the developed process is reliable and that the devices can be manufactured reproducibly with high efficiency. A photograph of fabricated CMOS compatible solar cell processed at the IMS after packaging in a ceramic housing with a transparent lid is shown in figure 1.

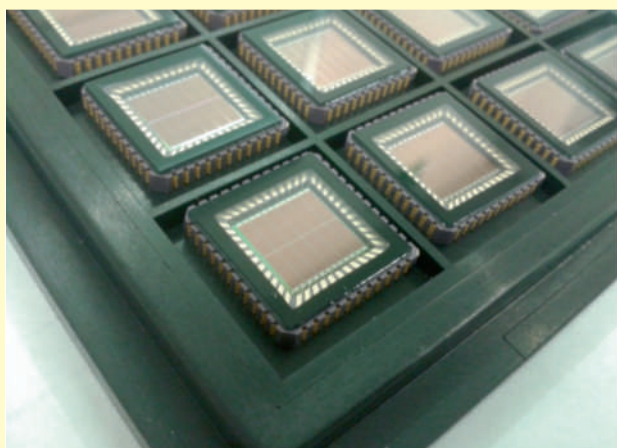


Figure 1: Packaged silicon chip with integrated solar-cell.

### Characterization of the CMOS-integrated Solar cell

The manufactured miniaturized CMOS-compatible solar cells have been characterized regarding their electrical behavior and their spectral characteristics.

A typical IV-characteristics of a PV-cell with and without illumination is shown in figure 2. In this case the illumination source of a microscope has been used. The shift of the IV-characteristics towards negative values with the illumination indicating the photo generated current is clearly observable.

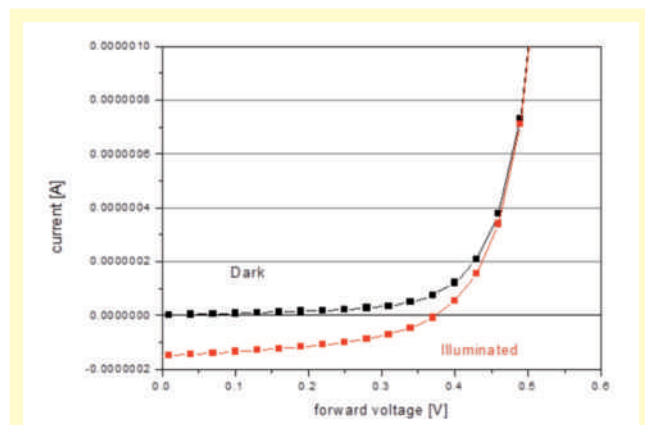


Figure 2: Typical measured IV-characteristics of the PV-cell with and without illumination. As the illumination source the light source of a microscope has been utilized.

Moreover the PV-cells have been characterized spectrally with the aid of a monochromator. The light beam of a broad band light source has been modulated by a chopper wheel and has been passed through a monochromator in order to select a narrow bandwidth interval of the incident spectrum. The modulated current generated by the exiting light beam has been detected with the aid of a lock-in amplifier. A typical plot of the spectral response (after normalizing the maximum to unity) together with an optical 1D-simulation is shown in figure 2. The optical simulation of the absorption spectrum is based on the matrix method [3] and takes into account the optical properties, i.e. dispersion and extinction of all optical

CUSTOMIZED DEVELOPMENT OF A CMOS COMPATIBLE SOLAR CELL FOR AUTONOMOUS SENSOR NODES

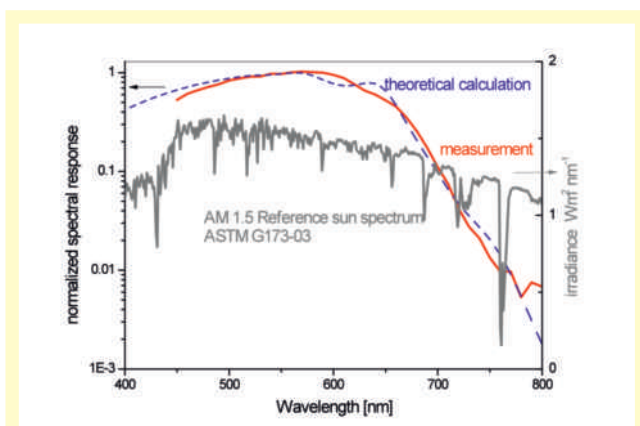


Figure 3: Spectral characteristics of the developed solar cell. For comparison the 1D-optical simulation and as well as the AM 1.5 standard sun spectrum is shown.

layers of the PV-cell. A qualitative agreement of the spectral dependence with the measurement is obtained. In this plot also the standard reference sun spectrum according to ASTM G173-03 with AM 1.5 is depicted for comparison. “AM” stands for Air Mass and is defined as the direct optical path length through the Earth’s atmosphere, expressed as a ratio relative to the path length vertically upwards. It is observed that the measured absorption profile matches the visible range of the solar illumination.

In particular the power delivered by the solar cell is an interesting parameter. In dependence of the effective area of the cell typically electrical power in the range of some milliwatts can be extracted in the case of sun light illumination. The performance of the cells is sufficient to power autonomous integrated sensor nodes with low power circuitry.

**Summary:**

In the framework of a customized development project conducted in collaboration with Solchip Ltd. a miniaturized solar cell has been developed, which is capable for direct integration on a CMOS substrate. The cell is deposited on a planarised CMOS-substrate containing the readout and

control electronics. The parameters of the cell (e.g. the area) can be adapted to the special requirements of the particular application. In this way a cost efficient solution for energy harvesting for autonomous sensor nodes is achieved. In near future further effort will be undertaken to further improve the efficiency of these cells.

**References:**

- [1] <http://en.wikipedia.org/wiki/Smardtust>
- [2] [http://en.wikipedia.org/wiki/Internet\\_of\\_Things](http://en.wikipedia.org/wiki/Internet_of_Things)
- [3] G.R.Fowles, “Introduction to Modern Optics”, 2nd. Ed., Dover Publications, N.Y. (1989)

# SMART FLIGHT CASE

R. C. Jacobi, G. vom Bögel

## Abstract

RFID is a well-known identification technology in logistics. It enables higher cost-efficiency in transport processes and in the inventory management. However, there are many applications where this principle malfunctions due to e.g. several contiguous metallic objects which are to be identified. This article is focused on one of these issues where common RFID technologies cannot be applied without further ado. An approach for a smart solution is presented which furthermore not mandatorily need stationary antennas and a stationary reader unit to read out tags at technical equipment in flight cases. This article is an abridged and modified version based on the paper [1], which is published in VDE conference proceedings and in the IEEE Xplore® Digital Library under IEEE-Copyright.

## Introduction

Wherever big events in sports, music or business are on, a sophisticated logistic is needed. Particularly this applies for touring events as Formula 1, a touring band or a road show. The equipment is usually packed in a flight as shown in Figure 1. These flight cases are manufactured in different sizes. There are some types of standard cases with the possibility of diverse insertions and of course customized cases, which contain normally major constituents like mixers or components of the PA-system. The flight case shown in Figure 1 is a small standard case.



Figure 1: Standard flight case for transporting technical equipment in the event sector [1]

It is desirable to register whether all equipment of the packing list is present and packed into the right case. From the economic point of view the most important issues are not only to avoid the disappearance of expensive equipment, but also to ensure an assembly with the complete equipment for the ongoing and the following touring event. A missing or not located case or just a particular component of the packing list can cause immense follow-up costs.

## Difficulties and Solutions for the Implementation of RFID at Technical Touring Equipment

Hence, it is promising to apply RFID in the event sector to optimize the process flow. It is aimed to overcome the barriers in practical use, which still exist.

The employed technical equipment varies from cables, to mixers or rigging equipment. This equipment has very different physical characteristics. A multitude of the equipment contains metal – rigging equipment consists predominantly of steel or aluminum. These materials have heavy reflective or damping characteristics dependent on the frequency.

Figure 2 shows a typical process flow with a smart event management system. An event management system consists usually of software where all equipment data as well as customer data or data of available freelancers are saved. During the planning process of the event the equipment is disposed. The storekeepers prepackage the equipment at the warehouse as described in the packing list. The prepackaged freight is

verified by the packing list (Figure 2 a)). These processes could easily be executed with the combination of an equipment management software and RFID. In practice some companies are working with bar code scanners, which demands to scan each label separately and with a small distance in a line of sight. Hence it is not possible to verify the packaged content of a case.

For each case of the freight a designated place for delivering at the venue can be stored in the system (Figure 2 b)). This saves time and resources. After the finalized event and the dismantling of the technical rigs, the freight is verified again with the packing list and can be shipped back to the warehouse or to the next venue (Figure 2 c)).

#### Novel Solution for the event sector

If the technical equipment is tagged and transported in the standard flight cases, RFID systems of the state of the art work not reliable due to damping or reflective environments or differing orientation. Moreover the solutions of the state of the art need stationary readers and antennas. For these reasons RFID technology is rarely applied in the event sector.

Our approach intends an internal reader in each case. This gets the antennas for energy supply of passive RFID tags and data communication as near as possible to the tags. In addition this principle allows applying a handy mobile reader device to read out the content of a case. Figure 3 shows the read operation in a so called smart flight case and the transmitting of the read data to an event management system.

The so called reader communication unit (RCU) is implemented in each case and exists of two parts – an internal RFID reader and a device for the outer communication (Figure 3 a)). The internal RFID reader (IRR) works in a low frequency range. Hence no reflection occurs since the transfer system is in accordance with a quasi-static system. For example LF-RFID technology with an anti-collision protocol is suitable to supply the tags with energy and receive the transmitted data (Figure

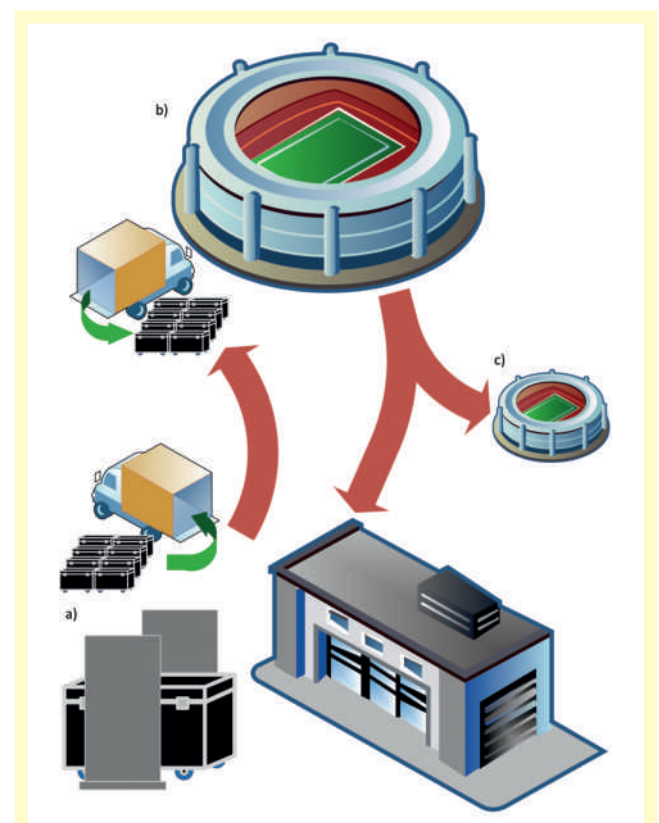


Figure 2: Process flow with a smart event management system: a) Disposing of the equipment at the warehouse and verification of the freight b) Delivery of the freight to the designated place at the venue c) Verification of the freight and shipping to the warehouse or to the next venue [1]

3 b)). The orientation of the RFID tags is not known. A smart flight case is equipped with a 3-D antenna array which ensures to read out a tag independent of the orientation. The read operation can take place with every closing of the case.

To transmit the read data, the information is transferred to an outer communication device (OCD). Due to the different requirements, it uses a higher frequency than the IRR. For example UHF-technology in an ISM-band can be used. Thus the OCD can transmit data over a range of several meters with comparatively small energy consumption.



In Principle two methods can be applied to collect the data – case by case or by read-out all cases in an area. The read data can be transmitted by an active transmitter. Hence the data of a case or several cases can be received easily with a smart mobile reader device (Figure 3 c)). Furthermore standard RFID gates can be used in a warehouse, in a truck or even at the venue to ensure the read-out of every case that is loaded (Figure 3 d)). The use of a central acquisition unit (CAU) is expedient in packing areas (Figure 3 e)). All principles which may have more than one smart flight case in their read-out area use a communication protocol with anti-collision to read the data of the smart flight cases successively.

The real time acquisition of the equipment supports the workflow and enables to retain control in the fast executing processes of an event. For example in the load process the data of scanned arriving cases can be verified with the load list. This ensures the right freight and load order as well as it gives the trucker the sureness not to have an excessive truck.

### Conclusions and Future Work

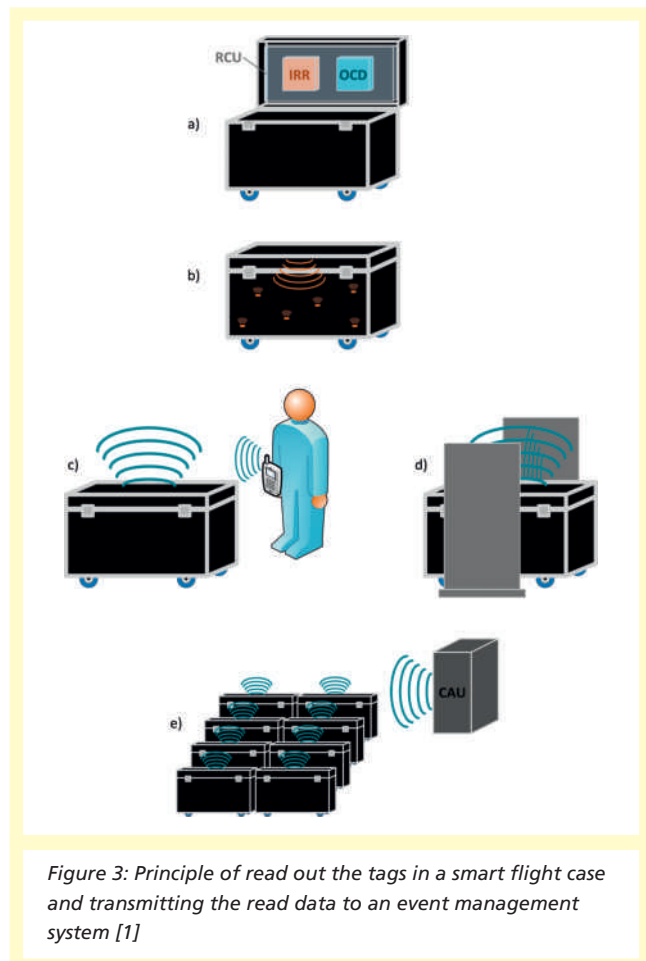
This article shows a novel solution for implementing RFID in a sector where this smart technology is not common so far for several reasons. Our solution intends a reader communication unit (RCU) for each smart flight case which contains an internal RFID reader (IRR) and a device for the outer communication (OCD).

Applying this principle, stationary antennas and a stationary reader unit are not mandatorily needed. There is a multitude of possibilities to transmit the read tag data to an event management system by the OCD. The data can be received with a mobile reader device or by a stationary system with gate antennas or a common UHF antenna.

In the next steps the buildup of a demonstration system is planned to verify the practical suitability.

### References

- [1] Jacobi, Rebekka C.; Hennig, Andreas; vom Boegel, Gerd, "Smart Flight Case" Smart Objects, Systems and Technologies (SmartSysTech), Proceedings of 2014 European Conference on, 01-02 July 2014





# DEVELOPMENT OF A WIRELESS AND SELF-SUSTAINING SENSOR SYSTEM IN INDUSTRIAL APPLICATIONS FOR A HIGH NUMBER OF SENSORS

G. vom Boegel, F. Meyer, M. Kemmerling

## Abstract

The industrial environment of a manufacturing plant is a suitable field of application for a variety of measuring tasks for process monitoring on the use of thermoelectric generators (TEG) for the power supply of wireless sensor modules. This paper describes the various aspects of the development of a self-sustaining system using the example of coolant monitoring and control. Subject is a continuous pressure and temperature measurement at each mold of a cooling system. Furthermore, wireless transmission of data to a central base station is required, wherein more than 50 sensor modules have to share one radio channel. The energy for operation of the sensor module is provided by a TEG using the temperature difference between the coolant tube and the "warm" environment. To attain a stable energy supply, various TEG and construction practices with controlled heat flow have been evaluated and optimized. In combination with a specific power management a robust, industry-compliant solution has been realized.

## 1 Introduction

Self-sustaining wireless sensor systems supporting process measurement technology have the advantage that they are maintenance free and easy to install in a process environment. Nevertheless such systems have to fulfil high demands on availability, measurement interval, communication security and data throughput.

The presented development addresses the monitoring and control of a cooling fluid within the manufacturing process for producing parts by injecting material like elastomers, polymers, metals or glasses into a mold (injection molding). The principle of the process is given in [1]. As parameters to be observed pressure and temperature of the coolant were given. The coolant is used to shorten the time between injection and opening the tool. Controlling the reflowing coolant allows to open the mold as early as possible.

The task of the development was to design a sensor system for a high number of about 50 measuring points spread over an area of about 2000 square meters. Due to occasional exchanges of machine parts, e.g. molds, handlers etc., a wired installation did not come into account. Furthermore the difficult access to measuring points for maintenance, a battery driven approach was prohibited. So it was obvious to implement wireless and self-sustaining sensor modules.

In principle two sources for local energy supply were usable for energy harvesting: the flow of the coolant or the temperature difference between the coolant and the ambient surrounding. The use of the flow energy would require a kind of a micro turbine and in order to that rotating parts with restricted life time. Therefore the choice falls on a thermoelectric generator as an energy harvester.

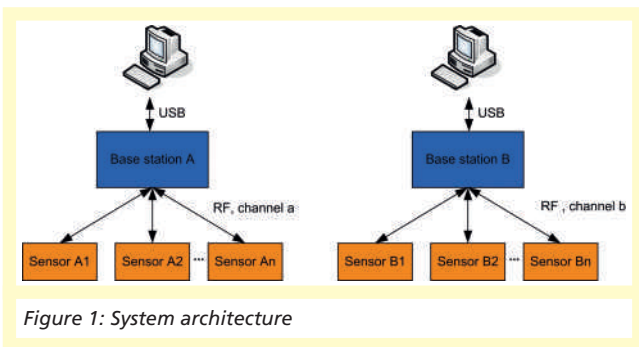
The considered temperature range is defined from -20 °C up to 125 °C.

## 2 Concept Design

### 2.1 System architecture

The system consists of a PC as control computer, one or more base stations and a large number of self-powered sensors. As shown in figure 1, each sensor is assigned to a dedicated base station.

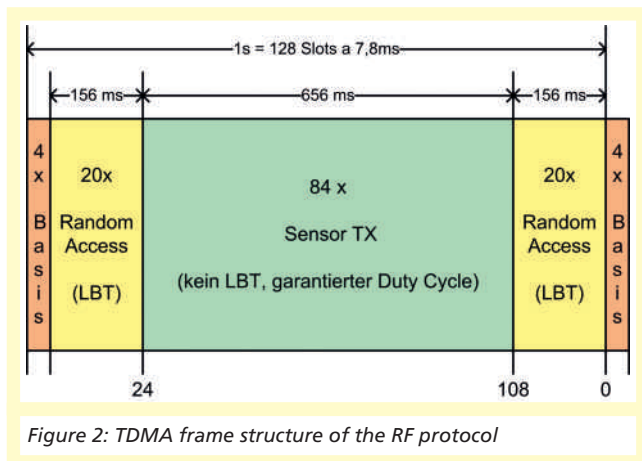
Limited by the wireless protocol, a base station can manage up to 80 participants. If more sensor nodes are needed for a special application, a second base station for further 80 participants must be added. In that case a new communication cell is created with its own carrier frequency similar to the technique known from mobile phone systems.



Very high demands are made on the wireless communications in industrial applications. The communication, especially in case of process control tasks, has to perform real-time operation. Although the amount of data per sensor is small, a large number of participants have to share the limited capacity of a channel.

For such applications stochastic primitive multiple-access methods, such as "Aloha" or "slotted Aloha" [2] are not suitable because of their high probability of collision with many participants in the system and the consequent lack of real-time capability.

From mobile phone systems synchronized time slot management (TDMA - Time Division Multiple Access) is known that results in guaranteed time slots for many participants by collision avoidance methods [2]. The system presented here shows the implementation of this technology, which is dimensioned for a large number of participants and a fixed data throughput. Due to the fixed allocation of time slots (see figure 2), this approach has real-time capability and is well suited for industrial applications that exceed sporadic data communication, such as continuous transmission of parameters for monitoring and control purposes.



Within the "basis" slots (figure 2) the base station sends a synchronization message containing additional information and configuration data. The "Random Access" slots are used as allocated time slots for the following transmission of sensor data. For time critical measurements, the base station can allocate several slots to one sensor modules in the "Sensor TX" phase. A second "Random Access" phase was added to the frame structure. Within this phase sensor modules can join the communication to a later point in time due to power aspects in power management. Especially during startup it is possible, that sensor modules need longer periods for recharge of the buffer capacitors.

**WIRELESS CHIPS AND SYSTEMS**  
**DEVELOPMENT OF A WIRELESS AND**  
**SELF-SUSTAINING SENSOR SYSTEM**  
**IN INDUSTRIAL APPLICATIONS FOR A**  
**HIGH NUMBER OF SENSORS**

In wireless sensor systems a carefully energy management has to be designed in order to achieve the best performance of the system. Figure 3 shows the involved building blocks in a block diagram.

The largest consumers of energy are the radio frontend and the sensor. The total energy demand has to be calculated from the demand of one measuring and transmission cycle and the cycle rate itself. Therefore high-efficient components and a low sampling and transmission rate are advantageous for the design of an energy-independent system. But in this case of a process monitoring application high measurement and communication rates are required.

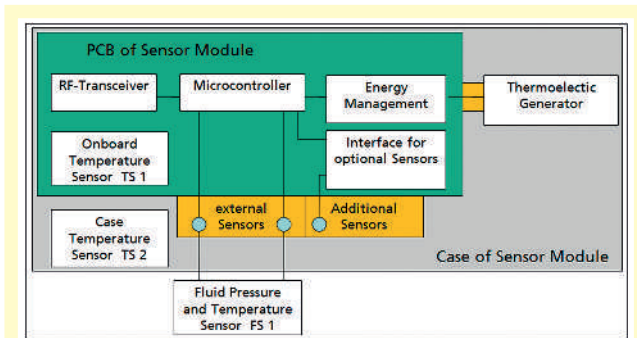


Figure 3: Block diagram of the sensor module

Based on the hardware concept the following figures for energy consumption can be made. The measurement and transmit phase (Sensor TX) is estimated with a duration of 100 ms, where:

- the measurement takes 80 ms,
- the sending takes 10 ms and
- the remaining jobs take 10 ms; this includes setup, calculation and storage tasks of the microcontroller.

The calculated power consumption for this cycle is 3.1 mWs. For the evaluation of the system two sample rates should be considered: 1/second and 1/minute. With a standby power of 36  $\mu$ W and the used sample rate the average power consump-

tion can be determined. The power for the operation of one hour results in dependency to the sample rate to:

a) 1/second:  $E_{sec} = 7.67 \text{ Wh}$

High sample rate for operation in injection operation and low latency requirements.

b) 1/minute:  $E_{min} = 0.25 \text{ Wh}$

Low sample rate in other operation phases, e.g. after ejection and handling.

Compared to the capacity of a primary battery cell - about 5 Wh for a AA size type – it is obvious, that a battery based approach is less promising.

**2.4 Power supply by TEG energy harvesting**

For the use of energy harvesting various technologies such as rectification of radio waves, conversion of kinetic energy by piezoelectric transducers, conversion of rotational energy by dynamos, solar cells or thermoelectric generators are available. For the application considered here a temperature difference provided by the process to be monitored was chosen as an appropriate energy source. A thermoelectric generator (TEG), also known as seebeck generator, converts the temperature difference between the cold coolant and the warm environment directly into electric energy for the supply of the sensor node. Reference [3] gives a comprehensive survey of the seebeck effect and the function of thermoelectric generators. Figure 4 shows the embedding of a TEG in the power supply of a sensor module.

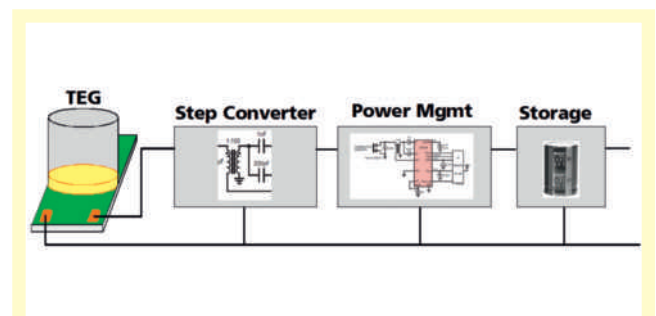


Figure 4: Embedding of the thermoelectric generator (TEG) into the sensor modules power supply

The output voltage of the TEG has to be transformed to one or more stable DC operating voltages. Depending on the used components, typical values for these voltages are 1.8 V, 3.3 V or 5.0 V. The power management unit supervises the operation voltages and indicates the power status to the processing unit.

A storage unit is optional for sensor modules. It is used to bridge either current peaks or power gaps and has to be designed carefully due to side effects. Especially in the startup phase, the storage unit can cause undesired behavior because of delays in charging.

During the concept phase of the presented development two TEGs were evaluated:

i) TGP-751 supplied by Micropelt [4]:

The TGP-751 is a packaged TEG in thin-film, solid state technology. The package is easy to be integrated into the mechanical design of the housing and mounting into the application environment.

Seebeck voltage is  $V_{sbi} = 110 \text{ mV/K}$ .

Thermal resistance:  $R_{th} = 18 \text{ K/W}$ .

Size (l \* w \* h): 15 mm \* 10 mm \* 15 mm.

ii) Power-Strap supplied by O-Flexx [5]:

The used sample of Power-Strap is an unpackaged TEG in thin-film, solid state technology with 20 TEG chips.

The TEG chips are bonded on a flexible stripe (see figure 5). The TEG can easily be adapted to the demand of power by cutting the length of the stripe, the number of determine the power. The package design and mounting into the application environment is more complex.

Thermal resistance per chip:  $R_{th} = 124 \text{ K/W}$ .

Thermal resistance per meter:  $R_{th} = 0.7 \text{ K/W}$ .

Size of used strap (l \* w \* h): 250 mm \* 20 mm \* 1 mm.

(values were taken from Preliminary Data Sheet O-Flexx "Power Strap" not published till press time of this article)

The following figures 6 and 7 are showing the test setup for the Power Strap evaluation. The stripe is fixed at the hot and cold side by pressing the thermal contacts against hot and cold heat conductors between the tube for coolant fluid and a dissipator. The dissipator is not shown in the figures.

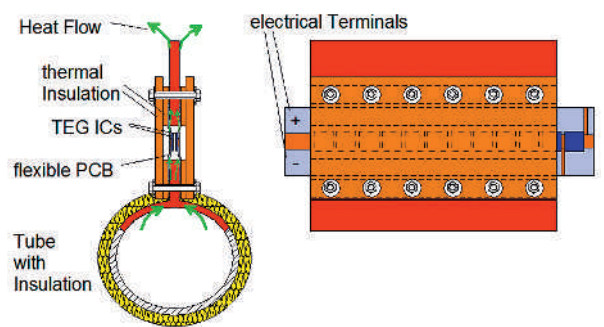


Figure 6: Example of integrating the "Power-Strap" test setup as cross section and side view

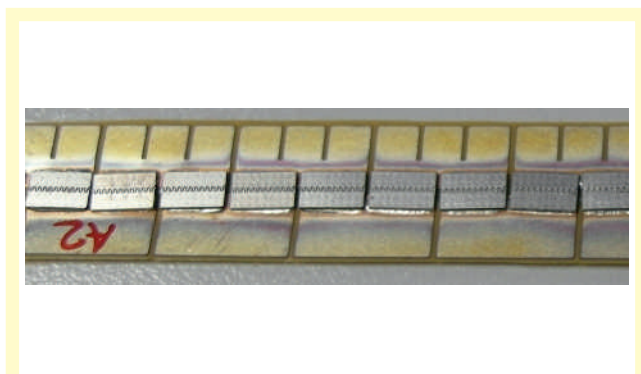


Figure 5: "Power-Strap" TEG (Source: O-Flexx)

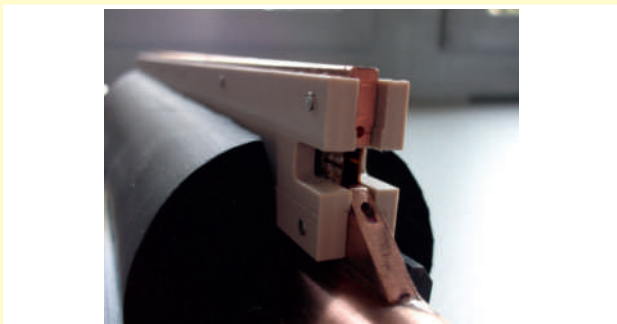


Figure 7: "Power-Strap" clamped between hot and cold terminals of the TEG (Source: Fraunhofer IMS)

**WIRELESS CHIPS AND SYSTEMS**  
**DEVELOPMENT OF A WIRELESS AND**  
**SELF-SUSTAINING SENSOR SYSTEM**  
**IN INDUSTRIAL APPLICATIONS FOR A**  
**HIGH NUMBER OF SENSORS**

The subject of the mechanical design is to concentrate the heat flow between the fluid ( source) and the ambient surrounding (sink) through the chips of the TEG. In practice a part of the heat flow goes parallel to the TEG chip path from source to sink. The behavior can be modelled in an equivalent circuit.

To limit the not usable heat flow in parallel to the flow through the TEG chips a careful mechanical design with selection of suitable materials has to be done. For the "Power Strap" the design is shown in figures 6 and 7, where figure 6 shows the heat flow in principle and figure 7 the realization with insulation materials.

After setup of both TEG test installations the open circuit voltages were measured over temperature difference. Figure 8 demonstrates the characteristics of the TEGs. The Micropelt TGP-751 indicates a good representation of the theoretical linear relationship between temperature difference and voltage output. The internal apparent resistance and the voltage level allow an easy impedance matching to the following circuitry. The input voltage of the DC-DC converter should cover a range from 0.15 V to 2.5 V. This range enables the design of an energy efficient converter.

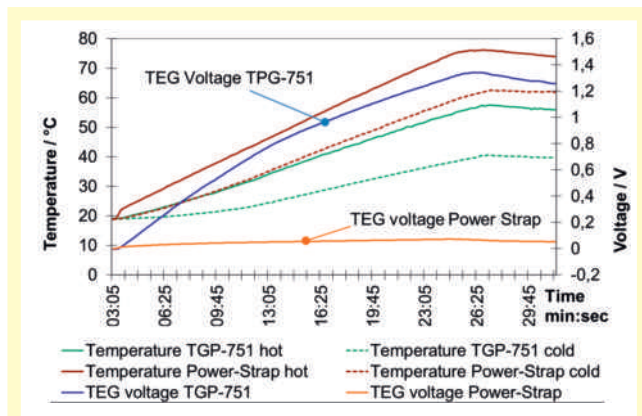


Figure 8: Comparison of open circuit voltages of TEGs

The "Power Strap" TEG is initially planned to be used for medium power applications in the power range of a few watts.

So the internal apparent resistance is designed for higher currents and the output voltage results in the sum of TEG chip output voltages. The short stripe used here comprises a relative low number of chips and so the output voltage of the TEG is low as well. For the further development the TGP-751 was chosen because of its higher output voltage.

**3 Realization**

**3.1 Mechanical design**

Due to the harsh environment in industrial applications, a housing with a protection class better than IP 65 is designed. The cold-side temperature provided by the process medium (coolant) is fed from the bottom to the thermal generator; the heating of the warm side of the generator is realized by capturing the heat radiation of the environment using a special shape of the housing itself (see figure 9).

The two housing halves are thermally decoupled from each other by means of a thermal insulator, which also ensures the tightness of the housing. The sensor is mounted externally to the measuring point using a separate housing. The use of an external sensor results in the possibility of an easy system expansion to other measurement scenarios by adding further external sensors.

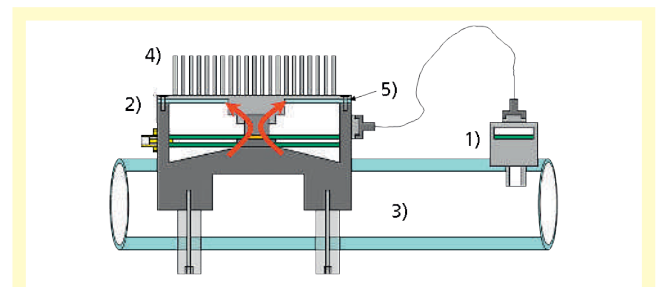


Figure 9: Mechanical assembly of the sensor module:

1. Pressure and temperature sensor
2. Electronics and thermoelectric generator (TEG)
3. Coolant (heat sink)
4. Ambient temperature (heat source)
5. Thermal insulation and seal

### 3.2 RF communication protocol

The radio protocol between a base station and the sensors is designed for a capacity of up to 80 nodes that can transmit measurement values every second. The realization of the time slot assignment method for this number of participants is a great challenge because of the very small amount of energy provided by the thermal generator and the temperature drift of the internal clock sources. The system shall be able to be used at a maximum ambient temperature of 125 °C, which greatly restricts the selection of usable components.

The implementation of the radio protocol includes special low-power synchronization algorithms which guarantee an optimum load profile matching with the current power generation. The protocol structure and other security measures make sure that after the synchronization phase any clock frequency drift is compensated over a temperature range from -20 °C up to 125 °C and thus each participant maintains its dedicated time slot for the wireless communication telegrams. With respect to the strong limitations and boundary parameters such as poor energy allocation, large number of participants, high measuring and transmission rate of up to 1 Hz and a wide temperature range of up to 125 °C the total system obtains its real-time capability and functionality.

### 4 Results

During the verification the system is tested on a specially built test environment. Figure 10 shows the results of such a measurement performed with realistic environment parameters. Due to easier setup the hot and the cold side were swapped and fluid delivers the heat energy. In the red curve the monitored temperature of the medium is shown; the dark blue curve shows the ambient temperature. The difference of these two temperatures is shown in the green curve.

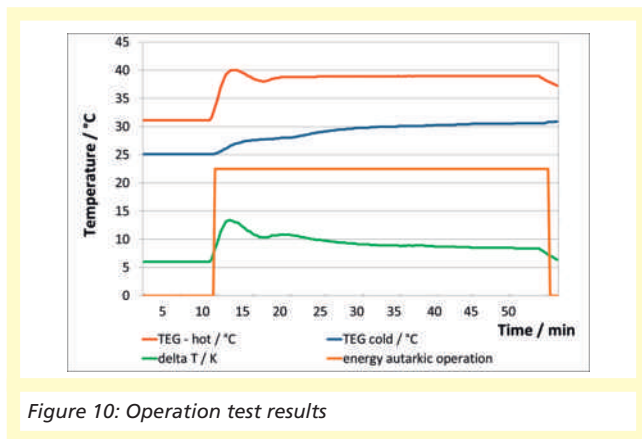


Figure 10: Operation test results

Based on the orange curve showing an internally generated signal that indicates the self-powered operation it is evident that a self-sustaining operation is possible if the temperature difference has an amount of at least 8 Kelvin. This value refers to a measurement and communication interval of 30 seconds. If the application provides a higher temperature difference, the number of measurements and transmissions can increase to more than one measurement per second.

In order to evaluate the startup phase and to monitor the charging of the buffer capacitors as well as the transmission rate, an auxiliary power source in form of a battery was temporary added to the sensor module. Figure 11 shows the startup sequence of the sensor module operating with a higher sample and transmission rate of 1 sample per second.

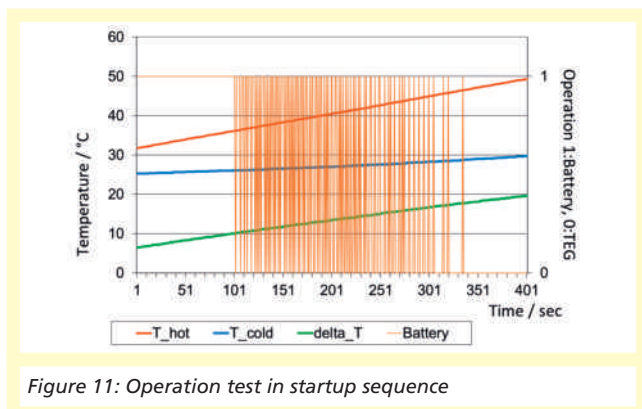


Figure 11: Operation test in startup sequence



WIRELESS CHIPS AND SYSTEMS  
DEVELOPMENT OF A WIRELESS AND  
SELF-SUSTAINING SENSOR SYSTEM  
IN INDUSTRIAL APPLICATIONS FOR A  
HIGH NUMBER OF SENSORS

At the beginning of this sequence the temperature difference is too low to power the sensor module. The supply comes from the battery. This corresponds with the orange curve of figure 11, this binary signal indicates battery operation when the signal is high (1) or TEG operation when the signal is low (0). With the increasing temperature difference at the TEG the sensor module achieves a transitional phase where the module is partly powered by the TEG. Due to current peaks caused by the RF transmitter the power management switches back to battery operation for a short bridging time. Only after exceeding a threshold in temperature difference – in the present prototype design of 17.5 °C – the module is completely powered by the TEG. This behavior was considered to optimize the power management and to obtain a robust startup operation. With the also measured temperature difference the transmission rate is automatically adapted and so unintentional resets are avoided.

Figure 12 shows the realized sensor module to be mounted at the coolant tube.



Figure 12: Realized sensor module with pressure and temperature sensor plug (Source: Fraunhofer IMS)

## 5 Outlook

Up to now the system was tested under laboratory conditions as well as in an industrial environment using a number of 20 modules. In this configuration the system fulfils the given requirements. After completion of field test, that is currently running for a period of three months, further modules will be manufactured and added to the test environment in subsequent steps.

For the development of the next system generation a smaller housing and a more efficient power management is planned.

## 6 References

- [1] Injection molding, from Wikipedia, 2014  
[http://en.wikipedia.org/wiki/Injection\\_molding](http://en.wikipedia.org/wiki/Injection_molding), last access: 10.1.2014
- [2] M. Schwartz, Mobile Wireless Communications, Cambridge Univ. Press, 2005
- [3] D.M. Rowe (Editor), CRC Handbook of Thermoelectrics, CRC Press, 1994
- [4] Datasheet TGP-751 Thin Film Thermogenerator, Micropelt GmbH, 2013 [http://www.micropelt.com/download/thermo\\_generator\\_package.pdf](http://www.micropelt.com/download/thermo_generator_package.pdf), last access: 8.1.2014
- [5] Product information "O-Flexx Power Strap", O-Flexx Technologies GmbH, <http://www.o-flexx.com/technologie/o-flexx-technologie/power-strap/>, last access: 8.1.2014

## Figures

Figure 1 System architecture

Figure 2 TDMA frame structure of the RF protocol

Figure 3 Block diagram of the sensor module

Figure 4 Embedding of the thermoelectric generator (TEG) into the sensor modules power supply.

Figure 5 "Power-Strap" TEG (Source: O-Flexx)

Figure 6 Example of integrating the "Power-Strap" test setup as cross section and side view

Figure 7 "Power-Strap" clamped between hot and cold terminals (Source: Fraunhofer IMS)

Figure 8 Comparison of open circuit voltages of TEGs

Figure 9 Mechanical assembly of the sensor module: 1. Pressure and temperature sensor, 2. Electronics and thermoelectric generator (TEG), 3. Coolant (heat sink), 4. Ambient temperature (heat source), 5. Thermal insulation and seal

Figure 10 Operation test results

Figure 11 Operation test in startup sequence

Figure 12 Realized sensor module with pressure and temperature sensor plug (Source: Fraunhofer IMS)

# SENSOR BASED CARE

M. Munstermann

## Introduction

The Fraunhofer Institute for Microelectronic Circuits and Systems (IMS) participates in a European project called "Hospital Engineering". Three research topics shall be presented in detail: "Sensor Based Care Cart", "Patient Protection System" and "Fall Detection Shower".

The first two systems are both designed to be retrofittable. E. g. regular care carts can either be replaced or enhanced to meet modern demands. The Patient Protection System can be installed in basically any patient room where it is required. The Fall Detection Shower currently replaces an existing shower, because the sensors are firmly attached to the shower tray.

Another common feature of the presented systems addresses the ability of digital and semi-automatic care documentation. Using sensor data from the environment the systems can generate recommendations of care services that are likely to have been performed or instances that might have happened. All the caretaker has to do then is acknowledge the correct recommendation which takes him much less time than hand-written documentation commonly does today. Those events that cannot be detected by sensors but are still important to write down can easily be input using the tablet PC of the Sensor Based Care Cart. This eliminates the well-known break in the information chain which would exist using a paper-based documentation.

## Motivation

The demographic change is referred to as the combination of fewer births and at the same time an increasing number of elderly people. Statistically this will lead to longer and more frequent hospitalisations. To face this trend society needs to come up with innovative solutions. In order to ensure comprehensive and high-grade health care in the future new ways have to be found. The legally required documentation for health and care services offers the most promising potential for optimisation.

## Objective

Three major objectives can be named as follows:

- Reduction of time spent for documentation and accounting
- Improvement of documentation quality (i. e. completeness and preciseness)
- Establishment of more time for patient care

In order to achieve the above mentioned goals techniques from the field of sensor analysis are applied. The Fraunhofer IMS has long-term experiences in regard to sensor analysis. Thereby activity recognition is the main key. Utilizing the installed sensors the system can then recognize which activities have been performed within the environment (i. e. patient room or shower). This also includes emergency situations (e. g. a fall in the shower).

The semi-automatic documentation process presents suggestions which only have to be acknowledged by the care or nursing personnel and can then be further enhanced or specified more precisely. This leads to a complete and precise digital documentation which will result in an easier accounting process.

By reducing the time needed for documentation and improving the documentation quality the staff has more time for those activities that really matter: the overall care quality!

## Activity Recognition

Both Sensor Based Care Cart and Patient Protection System utilize activity recognition as basic principles. The installation of appropriate sensors is an important precondition to be able to detect certain activities. An activity can then be defined by the sequence of sensor events which are fired during its execution. This simple correlation is shown in figure 1. Sensor events can appear anywhere on the timeline. The main task of the activity recognition is to classify sequences of sensor events into groups. These groups are then called activities. Figure 1 shows two examples: repositioning and rebandaging of the patient.

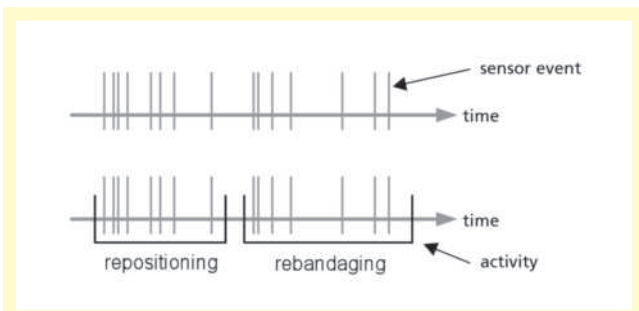


Figure 1: shows two examples: repositioning and rebandaging of the patient.

In general there are two different approaches in order to be able to classify activities with a certain probability: a rule-based one and one that is based on machine learning. Before a system using the latter approach can be productive some time is required for the so-called learning phase. This phase usually includes collecting sensor data and labelling it with the performed activities.

In case of the first approach a priori rules or models have to be defined. This is necessary because the system needs to know which sensor event sequence correlates to a certain activity. The main advantage of this approach is that it is ready for use immediately without the need for a learning phase.

In a hospital setting a combination of both approaches is most preferable. The time a patient spends in hospital is fortunately in general less than three to four weeks. This would be the duration a learning system would need to adapt to the patients habits in terms of activities he or she performs on a regular base.

The activities care or nursing staff performs are to unsteady as to be defined by static rules or models. Fortunately most staff members are present for more than three to four weeks. The learning phase is defined independently of the patient and determined by evaluation and the daily routine of care or nursing personnel.

The hospital is a quite well structured workplace with fixed daily routines which are proposed by patient's care plans. The rule-based approach heavily profits from that circumstance.

### Sensor Based Care

The Sensor Based Care Cart, Patient Protection System and Fall Detection Shower are all instruments of the sensor based care concept.

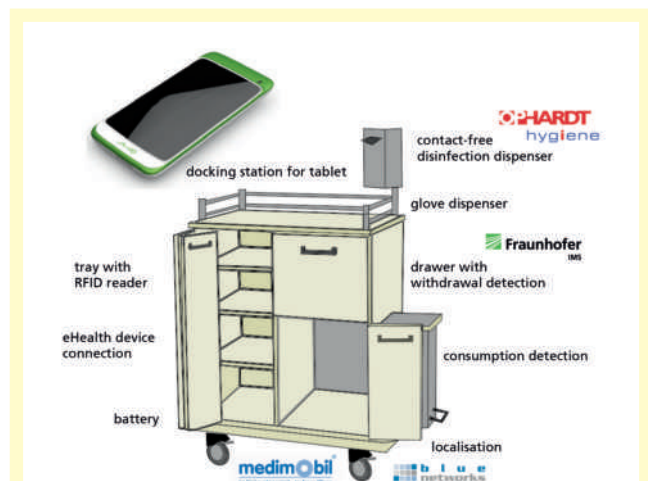


Figure 2: Drawing of all involved components (Sources: medimobil.com, miocare.mio.com)

Figure 2 shows all involved components of the Sensor Based Care Cart. The foundation of that concept is a care cart manufactured by medimobil. Medimobil's care cart already comes with a battery in order to supply electrical devices and sensors with power.

For the purpose of documentation and to be able to acknowledge suggested activities the cart is equipped with two kinds of human interfaces: a tablet PC and a documentation terminal (made by Winkel). For safe transportation and to be able to charge the tablet PC the care cart is additionally equipped with a docking station. For convenience and to save

time the cart has an eHealth connection. After a patient's body temperature or blood pressure has been measured the data can be transferred to the cart. There is no need for the care or nursing staff to write down the results manually thereby reducing the chance of false records.

Trays containing identifiable objects and material are furnished with RFID readers. A special drawer the Fraunhofer IMS has developed can detect the withdrawal of even not separately identifiable objects. Therefore there is no need to attached tags to material stored in that drawer. The waste bin automatically detects the event of throwing away material (e. g. packaging or bandaging material).

Wherever the cart may be placed: using the integrated localisation system (manufacturer: blue networks) the cart can easily be located. This localisation also enriches the automatic documentation. Knowing about the carts position, i. e. which patient's room it is located, helps drill down the possibilities of which patient is currently been treated. Additionally to that it is useful for regular maintenance and repair of all carts.

The Sensor Based Care Cart is equipped with two dispensers: a disinfection and a glove dispenser. When one of the dispensers is used the consumption will automatically be protocolled within the care documentation. Abnormalities from a certain norm can be detected and the corresponding staff member can be informed. Whenever disinfection fluid is low the cart

can report to the appropriate person to refill the dispenser. The Patient Protection System detects abnormalities considering predefined and disease-specific rules. It consists of the components presented in figure 3.

Detected abnormalities can be reported to the corresponding caretaker and thereby support him to appropriately care for his client. Chair, bed occupancy sensors and presence detectors provide information about the presence of the patient, care/nursing personnel or visitors. Door and window contacts can gather data about the ventilating behaviour. Light sensors can give an indication if the patient is currently sleeping or is awake in an unobtrusive way.

Another example for a sensor system that interprets context related information is the Fall Detection Shower. A custom-tailored combination of hard- and software specially designed for the bathroom setting detects the incidence of a patient lying on the shower tray for a certain amount of time. It has been evaluated under realistic conditions and can reliably distinguish water coming from the shower head (and other liquids such as shower gel) from the patient lying on the shower tray.

The Fall Detection Shower can be equipped with different types of interfaces. Therefore it is easy to integrate the shower into an existing emergency call system as found in modern hospitals and nursing homes. The system is intended to autonomously make emergency calls and thereby assist the patient when he needs help but can't call help on his own. The emergency will immediately be passed to the nursing staff in charge so that the patient will receive help as soon as possible.

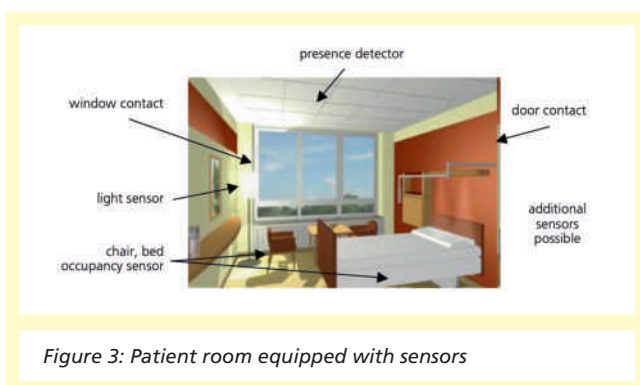


Figure 3: Patient room equipped with sensors

# ELECTROCHEMICAL MONITORING

T. Zimmermann, A. Hennig

The Fraunhofer IMS is a major R&D provider for wireless sensor system solutions worldwide. In this field the IMS covers the range from novel sensors as well as innovative solutions for standard measurement tasks. All developments are done according to ISO 9001. Further manufacturing will be realized in the ISO 16949 / ISO 9001 qualified cleanroom-production facilities. In the new and state-of-the-art biosensor lab integrated electrochemical and immuno-sensing capabilities will be implemented by production-compatible bio-functionalization technologies for customized integrated sensor systems. Wireless data and energy transmission using standard protocols provides access to mobile solutions and modern easy-to-use handheld devices. Recently, the IMS provides monitoring solutions for bioreactor processes and diabetics. Thereby, IMS customers are able to place innovative products on the market and expand its market share. Complete systems for continuous control of especially electrochemical/biological (glucose, lactate, bacteria), chemical (pH, solved oxygen), and physical (temperature, pressure) parameters can be customized. Those customized solutions can be offered by the Fraunhofer IMS to all interested parties.

One of the innovative solutions is a miniaturized short-term implant developed together with NovioSense BV. That system is measuring blood-sugar levels in tear fluid and can be comfortable placed in the under eye-lid by diabetics. An integrated nano-potentiostat designed and produced at FhG IMS guarantees accurate and reliable measurements in that electrochemical low-power sensor system. There is a growing demand for highly sensitive and portable devices that can measure quantitatively especially biological parameters real time and in a non-invasive manner. To measure those parameters, devices increasingly translate a binding event between receptors (e.g. glucose-oxidase) and their targets (e.g. glucose) into an electrical signal. These devices often require potentiostats, which can be offered by Fraunhofer IMS as a USB-stick potentiostat together with a basic software package, first. Later on, single nano-potentiostat-chips and its mass production for low-cost applications (e.g. disposables) can be provided, too. Due to

its reduced size, the USB-stick potentiostat is highly portable, making it ideally suited for field work.

The system can be used for detecting, measuring and monitoring a large variety of analytes, such as glucose, lactate, cholesterol and alcohol which are measured in an amperometric manner. The principle of measurement involves an electrochemical reaction that is activated with the aid of an enzyme. In the case of glucose-measurement the enzyme glucose oxidase converts glucose into gluconacid. A by-product of this conversion is hydrogen peroxide ( $H_2O_2$ ). Hydrogen peroxide will be reduced to water at a platinum-metal electrode. This electrochemical reaction delivers two electrons which can be measured by our potentiostat. The potentiostat in three-electrode configuration keeps the voltage between reference electrode and working electrode at a constant level. If there is a variation of hydrogen peroxide concentration in the solution the conductivity between the electrodes changes. Consequently, the potentiostat injects a current in the counter-electrode with an appropriate strength. That action stabilizes the voltage between reference and working electrode to a constant level. This highly accurate measurement is used for quantitatively measuring the glucose level. The special feature of this biosensor-system: the USB-stick potentiostat together with a basic software package brings electrochemical measurements as an easy-to-use plug-and-play solution to our customers. We are currently working on a wireless interface connecting sensor-system and handheld-device in an even more convenient way.

Based on its intuitive use the USB-stick measurement system can be used for teaching purposes and consumer-applications, as well. As education solution the system will come with a kit containing suitable samples and a workbook. In a playful manner students will learn to understand the mechanism of reduction and oxidation reactions.

Typical characteristics of the USB-stick potentiostat:  
Chrono-amperometry: yes



SYSTEMS AND APPLICATIONS  
ELECTROCHEMICAL MONITORING

Cyclic voltammetry: yes  
 Linear Sweep voltammetry: yes  
 Potential range: -3/+3 V  
 Current range: -10 pA to 750  $\mu$ A  
 Dimensions: 55 x 20 x 12 mm



Figure 1: Quality control of an electrode-surface functionalized with the enzyme glucose-oxidase. The modern AFM (atomic force microscopy) in the Biosensor-Lab of FhG IMS is dedicated for measurements in liquids and biological samples in the (sub-)nanometer range.



Figure 2: USB-stick potentiostat together with a software package brings electrochemical measurements as a plug-and-play solution to our customer.

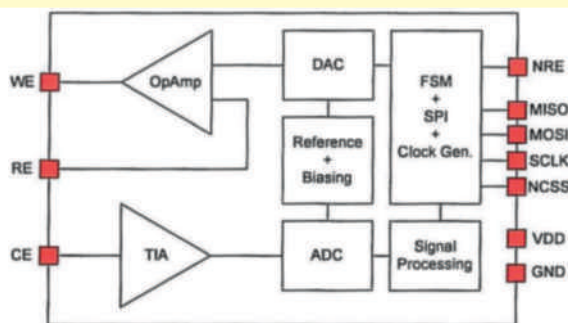


Figure 3: Functional blocks of the USB-stick potentiostat.

# LIST OF PUBLICATIONS AND SCIENTIFIC THESES 2013

## List of Publications and Scientific Theses 2011

---

1. Papers in Monographs	76
-----	
2. Journal and Conference Papers	76
-----	
3. Oral Presentations	79
-----	
4. Patents	
4.1 Granted Patents	80
4.2 Laid Open Patent Documents	81
-----	
5. Theses	
5.1 Dissertations	81
5.2 Master Theses	81
5.3 Bachelor Theses	81
-----	
6. Product Information Sheets	82
-----	

## 1. Papers in Monographs

März, M.; Eilers, D.; Gillner, A.; Schliwinski, H.-J.; Schneider-Ramelow, M.; Schubert, T.; Partsch, U.; Paschen, U.; Wilken, R.:  
**Leistungselektronik und elektrische Antriebstechnik.**  
In: Elektromobilität. Stuttgart: Fraunhofer Verlag, 2013,  
pp. 34–41

Möller, K.-C.; Althues, H.; Berger, T.; Günther, B.; Janietz, S.; Klieber, R.; Kusnezoff, M.; Latz, A.; Marquardt, K.; Pastewka, L.; Schiestel, T.; Schulz, J.; Thönnessen, T.:  
**Energiespeichertechnik.**  
In: Elektromobilität. Stuttgart: Fraunhofer Verlag, 2013,  
pp. 43–51

## 2. Journal and Conference Papers

Al-Eryani, J.; Stanitzki, A.; Konrad, K.; Tavangaran, N.; Brückmann, D.; Kokozinski, R.:  
**Continuous-time digital filters using delay cells with feedback.**  
(Analog <13, 2013, Aachen>).  
In: ANALOG 2013. Berlin [u.a.]: VDE-Verl., 2013, without  
pagination; [5 Bl.] (ITG-Fachbericht 239)

Bronzi, D.; Villa, F.; Bellisai, S.; Tisa, S.; Tosi, A.; Ripamonti, G.; Zappa, F.; Weyers, S.; Durini, D.; Brockherde, W.; Paschen, U.:  
**Large area CMOS SPADs with very low Dark Counting Rate.**  
(Quantum Sensing and Nanophotonic Devices <10, 2013, San Francisco, Calif.>).  
In: Quantum Sensing and Nanophotonic Devices X. Bellingham, Wash.: SPIE Press, 2013, Article number 86311B [8 Bl.] (SPIE proceedings series 8631)

Burmester, K.; Goehlich, A.; Celik, Y.; Schmidt, A.; Klieber, R.; Haas, N.; Greifendorf, D.; Vogt, H.:  
**CMOS integrated free standing circular membrane for the detection of allergens and biomarkers.**  
(Mikrosystemtechnik-Kongress <5, 2013, Aachen>).  
In: Mikrosystemtechnik Kongress 2013.  
Berlin [u.a.]: VDE-Verl., 2013, pp. 822–825 [4 Bl.]

Celik, Y.; Goehlich, A.; Jupe, A.; Vogt, H.:  
**Entwicklung eines hochtemperaturfesten Kondensators für die Mikrosystemtechnik.**  
(Mikrosystemtechnik-Kongress <5, 2013, Aachen>).  
In: Mikrosystemtechnik Kongress 2013. Berlin [u.a.]: VDE-Verl., 2013, pp. 834–836 [3 Bl.]

Durini, D.; Zappa, F.:  
**Advances in time-of-flight and time-correlated single-photon-counting devices.**  
In: SPIE newsroom 9. April 2013 [http://spie.org/documents/Newsroom/Imported/004768/004768\\_10.pdf](http://spie.org/documents/Newsroom/Imported/004768/004768_10.pdf)

Gembaczka, P.; Görtz, M.; Kordas, N.; Lerch, R. G.; Müntjes, J. A.; Kraft, M.; Mokwa, W.:  
**Kapazitive integrierte Drucksensoren für ein implantierbares System zur drahtlosen Druckmessung in der Pulmonalarterie.**  
(Mikrosystemtechnik-Kongress <5, 2013, Aachen>).  
In: Mikrosystemtechnik Kongress 2013. Berlin [u.a.]: VDE-Verl., 2013, pp. 169–172 [4 B.]

Goehlich, A.; Burmester, K.; Celik, Y.; Klieber, R.; Greifendorf, D.; Haas, N.; Vogt, H.:  
**Development of an universal allergen sensor system.**  
(International Conference on Sensors and Measurement Technology (Sensor) <16, 2013, Nürnberg>).  
In: Sensor 2013. Nürnberg: AMA Service GmbH, 2013,  
pp. 540–545 (AMA Conferences 2013)

Görtz, M.; Betz, W.; Mokwa, W.; Vogt, H.; Kraft, M.:  
**Verkapselungstechniken für implantierbare integrierte MEMS Drucksensoren.**  
(Mikrosystemtechnik-Kongress <5, 2013, Aachen>).  
In: Mikrosystemtechnik Kongress 2013. Berlin [u.a.]: VDE-Verl., 2013, pp. 586–587 [2 Bl.]

Grella, K.; Dreiner, S.; Schmidt, A.; Heiermann, W.; Kappert, H.; Vogt, H.; Paschen, U.:  
**High temperature characterization up to 450°C of MOS-FETs and basic circuits realized in a Silicon-on-Insulator (SOI) CMOS-technology.**  
In: Journal of microelectronics and electronic packaging 10 (2013), 2, pp. 67–72

Grella, K.; Dreiner, S.; Vogt, H.; Paschen, U.:  
**High temperature reliability investigations up to 350 °C of gate oxid capacitors realized in a Silicon-on-Insulator CMOS-technology.**  
(HiTEN <2013, Oxford>).  
In: HiTEN 2013. Washington, DC: IMAPS, 2013, pp. 116–121

Grella, K.; Dreiner, S.; Vogt, H.; Paschen, U.:  
**Reliability investigations up to 350°C of gate oxid capacitors realized in a Silicon-on-Insulator CMOS-technology.**  
In: Journal of microelectronics and electronic packaging 10 (2013), 4, pp. 150–154

Heiermann, W.; Gerschke, T.; Ruß, M.; Vogt, H.:  
**Flip-Chip Technologie für Anwendungstemperaturen > 250 °C.**  
(Mikrosystemtechnik-Kongress <5, 2013, Aachen>).  
In: Mikrosystemtechnik Kongress 2013. Berlin [u.a.]: VDE-Verl., 2013, pp. 709–712 [4 Bl.]

Jupe, A.; Goehlich, A.; Meißner, F.; Endler, I.; Vogt, H.:  
**CMOS kompatible, nanomodifizierte Multi-Elektroden-Arrays.**  
(Mikrosystemtechnik-Kongress <5, 2013, Aachen>).  
In: Mikrosystemtechnik Kongress 2013.  
Berlin [u.a.]: VDE-Verl., 2013, pp. 592–595 [4 Bl.]

Kahnert, S.; Goehlich, A.; Greifendorf, D.; Vogt, H.; Lennartz, K.; Kirstein, U.; Goellner, B.; Michelsen, U.; Bartels, F.:  
**Entwicklung einer Mikrochip navigierten Zellsortieranlage.**  
(Mikrosystemtechnik-Kongress <5, 2013, Aachen>).  
In: Mikrosystemtechnik Kongress 2013. Berlin [u.a.]: VDE-Verl., 2013, pp. 417–420 [4 B.]

Kißler, S.; Zimmermann, T.; Pierrat, S.; Klein, B.; Schiller, S.; Kraft, M.:  
**A new real time biomimetic membrane biosensor based on a capacitive readout ASIC for antibiotics.**  
(International Conference on Solid-State Sensors, Actuators and Microsystems (Transducers) <17, 2013, Barcelona>).  
In: Transducers. Piscataway, NJ: IEEE, 2013, pp. 349–352 [M3P.085]

Kraft, M.; Goehlich, A.; Burmester, K.; Haas, N.:  
**Resonant sensors for label-free biosensors.**  
(MicroNano Conference <9, 2013, Ede>).  
In: MicroNanoConference '13 [online].  
[Zugriff am 10. Februar 2014]. Verfügbar unter: <http://www.micronanoconference.nl/images/presentaties/SessieE/E3/michael%20kraft.pdf>

Kraft, M.; Görtz, M.; Müntjes, J. A.; Mokwa, W.; Cleven, N. J.; Schmitz-Rode, T.:  
**State of the art telemetric implantable sensors and their encapsulation.**  
(International Conference on Sensors and Measurement Technology (Sensor) <16, 2013, Nürnberg>).  
In: Sensor 2013. Nürnberg: AMA Service GmbH, 2013, pp. 633–637 (AMA Conferences 2013)

Kropelnicki, P.; Muckensturm, K.-M.; Mu, X. J.; Randles, A. B.; Cai, H.; Ang, W. C.; Tsai, J. M.; Vogt, H.:

**CMOS-compatible ruggedized high temperature Lamb wave pressure sensor.**

In: Journal of micromechanics and microengineering 23 (2013), 8, Paper 085018 [9 BI.]

Kuehn, S.; Barber, T.; Casse, G.; Dervan, P.; Driewer, A.; Forshaw, D.; Huse, T.; Jacobs, K.; Parzefall, U.:

**Signal and charge collection efficiency of nin- p strip detectors after mixed irradiation to HL-LHC fluences.**

(International Conference on Radiation Effects on Semiconductor Materials, Detectors and Devices <9, 2012, Firenze>).  
In: Nuclear instruments and methods in physics research / A 730 (2013), pp. 58–61

Marzouk, A. M.; Stanitzki, A.; Kokozinski, R.:

**High frequency pulse-density modulated switched-capacitor based functional electrical stimulation of retinal bipolar cells.**

(Artificial Vision <2013, Aachen>).  
In: Artificial Vision 2013. Aachen, 2013, pp. 5–6

Müntjes, J. A.; Häfner, J.; Görtz, M.; Mokwa, W.:

**Studies on thinned flexible integrated capacitive pressure sensors in tactile sensor arrays for the use in robotics and prosthetics.**

(International Conference on Solid-State Sensors, Actuators and Microsystems (Transducers) <17, 2013, Barcelona>).  
In: Transducers. Piscataway, NJ: IEEE, 2013, pp. 1460–1463 [T3P.138]

Obrebski, D.; Szymanski, A.; Tomaszewski, D.; Grodner, M.; Marczewski, J.; Pieczynski, J.:

**Development of ionizing radiation detectors integrated with readout electronics.**

(International Conference Mixed Design of Integrated Circuits and Systems (MIXDES) <20, 2013, Gdynia>).  
In: MIXDES 2013. Piscataway, NJ: IEEE, 2013, pp. 229–234

Pfennig, M.; Cleven, N. J.; Biela, S.; Urbaszek, A.; Ooyen, A. van; Görtz, M.; Mokwa, W.; Schmitz-Rode, T.:

**Ongoing development and first long-term trials of a cardiac output monitoring system in the pulmonary artery (COMPASS).**

(Jahrestagung der DGBMT <47, 2013, Graz>).  
In: Biomedizinische Technik 58 (2013), Suppl. 1, [2 B.]

Poklonskaya, E.; Durini, D.; Jung, M.; Schrey, O. M.; Brockherde, W.:

**Line sensor for fast, time-resolved spectroscopy measurements.**

(International Conference on Optical Technologies for Sensing and Measurement (Opto) <11, 2013, Nürnberg>).  
In: Opto 2013. Nürnberg: AMA Service GmbH, 2013, pp. 17–21 (AMA Conferences 2013)

Schmidt, A.; Kappert, H.; Kokozinski, R.:

**Analog performance of PD-SOI MOSFETs at high temperatures using reverse body bias.**

(PRIME <9, 2013, Villach>).  
In: PRIME 2013. Berlin [u.a.]: VDE-Verl., 2013, pp. 181–184

Schmidt, A.; Kappert, H.; Kokozinski, R.:

**Enhanced high temperature performance of PD-SOI MOSFETs in analog circuits using reverse body biasing.**

(HiTEN <2013, Oxford>).  
In: HiTEN 2013. Washington, DC: IMAPS, 2013, pp. 122–133

Schmidt, A.; Kappert, H.; Kokozinski, R.:

**Enhanced high temperature performance of PD-SOI MOSFETs in analog circuits using reverse body biasing.**

In: Journal of microelectronics and electronic packaging 10 (2013), 4, pp. 171–182

Schmidt, A.; Kappert, H.; Kokozinski, R.:

**High temperature analog circuit design in PD-SOI CMOS technology using reverse body biasing.**

(ESSDERC <43, 2013, Bucharest>).

In: ESSDERC ESSCIRC 2013. Piscataway, NJ: IEEE, 2013, pp. 359–362

Schmidt, A.; Kappert, H.; Kokozinski, R.:

**PD-SOI MOSFET performance optimization for high temperatures up to 400°C using reverse body biasing.**

(Analog <13, 2013, Aachen>).

In: ANALOG 2013. Berlin [u.a.]: VDE-Verl., 2013, without pagination; [5 Bl.] (ITG-Fachbericht 239)

Süss, A.; Nitta, C.; Spickermann, A.; Durini, D.; Varga, G.; Jung, M.; Brockherde, W.; Hosticka, B. J.; Vogt, H.; Schwöpe, S.:

**Speed considerations for LDPD based Time-of-Flight CMOS 3D image sensors.**

(ESSDERC <43, 2013, Bucharest>).

ESSDERC ESSCIRC 2013. Piscataway, NJ: IEEE, 2013, pp. 299–302

Vogt, H.; Heiermann, W.; Heß, J.:

**Galvanik in der Mikrosystemtechnik.**

In: ATZ-Elektronik 8 (2013), 2, pp. 88–93

Vom Bögel, G.; Meyer, F.; Kemmerling, M.:

**Radio frequency powering of microelectronic sensor modules.**

In: Technisches Messen 80 (2013), 2, pp. 61–66

Weiler, D.; Ruß, M.; Würfel, D.; Lerch, R. G.; Hochschulz, F.; Wang, Q.; Gerschke, T.; Heß, J.; Vogt, H.:

**Far infrared digital IRFPA based on uncooled microbolometer for automotive and military applications.**

(Infrared Colloquium <41, 2013, Freiburg>).

In: 41th Freiburg Infrared Colloquium: Abstract booklet. Freiburg, 2013, [Bl. 51–52; 5.4]

### 3. Oral Presentations

Gözüyasli, L.:

**Assistenz durch Sensorik – Unterstützung des Personals durch ein sensorgestütztes Pflegesystem.**

inHaus-Forum „Das Krankenhaus der Zukunft“ zur Eröffnung des Hospital Engineering Labors, inHaus Zentrum, Duisburg, July 18, 2013

Gözüyasli, L.:

**Einsatz von Sensorik im Krankenhaus.**

FKT-Fachtagung Krankenhaustechnika 2013, Fraunhofer inHaus Zentrum, Duisburg, June 20, 2013

Greifendorf, D.:

**Drahtlos überwachte Gebäudestatik mit passiven Sensortranspondern.**

9. Internationale Fachmesse Euro ID 2013, Frankfurt, Main, November 7, 2013

Grella, K.:

**Zuverlässigkeit von EEPROM-Speicherzellen auf SOI für den Einsatz bei 250 °C.**

VDE-ITG 8.5.6 Fachtagung, Freising bei München, May 13, 2013

Hennig, A.:

**Telemedizinische Sensorsysteme für die Medizin.**

FKT-Fachtagung Krankenhaustechnika 2013, Fraunhofer inHaus Zentrum, Duisburg, June 21, 2013

Kappert, H.:

**Integrierte Hochtemperatur-Schaltungen.**

Symposium SYSTEMS INTEGRATION 2013 „Mikrosysteme für extreme Umgebungen“, Berlin, June 13, 2013



Kappert, H.:

**Hochtemperaturschaltungen auf Dünnschicht-SOI.**

Symposium für Automotive, Aerospace und Medizintechnik  
"Elektronik am Limit II", Dortmund, March 6, 2013

Munstermann, M.:

**Patientinnen- und Patientenschutz zur Unterstützung  
der Autonomie.**

inHaus-Forum „Das Krankenhaus der Zukunft“ zur Eröffnung  
des Hospital Engineering Labors, inHaus Zentrum, Duisburg,  
July 18, 2013

Pieczynski, J.:

**Hot-carrier Untersuchungen zur Beurteilung der Qualität  
eines Submicron CMOS Prozesses.**

VDE-ITG 8.5.6 Fachtagung, Freising bei München,  
May 13, 2013

Schliepkorte, H.-J.:

**Neue Lösungen zur Verbesserung der Luftqualität mit  
Gebäudeleittechnik.**

Fachtagung Fraunhofer-Allianz BAU,  
München, November 20, 2013

Schliepkorte, H.-J.:

**Service-Wohnen – Trends und Technikausstattung.**

"Multimedia – Die Wohnung als dritter Gesundheitsstandort",  
VdW Rheinland Westfalen, Bonn, November 19, 2013

Vom Bögel, G.:

**INPACT: Intelligente Prozessautonomie im cloudbasierten  
Toolmanagement.**

4. Tag der Informations- und Kommunikationswirtschaft (IuK)  
NRW, Paderborn, November 20, 2013

Weyers, S.; Durini, D.; Stühlmeyer, M.; Goehlich, A.; Paschen, U.;  
Brockherde, W.; Tisa, S.; Villa, F.; Bronzi, D.; Tosi, A.; Zappa, F.:

**Integration of Single-Photon Avalanche Diodes with low  
dark counting rate in CMOS technology.**

Ninth International Nanotechnology Conference on Communi-  
cation and Cooperation (INC 9), Berlin, May 14–17, 2013

#### 4. Patents

##### 4.1 Granted Patents

Hennig, A.; Vom Bögel, G.:

**Antennenanordnung und Transponderlesegerät.**

July 11, 2013

DE102010028993 B4

Hennig, A.; Vom Bögel, G.:

**Antennenvorrichtung, Transponderlesegerät,  
Induktionsherd.**

October 17, 2013

DE102010028992 B4

Hochschulz, F.; Dreiner, S.; Paschen, U.; Vogt, H.:

**Photodetektor, Bildsensor und Verfahren zur  
Herstellung.**

July 18, 2013

DE102011079990 B4

Kropelnicki, P.; Ruß, M.; Vogt, H.:

**Diode bolometer and method for producing a diode  
bolometer.**

October 29, 2013

US8569857 B2

Lerch, R. G.; Görtz, M.:

**Vorrichtung zum Messen und zum Ansteuern einer Elektrodenanordnung und ein Verfahren zum Messen und zum Ansteuern von Elektroden.**

November 21, 2013

DE102008024972 B4

Vogt, H.; Bauer, J.:

**Package comprising an electrical circuit.**

November 12, 2013

US8581357 B2

#### 4.2 Laid Open Patent Documents

Marzouk, A. M.; Stanitzki, A.; Kokozinski, R.:

**Konzept zum Stimulieren von Nervenzellen.**

September 5, 2013

DE102012203192 A1

Süss, A.; Brockherde, W.; Hosticka, B. J.:

**Halbleiterstruktur, Verfahren zum Betreiben derselben und Herstellungsverfahren.**

September 19, 2013

DE102012206089 A1

Vogt, H.; Goehlich, A.; Jupe, A.:

**Integrierte Sensorstruktur.**

August 29, 2013

DE102012202846 A1

Vogt, H.; Weiler, D.; Kropelnicki, P.:

**Sensor und Verfahren zum Herstellen eines Sensors.**

March 27, 2013

EP2573530 A2

## 5. Theses

### 5.1 Dissertations

Heiermann, W.:

**Entwicklung mikroelektronischer Kontaktierungsmethoden für Hochtemperatur-Anwendungen über 250 °C.**

Duisburg, Essen, Univ., Diss., 2013

### 5.2 Master Theses

Beckmann, N.:

**System für dynamische Hochtemperaturlebensdauertests eines ASICs.**

Düsseldorf, Fachhochsch., Master Thesis, 2013

Eimers, C.:

**Prozessschrittentwicklung für einen Rückseiten-beleuchteten Bildsensor: direktes Wafer-zu-Wafer Bonden und Abscheidung eines leitfähigen transparenten Oxides mit Hilfe der ALD-Technik.**

Duisburg, Essen, Univ., Master Thesis, 2013

Sun, L.:

**Near field RFID-based positioning of objects for underwater robots.**

Duisburg, Essen, Univ., Master Thesis, 2013

Wagner, A.:

**Entwicklung eines Opferschichtprozesses durch Ätzen von Siliziumdioxid mittels gasförmigem Fluorwasserstoff.**

Duisburg, Essen, Univ., Master Thesis, 2013

### 5.3 Bachelor Theses

Adar, B.:

**Entwurf eines Testsystems für den Test von Time-to-Digital Converter.**

Bochum, Univ., Bachelor Thesis, 2013

Caspers, F.:  
**Simulation und Charakterisierung von Lateral Drift Field Photodioden (LDPD) in einem 0,35  $\mu\text{m}$  Standard-CMOS-Prozess.**  
Düsseldorf, Fachhochsch., Bachelor Thesis, 2013

Cheng, Y.:  
**Characterization of the CMOS line sensor based on the lateral drift-field photodetector (LDPD) by means of the charge transfer time measurement and simulatin and the cross-talk measurement.**  
Duisburg, Essen, Univ., Bachelor Thesis, 2013

Fischer, K.:  
**Entwicklung, Durchführung und Bewertung einer Prüfmittelfähigkeitsanalyse für ein Parametertestsystem.**  
Düsseldorf, Fachhochsch., Bachelor Thesis, 2013

Haunschild, F.:  
**Entwicklung eines USB-Potentiostaten zur amperometrischen und voltammetrischen Vermessung von Glucose-sensoren.**  
München, Hochsch., Bachelor Thesis, 2013

Körschgen, M.:  
**Entwurf, Simulation, Aufbau sowie Anpassung einer RFID UHF Transponderantenne für metallische Oberflächen.**  
Gelsenkirchen, Hochsch., Bachelor Thesis, 2013

Maslim, D.:  
**Verbesserung der gestenbasierten Interaktion innerhalb einer Wohnumgebung mittels ambienter Eingabegeräte.**  
Duisburg, Essen, Univ., Bachelor Thesis, 2013

Mentrup, M.:  
**Analyse von Energieverbrauchsdaten zur Betriebsoptimierung am Fallbeispiel: Einsatz eines Blockheizkraftwerkes im inHaus2.**  
Gelsenkirchen, Hochsch., Bachelor Thesis, 2013

Niehoff, S.:  
**Entwurf, Simulation, Aufbau sowie Anpassung einer RFID UHF Reader-Antenne.**  
Gelsenkirchen, Hochsch., Bachelor Thesis, 2013

Pollmann, J.:  
**Lokale Interaktionskonzepte für eine iTV Anwendung in einer Smart Home Umgebung.**  
Duisburg, Essen, Univ., Bachelor Thesis, 2013

Zunic, E.:  
**Entwicklung eines LabVIEW Messprogramms zur Modellierung von CMOS Bauelementen mit IC-CAP.**  
Krefeld, Hochsch., Bachelor Thesis, 2013

## 6. Product Information Sheets

**Measuring Glucose Without Needle Pricks**  
IMS-Duisburg 2013

**Miniaturized Solar Cells**  
IMS-Duisburg 2013

**A Universal Test System for DC/DC Converters**  
IMS-Duisburg 2013

**USB-Stick Nano Potentiostat For Innovative Bio Sensors**  
IMS-Duisburg 2013

# CHRONICLE 2013

---

## Chronicle

Opening of Hospital Engineering Laboratory	84
Microsystems Technology Congress	85
Visit of the Dutch Commissioner, Ms. Annemieke Slow, at Fraunhofer IMS	86



## OPENING OF HOSPITAL ENGINEERING LABORATORY

On July 18, 2013 the Hospital Engineering Laboratory at the Fraunhofer inHaus in Duisburg opened. Among the 180 guests of the opening was Barbara Steffens, Health Minister of North Rhine-Westphalia, who is aware of the need for research and development in the field of hospital engineering: for cost pressure and workload of staff continue to increase in the health sector, solutions must be developed to reduce costs while quality of care is ensured at the same time. On 350 m<sup>2</sup> the Hospital Engineering Laboratory serves as a novel development and test environment for researchers, manufacturers and practitioners in the health sector - including a reception area, a doctor's office, a patient room, an operating room, a rehabilitation area and several store and functional rooms. Besides four Fraunhofer Institutes - for Microelectronic Circuits and Systems IMS in Duisburg, for Software and Systems Engineering ISST in Dortmund, for Environmental, Safety, and Energy Technology UMSICHT in Oberhausen and for Material Flow and Logistics IML in Dortmund – eight hospitals in North

Rhine-Westphalia and more than 60 industrial partners are involved. Together they analyzed the present situation in hospitals regarding state of the art technology and materials, energy consumption and common processes in order to identify optimization potential. While existing hospitals do not have any capacities for experiments in their facilities, the Hospital Engineering Laboratory provides an ideal environment to test, optimize and evaluate solutions. There are various approaches arising in the Hospital Engineering Laboratory that show ways into a future in which hospitals are competitive while providing the best possible medical treatment: from lighting concepts increasing the well-being of patients and staff while saving energy to a fall detection integrated into a shower tray through to RFID-based presence detection for automated documentation and scheduling purposes.



## MICROSYSTEMS TECHNOLOGY CONGRESS

Fraunhofer IMS participated in the Microsystems Technology Congress in Aachen. At our booth we presented the following new developments: the infrared camera, the miniaturized solar cell, the shunt sensor. The NRW-Minister for Innovation, Science and Research, Ms. Svenja Schulze, visited our booth and she was impressed by our innovations. Professor Vogt explained "In a first step we manufacture CMOS-chips which contain the whole electronics of the sensors. These CMOS-chips are later extended by the sensory functions, e.g. by elements which detect heat radiation. The application fields of for instance **bolometers** are widely spread: **Infrared sensors** are used to measure the heat radiation of objects such as people, cars, buildings and animals".

We also presented a **miniaturized solar cell** which can be integrated on an ASIC. This allows the so-called energy harvesting directly on a chip. Energy harvesting is the collection of energy from sources that provide only small amounts of energy: Possible application areas include autonomous sensor

nodes and transponders for the detection of environmental parameters such as temperature and humidity.

Furthermore the **shunt sensor**, which measures the intracranial pressure in the patient's brain, was presented. The continuous control of the pressure protects the patient from further possible complications.





## VISIT OF THE DUTCH COMMISSIONER, MS. ANNEMIEKE SLOW, AT FRAUNHOFER IMS

On July 9<sup>th</sup> a high-level meeting concerning a biomedical project with NovioSense BV, a Dutch medical technology firm, took place at Fraunhofer IMS.

During the visit Ms. Slow symbolically received the first wafer with the glucose sensor chip which is developed and produced at IMS and which is planned to be on the market in 2017.

In various presentations and also during the cleanroom tour the principle of how to measure glucose without needle pricks was explained.

The tiny chip with the glucose sensor is placed under the patient's eyelid where it measures continuously the sugar values. The data is sent to a mobile device, e.g. a smart phone, in order to read the sugar values. Thus the diabetic patient can continuously monitor the glucose level and may take action at too high or too low values. This is a major breakthrough which makes the patient's life easier and safer.

Since the chip can be manufactured very cost-effectively, it is best suited for mass production.

This joint project is an innovative cross-border cooperation between a German research institution and a Dutch company.

# PRESS REVIEW

## RFID-Sensoren schützen Rotterdamer Kaimauer

Tag ein Tag aus nagt das salzige Meerwasser am Beton der Kaimauer. Schwerste Bedingungen also, die der Stahlbeton aushalten muss. In Form von Salzionen dringt das Salz in den alkalischen Beton ein und neutralisiert ihn, es verändert ihn also chemisch. Kritisch wird es, wenn die Salzionen die Stahlbewehrung erreichen: Die Stahlstäbe korrodieren, es bilden sich Risse, Betonstücke können abbrechen und die Kaimauer verliert ihre Stabilität. Wann die Eindringlinge sich soweit durch den Beton gekämpft haben, dass sie auch dem Stahl zusetzen, lässt sich allerdings nur schwer beurteilen.

Anders in einer neuen Kaimauer in Rotterdam: Bei ihrem Bau integrieren die Bauherren passive RFID-Sensoren an den Bewehrungsstäben. Erreichen die Salzionen einen der Sensoren, »zerfressen« sie dessen spezi-

sind, desto weiter ist auch die Korrosion des Stahls fortgeschritten. Ein Transponder im Sensor übermittelt die Daten an ein Lesegerät und zeigt an, ob die Kaimauer gefährdet ist. Die Verantwortlichen können das Bauwerk somit instandsetzen lassen, bevor die Bewehrung Schaden nimmt. Auf diese Weise können bei vielen Betonbauwerken Kosten in Millionenhöhe eingespart werden. Entwickelt wurde der Sensor von

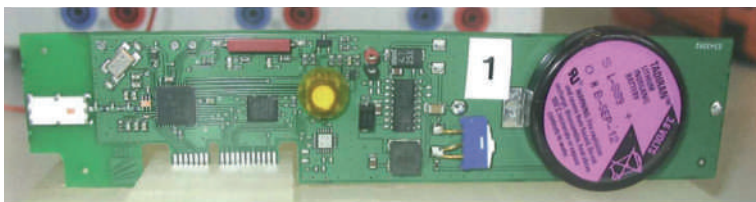


VuE Nachrichten, Dezember 2013

## Datendetektive in Isolierfenstern

Pralle Sonne, eisiger Wind, klirrende Kälte – Isolierfenster müssen einiges aushalten. Denn steigt oder fällt die Temperatur, ändert sich auch der Druck zwischen den beiden Fensterscheiben. Sie beulen aus oder ziehen sich zusammen. Diese Belastungen können zu kleinsten Rissen an den Rändern der Scheiben führen. Für das bloße Auge kaum sichtbar, kann das Isoliergas durch diese Risse entweichen. Die Folge: Die Fenster verlieren ihre isolierende Wirkung. Spezielle Messgeräte, sogenannte Datenlogger, geben Fensterherstellern Aufschluss darüber, welche Temperaturen und Drücke im Inneren des Fensters herrschen. Die Daten helfen, die Produktionsprozesse und die Kon-

struktion der Fenster zu optimieren. Forscher vom Fraunhofer-Institut für Mikroelektronische Schaltungen und Systeme IMS haben die Sensoren entwickelt. Sie sind nur wenige mm dick und passen somit in den schmalen Raum zwischen den Fensterscheiben. Mitarbeiter der Materialprüfanstalt der TU Darmstadt haben die Datenlogger in 40 verschiedene Isolierfenster eingebaut und diese in einen Klimaschrank gesteckt. Dort müssen sie zwölf Wochen lang Temperaturschwankungen zwischen -18 und +53 °C überstehen. Die Sensoren messen in diesem Zeitraum Druck und Temperatur zwischen den Scheiben, funken die Daten nach außen und speichern sie zudem auf einem integrierten Speicher. So helfen sie, Isolierfenster noch dichter zu machen.



VuE Nachrichten, Dezember 2013

## Aktives Türdichtungssystem verbessert Raumluft

Werden Konferenzräume nicht ausreichend belüftet, sinkt rasch die Raumluftqualität. Die Folgen: Die Luft im Konferenzraum ist stickig und verbraucht, der erhöhte Gehalt an Kohlendioxid (CO<sub>2</sub>) verursacht bei den Teilnehmern Müdigkeit und schwächt deren Konzentrationsfähigkeit.

### CO<sub>2</sub>-Gehalt ist noch immer ein Problem

Besonders in neueren Bauten sei der CO<sub>2</sub>-Gehalt in Zimmern noch immer ein Problem. „Moderne Gebäude werden immer dichter“, sagt Dipl.-Ing. Hans-Jürgen Schliepkorte, Gruppenleiter am Fraunhofer IMS in Duisburg. Bessere Fenster und Bausubstanzen sorgen zwar für eine gute Wärmedämmung, was lange Zeit ein großes Thema gewesen sei. Dafür sei aber die Luftqualität auf der Strecke geblieben. „Vielfach wird noch immer durch Fensteröffnen gelüftet“, so Schliepkorte. „Das wirkt sich auf die Energieeffizienz aus.“

Ein CO<sub>2</sub>-Sensor registriert die Konzentration in der Luft. Steigt diese über einen bestimmten Schwellenwert, steuert ein kleiner Motor die Türdichtung am unteren Teil des Türflügels. Eine Feder zieht die Dichtung nach oben, Raumluft kann über den Schlitz



Quelle: Fraunhofer IMS

### Sensor misst den CO<sub>2</sub>-Gehalt in der Raumluft

Forscher vom Fraunhofer-Institut für Mikroelektronische Schaltungen und Systeme IMS haben in Ko-

Elektro Praktiker, Juli 2013

## Technik: Dichtung checkt Luftqualität



**Sorgt für Frischluft:** Die intelligente Türdichtung öffnet sich von selbst, wenn die Raumluft verbraucht ist. Foto: Fraunhofer IMS

VDI nachrichten, Juni 2013



## Kranke unterm Strichcode

**MEDIZINTECHNIK:** Im Krankenhaus der Zukunft wird alles besser, sicherer, effizienter – das versprechen Fraunhofer-Forscher des Hospital Engineering Labors. Sie testen im Duisburger inHaus-Zentrum, ob und wie elektronische Assistenzsysteme Patienten und Personal das Leben erleichtern.

VDI nachrichten, Dülmen, 16. 8. 13, 107  
Die Wände sind in Creme und Lindgrün gehalten, die Bettwische blütenweiß und die Möbel tragen freundliches Birken Dekor. Das Licht wurde gedimmt, die Luft ist angenehm kühl und das großzügige Fenster lenkt den Blick ins Grüne. Zwei Schritte weiter präsentiert sich ein Bad mit erstaunlich viel Platz. Armaturen vom Feinsten und einer gro-

Auswirkungen, die Amortisation und Praktikabilität prüfen.

Zurück im Patientenzimmer. Erst beim genauen Hinsehen fällt der Blick auf Dinge, die man aus einem normalen Krankenhaus nicht kennt: Im Bettgestell sind seitlich mehrere Sensoren integriert, am Fußende ist ein kleines Display mit Touchscreen montiert und der Türrahmen trägt Bewegungsmelder.

Punk, ob und wann der Kranke das Bett oder das Zimmer verlässt.

Ein selbstklebendes Papierband mit Namen und Strichcode am Arm identifiziert jeden Patienten während des gesamten Aufenthalts und ist zugleich Steuerinstrument: Führt der Kranke den Barcode des Armbands im Bad über den kleinen Scanner an der Wand, werden automatisch WC und Waschtisch auf eine der Körpergröße angepasste Höhe gefahren.

Selbst auf einen Sturz in der Dusche ist die Elektronik vorbereitet: Unter der Duschwanne sitzt ein Netz aus kapazitiven Sensoren, die einen stehenden Menschen von einem gestürzten unterscheiden können, weil



VDI nachrichten, August 2013

## Hier ist aber dicke Luft!

Stickige Konferenzräume, Konzentrationsschwierigkeiten und müde Augenlider – jeder kennt diese Situationen aus dem Arbeitsleben. Grund ist die hohe CO<sub>2</sub>-Konzentration. Nachdem lange nur die Wärmedämmung zählte, haben die Forscher des Fraunhofer IMS jetzt eine Lösung entwickelt, mit der ständiges Lüften passé ist: ein intelligentes Türdichtunassystem.



µE Nachrichten, Juli 2013



## Fit für die Zukunft: Smarte Sensortechnologien optimieren Krankenhausprozesse

Im Krankenhaus der Zukunft denkt auch die Infrastruktur mit. Doch heute sind viele Bereiche des Krankenhauses mit Blick auf ihre technische Infrastruktur noch unterversorgt: „Bisherige Innovationen konzentrieren sich meist auf den OP-Bereich oder dessen direkte Umgebung – doch das alleine genügt nicht mehr, um diesen umfassenden Anforderungen gerecht zu werden“, ist Levent Gözüyüslü vom Fraunhofer-Institut für Mikroelektronische Schaltungen und Systeme IMS überzeugt. Gözüyüslü und sein Projektteam sind im Hospital Engineering Labor

Hospital Engineering Magazin, Juli 2013

## Ein Inkubator für gemeinschaftliche Innovationsentwicklung

Das Fraunhofer inHaus-Zentrum zielt darauf ab, gemeinsam mit den späteren Nutzern und Wirtschaftspartnern Systeminnovationen zu entwickeln, die gesellschaftliche Nutzeffekte in Bereichen wie z. B. Energieeinsparung (Energy efficiency), Arbeitsprozessverbesserung und Umweltschutz erzielen und den Industrieunternehmen neue Markchancen eröffnen. Durch die integrierte Innovationskette von Forschung bis Praxis (inHaus-Pilotprojekte im Markt), werden dabei die Erfolgchancen neuer Entwicklungen ganz entscheidend gesteigert.

trieren, ohne dass die Krankenhäuser die Innovationen direkt im eigenen, hoch sicherheitskritischen Live-Betrieb einsetzen müssen. Das Labor ist ein Living Lab – die Projekte und Themen werden sich immer wieder anpassen und erweitern.

### Interdisziplinär zum Ziel

Wer heute, aber besonders in der Zukunft Gebäude baut, wird das unter ökonomischen und gesellschaftlichen



Hospital Engineering Magazin, Juli 2013



## Tränen statt Blut: Neue Messlösung für Diabetiker

Ein RFID-Miniatursensor soll den Blutzuckergehalt anhand der Tränenflüssigkeit messen und die Ergebnisse kontaktlos weiterleiten

Für die meisten Diabetiker gehört es zum Alltag, sich mehrmals täglich den Finger stechen zu müssen. Nur so können Messwerte über das austretende Blut des Glukosewerts ermittelt, um die nötige Insulindosis zu ermitteln. Non-invasive Messmethoden befinden sich in der Entwicklung. Sie sollen schmerzfreie Alternativen bieten

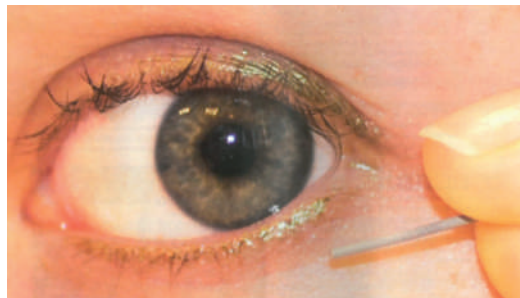
und zugleich genauere Messergebnisse liefern. Mit dem Noninvasive Glucose Sensor hat das Unternehmen Novionics BV einen Weg gefunden, den Blutzucker ohne Blut zu bestimmen: Ein RFID-fähiger Sensor analysiert die Tränenflüssigkeit und sendet die Ergebnisse an ein Lesegerät.

### Komfort und Langlebigkeit durch RFID

Blutzuckermessung könnte zukünftig am Auge erfolgen, ohne dass der Benutzende etwas davon merkt. Mit 0,7 Millimetern Durchmesser und 10 Millimetern Länge soll sich der Noninvasive Glucose Sensor zwischen Augen und innerem Augenlid platzieren lassen, um anhand der Tränenflüssigkeit kontinuierlich in Echtzeit den Blutzuckergehalt des Patienten zu messen. Ein integrierter passiver RFID-Transponder macht diese Lösung kontaktlos. Nach der Messung in jeder Messung heruntergeladen und wieder einsetzen zu müssen, lassen sich die Daten kontaktlos beispielsweise durch ein NFC-fähiges Smartphone oder eine Glukose-Teststation auslesen. Bild



Die Maße des Noninvasive Glucose Sensors betragen 0,7 mit einer Millimeter. Der integrierte Chip misst 0,5 mit einer Millimeter und ist nur ein Phosphor, als auch ein Transponder.



RFID im Blick, März 2013

## SonnenKRAFT für Sensorknoten

Winzige Solarzellen, die direkt auf einen Siliziumchip aufgebracht werden, könnten zukünftig drahtlose Sensornetze effizient und zuverlässig mit Strom versorgen. Das erleichtert vor allem großflächige Anwendungen, etwa in der Landwirtschaft.

der Wartungsaufwand durch die regelmäßig nötigen Batteriewechsel, gerade bei großen Netzwerken.

Forscher des Fraunhofer-Instituts für Mikroelektronische Schaltungen und Systeme IMS haben jetzt gemeinsam mit der SOLCHIP Ltd. eine Alternative entwickelt und nutzen für die Energieversorgung eine Ressource, die fast überall umsonst zur Verfügung steht: Das Sonnenlicht. „Wir bringen

Sensornetze, deren einzelne Module drahtlos miteinander kommunizieren, sind in der Lage, großflächig Parameter in ihrer Umwelt zu messen und diese Daten untereinander bis an eine zentrale Station weiterzugeben. Damit eignen sie sich für unterschiedlichste Einsatzgebiete – vom Brandschutz bis zum Monitoring von großen Anbauflächen in der Landwirtschaft. Einen Knackpunkt ist bei solchen Anwendungen nach wie vor die Ener-



tema, Juni 2013

## Kupfer, Gold und Zinn für effiziente Chips

### PRODUKTION NR. 15, 2013

Für zuverlässige Leuchtkraft muss durch die Schaltkreise der LED-Treiber ein höherer Strom fließen. Forscher des Fraunhofer IMS haben ein Verfahren für entsprechende Chips entwickelt.



Eine Mitarbeiterin des MST Lab & Fab, in dem das Post Processing von Chips stattfindet. Bild: Fraunhofer IMS

DUISBURG (BA). Um auf noch kleineren Chips genauso viel Strom wie auf größeren fließen lassen zu können, sorgen Forscher des Fraunhofer-Instituts für Mikroelektronische Schaltungen und Systeme IMS dafür, dass dank Galvanisierung Kupfer auf den Halbleitern abgeschieden wird. Doch ist die Integration von neuen Materialien auf den Chips nicht ohne Weiteres möglich, da den Herstellungsprozessen Grenzen gesetzt sind.

Die Forscher haben deshalb eigene eine Fertigungslinie für das „Post-Processing“ aufgebaut, um die Chips auf den Substratwafern je nach Anwendungsbedarf verbessern zu können. Neben Kupfer sind die Ingenieure in der Lage, auch

andere Metalle oder Verbindungen wie Kupfer-Zinn oder Gold-Zinn auf Chips abzuscheiden. Da diese Schichten lösbar sind, ergibt sich der Vorteil, dass direkt auf dem Wafer der Deckel auf den Chip gelötet werden kann. Damit entsteht laut den Forschern das kleinste Gehäuse für einen Chip, das man

haben kann. Mit ihm lassen sich sensible Sensoren schützen, ohne ihre Funktionsweise zu beeinträchtigen. Ein Beispiel sind Bolometer, Sensoren, die zur Temperaturmessung dienen. Weil die Gehäuse für Bolometer für eine unverfälschte Messung auch unter Vakuum gelegt werden müssen, war deren Fertigung bisher sehr aufwändig und teuer.

Mit Hilfe der Fraunhofer-Fertigungslinie lassen sich jedoch kostengünstige und damit massentaugliche Gehäuse herstellen. Zudem ist es den Forschern möglich, komplexe Bauelemente innerhalb eines Gehäuses zu produzieren. Über die Galvanisierung mit Kupfer können sie zwei Chips miteinander verlöten, etwa einen Opto-Chip mit hochempfindlichen Photosensoren mit einem CMOS-Chip (Complementary Metal Oxide Semiconductor), der einzelne Photonen messen kann. Solche mikroelektronischen Bauelemente eignen sich für Nachtsichtgeräte oder lichtarmen Mikroskopie-Anwendungen.

Produktion, April 2013

## Wie das Gehirn Beinprothesen steuern kann

Die SNAP GmbH in Bochum entwickelt einen Versuchsstand, der neuronale Impulse beim Gehen misst

Von Frank Mölling

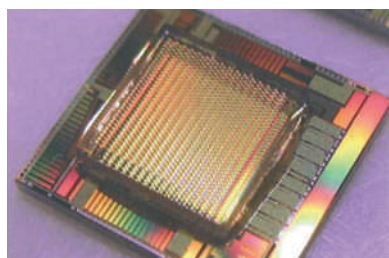
Bochum. „Ich denke, ich grüße dich.“ Diese These ist für Gesunde eine Selbstverständlichkeit. Das Gehirn steuert die Beine. Für amputierte Menschen ist dieser Mechanismus allerdings eine Vision. Noch. Denn in Bochum arbeitet ein kleines Team daran, neuronale Signale auf Prothesen zu übertragen. „Sensorisierte Neural Adaptive Prothesen“ heißt die Pflanz auf dem Campus der Ruhr-Universität Bochum, die sich kurz und prägnant SNAP nennt. Um neuronale Signale für Beinprothesen nutzbar zu machen, ist eine Menge Vorarbeit zu



SNAP-Chief Uwe Sabel steht mit EEG-Headset auf dem Versuchsstand. Foto: Frank Mölling

der Steuerung einer Prothese wichtig sein können. So die Knoch, die beim Ausführen des Fußes entsteht. Anhand der gewonnenen Informationen soll es irgendwann möglich sein, dass ein Mensch über einen kleinen Sensor am Kopf mit seiner Prothese kommuniziert, als wäre sie sein eigenes Bein. Beid: „Entscheidend ist, dass für den Einsatz des Sensors keine Operation erforderlich sein wird.“ Der Sender wird von außen aufgebracht. und das Versuchsstand zu stabilisieren. Das sehen die Probenrichtlinien von Europäischen Union und Land NRW vor. Denn die Sensorprothese ist ein Projekt des ZNS-Programms. Die Leitung hat die SNAP GmbH in Bochum und unter anderem das Fraunhofer Institut für Mikroelektronische Schaltungen und Systeme, die Ruhr-Universität Bochum. Die zu erwartenden Gesamtinvestitionen für Hilfe von 1,88 Millionen Euro werden zu 85 Prozent von der öffentlichen Hand aus ZNS-2-Mitteln gefordert. „Wann aus der Vision „Ich denke, ich grüße dich“ auch für Prothesen-

WAZ, Oktober 2013



Für einen neuen BILDSSENSOR haben Wissenschaftler des FRAUNHOFER IMS (Institut für Mikroelektronische Schaltungen und Systeme) in Duisburg die Complementary-Metal-Oxide-Semiconductor (Cmos)-Technik weiterentwickelt und mit der neuen Technik, die auf Single-Photon-Avalanche-Photodioden (Spad) basiert, einen hochempfindlichen Bildsensor vorgestellt. Die Pixelstruktur des neuen Sensors könne einzelne Photonen innerhalb weniger Pikosekunden zählen und sei damit

ATZ, Januar 2013

## Imprint

---

Copyright 2014 by Fraunhofer-Gesellschaft  
Hansastraße 27 c  
80686 München

Annual Report  
Fraunhofer-Institut für Mikroelektronische  
Schaltungen und Systeme

Director: Prof. Dr. rer. nat. A. Grabmaier

Adresses:

IMS Duisburg  
Finkenstraße 61  
47057 Duisburg

Phone +49(0)2 03/37 83-0

Fax +49(0)2 03/37 83-2 66

E-mail [martin.van.ackeren@ims.fraunhofer.de](mailto:martin.van.ackeren@ims.fraunhofer.de)

Internet [www.ims.fraunhofer.de](http://www.ims.fraunhofer.de)

Editorial Staff: Martin van Ackeren





